KINETIC STUDY OF THE CRYSTALLIZATION OF LLDPE AND WAX IN LLDPE/WAX PHASE CHANGE BLENDS USED FOR THERMAL ENERGY STORAGE

by

THANDI PATRICIA GUMEDE (B.Sc. Hons.)

2008115624

Submitted in accordance with the requirements for the degree

MASTER OF SCIENCE (M.Sc.)

Department of Chemistry

Faculty of Natural and Agricultural Sciences

at the

UNIVERSITY OF THE FREE STATE (QWAQWA CAMPUS)

SUPERVISOR: PROF A.S. LUYT

CO-SUPERVISOR: PROF A.J. MÜLLER

December 2014

DECLARATION

I hereby declare that this M.Sc. thesis submitted by me at the University of the Free State is the product of my own independent work. All content and ideas drawn directly or indirectly from external sources are indicated as such. The thesis has not been submitted by me to any other examining body. I furthermore cede copyright of the dissertation in favour of the University of the Free State.

Gumede T.P. (Ms)

DEDICATION

To my mom and dad (Busisiwe Minah Gumede and Mvulani Alfred Gumede):

Throughout my life, you have always been the strength that holds me up in the storm of life. Thank you for giving me a chance to prove and improve myself through all my walks of life. Thank you once again for the unconditional support through my studies and for always believing in me. I am blessed to have you in my life. I love you mom and dad.

To my granny (Nomadlozi Lephinah Mofokeng):

Words cannot express the true appreciation I have for you gogo. You always opened your arms for me. When people shut their ears for me, you always opened your heart for me. Thank you for always being there for me in good and bad times. You are highly appreciated.

To my brother and nephew (Sibusiso Edward Gumede and Kabelo Mofokeng):

Never forget the three powerful resources you always have available to you: love, pray and forgive and I hope that with this research I have proven to you that there is no mountain higher as long as God is on our side. I hope that you will walk again and be able to fulfill your dreams.

To my baby boy (Bokang Siphosethu Gumede):

I dedicate this entire thesis to you. You were there with me from the beginning of this thesis until the end. I believe that you are a gift from God. Everything that I do, I do it for you. I ask God for grace and wisdom in carrying out the responsibilities of being a mother.

ABSTRACT

The main purpose of this research was to kinetically study the influence of each component in an LLDPE/wax blend on the crystallization behaviour of the other component, and also to evaluate the effectiveness of wax as a phase change material when blended with LLDPE. Phase change materials are used to store and release energy through phase changes, be it melting and solidification processes or solid state phase transitions. Paraffin wax is one of a large number of phase change materials that store and release large amounts of thermal energy through melting and solidification. Since molten wax has a low viscosity, it is important to contain the wax in some medium. A lot of research has gone into the preparation and characterization of immiscible polymer/wax blends, in which the wax crystallizes separately in the amorphous phase of the polymer. These wax crystals can then melt and solidify without affecting the polymer, which should have a significantly higher melting temperature than the wax. It is, however, possible for some of the wax to be trapped in the amorphous part of the polymer, in which case this wax fraction will not be available for thermal energy storage, making the system less effective as a phase-change blend. The crystallization kinetics results described in this thesis showed that the overall crystallization rate of LLDPE decreased with an increase in wax content, due to the dilution effect of the wax. Although the wax crystallized faster when blended with LLDPE, it showed lower melting enthalpies indicating fewer wax crystals, which directly impacts on its effectiveness as a phase-change material for thermal energy storage. The results obtained by successive self-nucleation and annealing (SSA) indicated that LLDPE can be thermally fractionated, whereas the medium-soft paraffin wax was not susceptible to thermal fractionation because of its linear short chain hydrocarbons. It was also shown that the wax acts as a solvent for LLDPE inducing a 'dilution effect' without co-crystallization.

PEs	polyethylenes
PP	polypropylene
φ	cooling rate
q	work done by the chain to form a fold
rpm	revolutions per minute
R	gas constant
R^2	correlation coefficient
SC	step crystallization
SCBs	short chain branches
SEM	scanning electron microscopy
SFE	supercritical fluid extraction
σ	lateral surface free energy
σ_e	fold surface energy
SN	self-nucleation
SPD	short path distillation
SSA	successive self-nucleation and annealing
$t_{1/2}(e)$	experimental half crystallization time
$t_{1/2}(t)$	Avrami fitting half crystallization time
T_c	crystallization temperature
T_{c1}	pre-established temperature
t_c	crystallization time
T_m	melting temperature
$T_{m(obs)}$	observed melting temperature
T_m°	equilibrium melting temperature
$T_{o,m}$	onset temperatures of melting
TREF	temperature rising elution fractionation
T_s	self-seeding temperature
$T_{s(ideal)}$	ideal self-nucleation temperature
T_α	temperature at which chain mobility ceases = T_g–30 K
U*	activation energy for the transport of the chains to the growing front = 1500 calmol^{-1}
V_c	relative volumetric transformed fraction
$X_{(t)}$	relative crystallinity
Z	crystallization rate constant

TABLE OF CONTENTS

LIST OF TABLES

Page

LIST OF FIGURES

CHAPTER 1

INTRODUCTION AND LITERATURE REVIEW

1.1 General introduction

The crystallization behaviour of crystallizable polymers is of importance for controlling the microstructure and therefore the properties of materials [1-2]. Differential scanning calorimetry (DSC) has been traditionally used for studying the thermophysical properties of polymers such as the crystallization behaviour [3-5]. The process of crystallization can be studied at a constant temperature, i.e., isothermal crystallization, or at a constant cooling rate, i.e., non-isothermal crystallization [6].

The isothermal crystallization experiment is very useful for determining the crystallization kinetic parameters such as the crystallization enthalpy (ΔH_c), relative crystallinity ($X_{(t)}$), and to provide data suitable for fitting with crystallization theories such as the Avrami model or the Lauritzen and Hoffman nucleation and growth theory [7]. The isothermal crystallization experiment can be conducted for a series of suitable crystallization temperatures (T_c), but the DSC must be able to detect the isothermal crystallization. If a lower crystallization temperature is chosen, the isothermal crystallization will be so fast that only part of the curve will be recorded, because the sample starts to crystallize before the selected crystallization temperature is reached. At higher temperatures the amount of heat flow evolved per unit time will be too small for the DSC sensitivity [8].

During an isothermal crystallization experiment, the sample is first heated to above its melting temperature. Holding for a crystallization time (t_c) at approximately 30 °C above the sample peak melting temperature (T_m) is necessary to fully melt out any existing crystals [9]. The sample is then rapidly cooled (at a constant and controlled rate, usually 60 °C min^{-1}) from above its melting temperature T_m, to the desired isothermal crystallization temperature T_c. The sample is left to crystallize at this temperature and the heat generated during this crystallization process is recorded by the DSC instrument. The experiment may stop when the crystallization finishes and

the heat flow signal reaches the baseline [10]. The Avrami model and the Lauritzen and Hoffman theory (L-H) can be evaluated if they can predict the isothermal crystallization. The curves obtained from DSC can be processed by a plug-in to the Origin® graphics software, developed by Lorenzo *et al.* [9]. This plug-in was designed to analyse the DSC isotherms, establish the baseline, calculate its integral, perform a linear fit according to the Avrami equation [11-13], calculate fitting errors and perform graphical comparisons between the experimental data and the predictions. The L-H theory predicts that the overall crystallization rate ($1/\tau_{50\%}(T)$) can be expressed as a function of supercooling [14].

In studying the crystallization kinetics of crystalline polymers, it is also important to know the true reflection of the microstructure and the morphology of the material. It can be obtained by determining the equilibrium melting temperature ($T_m°$) or the melting temperature of a perfect crystal. The procedure suggested by Hoffman-Weeks [15] may be used to obtain the $T_m°$ which was adopted by plotting the observed melting temperature ($T_{m(obs)}$) against T_c to observe the intersection of this line with another line with a slope equal to 1 ($T_m = T_c$). Usually, the lamellar thickness is in the range between 5 and 50 nm and, for this reason, the melting temperature, T_m is always lower than $T_m°$. At the beginning of the crystallization process, the longest and more regular chains attach to the primary nucleus. Only at later stages, the shortest chains and those containing a large amount of constitutional and configurational defects add to the crystalline phase, giving rise to crystalline systems characterized by a spectrum of crystal thicknesses and defect concentrations. It should be mentioned that these crystals may undergo melting and re-crystallization phenomena. During heating, thin and highly imperfect lamellar crystals develop at low solidification temperatures and, characterized by a low melting temperature, these crystals are first destroyed giving rise to an undercooled metastable melt. In this situation, the thermodynamic conditions may be suitable for the formation of new, thicker and more perfect crystalline entities that will melt at higher temperatures [16].

Another way of using DSC to study the crystallization behaviour of crystalline polymers is by performing a non-isothermal crystallization experiment [10]. During non-isothermal crystallization, the sample is allowed to crystallize upon cooling at various rates from the melt to room temperature or below [17]. Some useful parameters such as the crystallization temperature,

T_c, and relative crystallinity, $X_{(t)}$, as functions of the crystallization behaviour of the system can be obtained. The relative crystallinity of the sample, $X_{(t)}$, can be calculated by the integration of the crystallization exotherms at specific temperature intervals divided by the total crystallization exotherm [18]. To study the kinetic parameters for non-isothermal crystallization processes, several methods were developed by Jeziorny [19] and Mo [20-22], and their formulations are based on the Avrami equation [11-13]. All the theories used to interpret the data are extrapolated from isothermal theories, but taken under non-isothermal conditions; however, this method is not effective because the parameters obtained hardly have a physical meaning for polymers (i.e., the non-isothermal "Avrami" indices are lower than 2 in polymers like PE). It is well known that in polymers only 2 and 3 dimensional structures are commonly obtained as they would represent axialites for two-dimensional lamellar aggregates and spherulites for superstructural three-dimensional aggregates of radial lamellae [9]. New evidence [23] on the correlation between sensitivity and sample mass indicates that unless the sample mass is compensated for upon changing the scanning rates, the values obtained are greatly affected by superheating. In other words, the shifts in T_c with scanning rates if the mass is held constant can be due to heat transfer effects. The faster the cooling rate, the smaller the sample mass should be, in order to reduce the thermal gradients in the sample caused by the heat transfer from the sample pan to the sample.

Polyethylenes (PEs) have high crystallization rates that cause faster solidification and faster production in industry. However, polymer blending is essential to produce polymeric materials from existing polymers with improved properties, such as thermal energy storage [2]. The advantages of polymer blending include cost effectiveness and less time-consumption as in the case of the development of new monomers as a basis for new polymeric materials. Additionally, a wide range of material properties is within reach by merely changing the blend composition [24]. The blending of polymers with phase change materials (PCMs) received attention due to its non-toxic nature, availability and low cost. PCMs can possess high energy storage density and isothermal operating characteristics that make them efficient materials for utilizing latent heat. Organic, inorganic and eutectics are forms of PCMs and have been widely investigated for storage of passive solar energy for deployment in the walls or floors of buildings. In this application, they act as a temperature buffer for energy conservation in the building. When the building's interior temperature approaches the melt temperature of the PCM, the PCM changes

from solid to liquid and absorbs energy. Later, when the ambient temperature drops, the PCM begins to crystallize, releasing stored thermal energy to the building and stabilizing the interior temperature. The PCM temperature will be maintained closer to the desired temperature during each phase transition period until the phase change is complete. In this manner, the PCM decreases the interior temperature fluctuations, maintain human comfort while conserving energy through this reversible phase change [25-28].

Amongst the various kinds of PCMs, paraffin waxes have been widely used for blending with polyethylenes due to their high heat of fusion, chemical resistance, commercial availability and low cost [29-30]. The blending of paraffin waxes with polyethylenes possesses many useful properties such as light weight, good processability and low cost. There are various kinds of paraffin waxes. Each of these waxes differs in the melting temperature and degree of crystallinity. Although medium-soft paraffin wax has a lower melting enthalpy than hard paraffin wax, its high level of immiscibility with polyethylenes makes it a material of choice to be used as an energy storage material [31]. It is also important to mention that paraffin waxes are more compatible with PE based materials than polypropylene (PP) due to the difference in their chemical structures. PEs and paraffin wax are made up of just CH_2 units and PP has stereo-defects, i.e., non-isotactic units in the chain or any other irregular monomer incorporation.

In this study, linear low-density polyethylene (LLDPE) has been selected because it is a more regular polymer with an ethylene/α-olefin composition having uniform short chain branches. Low-density polyethylene (LDPE) has an irregular backbone structure of short and long branches; for applications requiring high tensile strength, LLDPE has better thermal and mechanical properties than LDPE (although LDPE is easier to process). Therefore, in this study, a simple and fast technique with a high resolution has been used to investigate the interaction of medium-soft paraffin wax with LLDPE in order to ascertain if the wax can co-crystallize with LLDPE or act as a diluent. This technique (successive self-nucleation and annealing (SSA) [32]) is useful for studying the degree and distribution of short chain branches produced by the copolymerization of ethylene with α-olefins [33]. It is very sensitive to branches or any other defect that interrupts the methylene linear sequence that crystallizes [23]. It fractionates the polymer according to the different lamellar thicknesses. This technique does not require special

instrumentation except for conventional DSC equipment [32,34]. However, other materials (i.e., polymer blends or block copolymers) have also been examined by this technique [34-35]. The SSA technique has great potential as a characterization tool of anyheterogeneous system capable of crystallization. The blending of medium-soft paraffin wax with LLDPE can result in an improvement of the quality of thermal fractionation curves and a reduction of the overall crystallization rate of the polyethylene. The reduced overall crystallization rate is related to a dilution effect caused by the wax when the materials are compared at identical crystallization temperatures [14]. To our knowledge, there are no reports on the overall crystallization kinetics of polyolefin/wax blends and it is important to understand the influence of other components in a blend on the crystallization behaviour of a particular component.

1.2 Literature review

1.2.1 Thermal behaviour and morphology (polyethylene/wax blends)

The blending of polymers with phase change materials (PCMs) is a method of obtaining materials with practical importance for various applications. Since the blended constituents have different chemical compositions and physical properties, materials with improved properties can result [31]. A number of studies were conducted on the thermal properties of various paraffin waxes blended with different polyethylenes [31,36-46]. The used paraffin waxes were of different grades and melting temperatures. The preparation of these blends was mostly based on extrusion, injection molding, mechanical mixing and melt-mixing methods. Each preparation method gave different characteristics to the final materials. Some studies [36-39,44-45] demonstrated that an increase in wax content when blended to polyethylenes resulted in a decrease in the onset temperature of melting as well as the melting and crystallization temperatures of the blends. This indicated that the polymer exhibited more pronounced plasticization when mixed with wax. The authors attributed this to a non-uniform distribution of short chain branching density along the LLDPE main chain, which can interact with the wax structure. The specific enthalpy values of melting were shown to increase with increasing wax content indicating an increase in the crystallinity of the blends. Several reasons were given for this: (i) the higher melting enthalpy of the wax compared to that of the pure polymer; (ii) partial

miscibility of the polyethylene and wax at low wax content; (iii) the incorporation of short and linear wax chains into the crystal lattice during crystallization.

Two studies [39-40] showed that for LDPE mixed with two different hard waxes, the enthalpy values increased with increasing wax content. However, for an oxidized paraffin wax and medium-soft paraffin wax containing blends, different behaviour was observed. The melting enthalpies of these blends were found to decrease with an increase in wax content. Thermal properties such as melting temperatures (T_m), onset temperatures of melting ($T_{o,m}$) and melting enthalpies (ΔH_m) are also strongly affected by the use of crosslinking agents [36-37,46]. Generally there was a decrease in melting temperatures and enthalpies with an increase in the content of the cross-linking agent, probably because of a combination of polymer crosslinking and grafting of the wax onto the polymer chains.

Various studies [31,38,42-43,45] investigated the morphology of polyolefin/wax blends using techniques such as scanning electron microscopy (SEM) and differential scanning calorimetry (DSC). Limited studies were conducted on this system using atomic force microscopy (AFM). The wax dispersion in the matrix strongly depends on (i) the percentage of wax added to the polymer and (ii) the morphology of the polymer. Increasing the wax content caused an increase in phase separation. The results obtained also showed that the wax loading affected the surface morphology. The roughness increased due to a restriction of the free flow of the resin and an increase in contact area. It also increased with the degree of branching because flow decreased because of long chain branch networks. Generally, all the polyethylene/wax blends showed a homogeneous surface and good dispersion of the wax at low wax content (10 and 20%), although the blends were not uniform. At higher wax content the miscibility of the wax with the polymer matrix became poor (two distinct phases) and agglomeration of the wax was observed. The clear phase separation supported the notion that the PEs and paraffin were not totally miscible. According to a paper by Al Madeed *et al.* [45] LDPE showed less phase separation with the wax than with HDPE and LLDPE. The results were interpreted by arguing that LDPE is composed of a network of short and long chain branches, and it has larger open amorphous areas due to its low crystallinity. High density polyethylene (HDPE) was found to have lower miscibility with wax than LDPE and LLDPE. Due to the influence of miscibility on the thermal behaviour of the

paraffin, it was suggested [25-28,42] that HDPE should be used in PE/paraffin form-stable PCM to maintain the energy saving behaviour of paraffin in building applications for reducing interior temperature fluctuations.

1.2.2 Polymer fractionation

Polymers need to be fractionated to ensure that the properties are tailored for a particular application. Polymer fractionation is a process of separating polymer fractions according to specific characteristics of their microstructures. The most important techniques used for this are temperature rising elution fractionation (TREF), crystallization analysis fractionation (CRYSTAF), and thermal fractionation. TREF is a technique that separates the polymer fractions, at successively rising temperatures, of a material that has been previously crystallized from solution on an inert support during very slow cooling or multiple steps [47-49]. Such slow crystallization from solution favours molecular segregation by short chain branching content and distribution, with a limited influence of molecular weight. Chains with fewer branches precipitate at higher temperatures and those with higher comonomer content do so at lower temperatures. Even though the technique has been successively applied, its implementation is not easy, because it can be expensive and measurement times can be very long. In order to improve the analysis time, a related technique called CRYSTAF was developed [50-51]. The main difference between analytical TREF and CRYSTAF is that, while TREF monitors the concentration of the polymer in solution during the elution step, that takes place after the polymer has been previously crystallized, CRYSTAF monitors the concentration of the polymer in solution during the crystallization stage. Therefore, analysis times in CRYSTAF are shorter but still significant and both TREF and CRYSTAF employ solvents and involve costly equipment [23].

Several researchers [23,32,34-35] reported that in order to improve implementation, rapid characterization and for less costly equipment, thermal fractionation techniques can be used. Thermal fractionation methods have been developed to provide qualitative information on the content and distribution of short chain branches (SCBs) of the polymer under study with only a conventional DSC instrument. The term 'thermal fractionation' refers to DSC based techniques

that are able to 'fractionate' the polymer starting from the melt (even though adding a solvent is also possible) by carefully designing a temperature programme applied to the sample. It is based on the molecular fractionation capacity of polymer chains when they are held at a temperature where only part of the chains or chain sequences respond by isothermal crystallization and/or annealing. Such a thermal treatment creates thermal fractions whose nature depends on the specific temperature and thermal history applied to the material. There are two thermal fractionation techniques: step crystallization (SC) and successive self-nucleation and annealing (SSA) [23]. SC is a technique that employs the step crystallization from solution that is applied in some TREF techniques but solvent-free experimental protocols are usually used. The disadvantage of using SC is that it is time consuming and the resolution is not so good. To improve analysis time and resolution, SSA was developed [34-35]. SSA is based on the sequential application of self-nucleation and annealing steps to a polymer sample where each cycle is similar to those reported elsewhere in the literature [23]. The SSA technique is an effective method of characterizing the fine structure of semi-crystalline polymers that undergo molecular segregation when cooled from the melt and therefore can be thermally fractionated. It is particularly useful to fractionatepolymers that incorporate defects in their linear crystallizable chains (e.g., branches, comonomers, crosslinks, stereo-defects or any other molecular defect that cannot enterthe crystalline lattice).

Previous studies [23,52] reported that before applying SSA thermal fractionation, a self-nucleation (SN) thermal protocol [52] must be applied to determine the ideal self-nucleation temperature (T_s), which is the temperature that causes maximum SN without any annealing. This temperature is in *Domain II*, where self-nucleation occurs. If no changes in T_m (melting temperature) and T_c (crystallization temperature) values are detected after the SN protocol, the polymer is said to be in *Domain I*, where complete melting of the crystallites occurs. When the T_s temperature is high enough to melt the sample almost completely, but low enough to leave some self-nuclei that provoke nucleation during the subsequent cooling from T_s, the polymer is said to be in *Domain II*. When the T_s temperature is too low, only part of the crystals will melt. The unmolten crystals will be annealed during the five minutes at T_s, while the rest of the polymer will be self-nucleated during the subsequent cooling from T_s. The polymer is said to be in *Domain III* where self-nucleation and annealing occurs.

Several researchers [23,32,48,53] investigated the characterization of LLDPE by an SN thermal protocol. It is important to note that for different LLDPE samples, SN must be applied to each sample, since the location of self-nucleation domains vary from sample to sample. In previous studies of specific LLDPE samples, 123 °C was found to be the minimum temperature of *Domain II*, and therefore the first T_s temperature for the SSA thermal protocol. This is the maximum temperature that induces self-nucleation without any annealing. After thermal conditioning by SSA, a final DSC heating run revealed the distribution of melting temperatures induced by the SSA thermal treatment as a result of the heterogeneous nature of the chain structure of the analysed polymer. The final distribution of melting points depends on how close to equilibrium the generated crystals are, since chain folding occurs beyond a critical number of linear and uninterrupted chain sequences and will most probably be present in a great number of high-melting point thermal fractions. The melting behaviour of copolymers suggests that the melting peaks come from different crystal populations that are formed from chains with different crystallizable lengths, after being annealed for a certain time. The series of multiple melting peaks are a reflection of multiple mean lamellar thicknesses. The highest melting point fraction corresponds to the fusion of the thickest lamellae that are formed by the longest uninterrupted chain sequence. The shorter sequences crystallize in thinner lamellae that melt at lower temperatures. The melting curve of LLDPE was shown to have 13 melting peaks after a 14 step SSA protocol was applied. This behaviour illustrated the capability of the technique to induce thermal fractionation as a result of the broad short chain branching distribution of the copolymer. Each endothermic peak was said to be proportional to the amount of crystals with the same stability.

A number of studies [54-60] were conducted on the effect of thermal fractionation conditions such as the number of isothermal steps, fractionation window and annealing time, on the melting behaviour of LLDPE by SC thermal fractionation. The best SC thermal fractionation conditions for the LLDPE sample, producing sharp multiple melting peak curves with good profiles, included five isothermals, fractionation windows of 10 °C, and annealing times of 80 min. However, these are incredibly long times. With SSA, thermal fractionation times are shorter and the resolution is better than that of SC. The number of melting peaks produced by SSA depends

on how broad the melting temperature range is, and also on the selection of the thermal fractionation conditions.

A large amount of work was done on the thermal fractionation of polymers, especially polyethylenes [32,39,48,54,61-63]. Generally the authors investigated co-crystallization and phase segregation in polyethylene blends. The factors affecting co-crystallization are similarity in molecular structures, crystalline lattice structures, crystallization rates, and miscibility in the melt. The first and second conditions are requirements for thermodynamic stability of crystals, while the third and fourth conditions are for kinetic accessibility to form crystals. It was also mentioned that even if the similarity in the structures ensures the co-crystallization in the equilibrium state, immiscibility and difference in the crystallization rate between the component polymers prevent the crystallization at the same time and at the same place. Co-crystallization can also occur if there is an overlap between the melting temperatures of the pure components. It was reported [32,61-63] that for HDPE/LDPE and LLDPE/LDPE blends, phase segregation was observed when cooled slowly from the melt. However, contradictory results were reported [61] for LLDPE/HDPE and LLDPE/LDPE blends, where co-crystallization in the blends was observed. This behaviour was explained as follows: the most linear fractions of both polymers were able to co-crystallize since the interaction between LLDPE and HDPE or LDPE molecules resulted in a new fraction forming with an intermediate lamellar thickness. Therefore crystal separation and co-crystallization are dependent on the selected PEs, the crystallization conditions, molecular weight, the amount of SCBs and the type of catalyst used.

A few studies investigated the possibility and extent of co-crystallization of different waxes with different polyethylenes using CRYSTAF and SC thermal fractionation [39,64]. According to these studies the blends of LDPE and LLDPE with respectively an oxidised and an unoxidised hard wax showed co-crystallization due to the overlap between the melting temperatures of the pure components. This observation was evident from the SC thermal fractionation curves. However, the blends of HDPE with these waxes did not show co-crystallization. It was also shown that in PE/wax blends, the lamellar thickness of the samples decreased with an increase in wax content due to the dilution effect of wax. There were no reports on investigating the

interaction of wax with different PEs using SSA thermal fractionation, in order to ascertain if wax can co-crystallize or act as a diluent.

There were also studies on paraffin wax fractionation by state-of-the-art modern crystallization processes (short path distillation (SPD) and static crystallization) and supercritical fluid fractionation [65-66]. SPD is commonly used to separate or recover low volatility or heat labile components. It is typically used to fractionate waxes since an SPD unit can operate at very low pressures, much lower than is possible in standard vacuum distillation units. It is necessary to operate at low pressures to prevent high temperatures that may lead to thermal degradation of the wax. SPD seems to be a cheaper fractionation process for light paraffin wax. The advantages of wax fractionation by static crystallization, compared to wax sweating and solvent based deoiling processes, are: (i) low energy consumption, (ii) high yield, (iii) no residual solvent in product, and (iv) preferential removal of iso-paraffins and aromatics. Due to these advantages, static crystallization is chosen as the preferred state-of-the-art modern crystallization process. Supercritical fluid extraction (SFE) is a fractionation process used for waxes with a significant amount of material heavier than n-C45, and is preferred because of its low environmental impact. SFE is a process separating one component from another using supercritical fluid such as CO_2 as the extracting solvent.

1.2.3 Polymer crystallization

Polymer crystallization has been a fascinating topic in the last decades since the discovery of the chain folded lamellar crystal structure in 1957 [67]. The properties of a semicrystalline polymer – thermodynamic, spectroscopic, physical and mechanical – depend on the details of crystal structure and morphology that develop from the melt. Understanding the crystallization mechanism is a key to understanding these properties. A previous report [68] mentioned that the overall crystallization of semi-crystalline polymers involves two main processes: primary and secondary crystallization. Primary crystallization relates to the macroscopic development of crystallinity as a result of two consecutive microscopic mechanisms, primary and secondary nucleation. For polymer crystallization to start, primary nucleation first needs to occur. Primary nucleation is the process by which a stable crystalline nucleus is formed in the melt state by

homogeneous or heterogeneous nucleation. In homogeneous nucleation nuclei formation occurs spontaneously as a result of supercooling. In heterogeneous nucleation, a secondary phase is required (it may be a foreign particle or the surface of the vessel) for nucleation to occur. Another way of categorizing primary nucleation is on the basis of the time dependent effects at any temperature. If nucleation is such that all the nuclei start forming spontaneously at approximately the same time, then the nucleation is referred to as athermal nucleation. One aspect of such nucleation is that it leads to spherulites of roughly the same size during isothermal crystallization. If the nucleation on the other hand is such that new nuclei form throughout different times at a particular temperature, different spherulitic (crystal) sizes are obtained and the nucleation is referred to as thermal nucleation. Homogeneous nucleation is almost always of the thermal type, whereas heterogeneous nucleation may be thermal or athermal. Crystallization does not generally stop with the growth of crystals, but a process called 'secondary nucleation' occurs whereby crystallization continues on the growth surface by the introduction of more polymer molecules. It produces an increase in crystallinity.

Crystallization studies are generally conducted under isothermal conditions, since the use of a constant temperature permits easier theoretical treatment and limits the thermal gradients within the samples. Analysis of the overall crystallization rate under isothermal conditions is generally accomplished with the use of the Avrami equation [11-13]. This is the reason for our use of this model in describing our experimental data in the present manuscript. However, the Avrami model has some drawbacks. It holds well for primary crystallization only, and it provides a good fit of the experimental data at least in the conversion range up to the end of primary crystallization, i.e., up to the impingement of spherulites at approximately 50% conversion to the solid semi-crystalline state [9,69]. The Lauritzen-Hoffman model (L-H) [14] has been developed to describe secondary nucleation which is the growth process and therefore occurs during primary crystallization. The crystallization kinetics analysis according to the Lauritzen and Hoffman Theory (L-H) can also be extended to overall crystallization (including both primary and secondary nucleation) by fitting rate data obtained by DSC as the inverse of the half-crystallization time $1/\tau_{50\%}(T)$ as a function of supercooling ΔT.

A number of reports were published on the crystallization behaviour of polymers, polymer blends and polymer composites/nanocomposites [3,69-80]. Samples crystallized at higher temperatures required longer times to complete the crystallization process, which is the result of slower crystallization rates. The slow rate at these temperatures is the result of the high mobility of the chains, which means they detach from lamellae almost as fast as they attach to lamellae at the growth front. However, slower crystallization rates in blends and composites may be the result of immobilization of polymer chains by the other component(s) in the blend/composite. In blends the slow crystallization rate is due to the fact that crystallization occurs before phase separation and starts from a relatively homogenous liquid state. The slower crystallization rate is therefore mainly caused by a dilution effect. In fact, in miscible blends, the crystallization rate depression depends on the equilibrium melting point. The diluent can reduce the viscosity of the polymer, thus reducing the crystallization rate of the polymer and also changing the rate of crystallization of the other components in the blend. If the viscosity is reduced, the polymer chains are more mobile and therefore they detach from the growth front almost as fast as they attach to the front, thus reducing the crystallization rate.

The Avrami model [11-13] was used to check if it can predict the isothermal crystallization. For most crystallizing polymers, the value of the Avrami exponent, n, was found to vary between 1 and 4, corresponding to various growth forms from rod-like to spherical [69,71,76-77]. It was reported [71,80] that the value of n sometimes decreased with the addition of nucleating agents or diluents, indicating that the crystallization mode and therefore the overall nature of the nucleation and growth process in the system changed. At higher diluent concentrations, the diffusion process of the diluent chains from the growth front was the dominant effect. The non-crystalline diluent chains at the crystal growth front can prevent the dimensional crystal growth of the polymer, which induces a decrease in the Avrami exponent. However, other reports [76-77] showed that the value of the Avrami exponent remained constant for all the blends used in these studies, indicating that the crystallization mechanism has not changed and the geometric dimension of crystal growth was not affected.

1.2.4 Wax crystallization

Waxes are highly crystalline materials with a large melting enthalpy. Due to its high crystallinity, it can be regarded as an efficient PCM because of its ability to store and release large amounts of energy through melting and solidifying at certain temperatures [25-31].

It was reported [81-82] that the remediation of wax deposition is costly and needs much effort. One of the methods that are used to manage this problem is the use of inhibitors. Inhibitors are polymeric compounds that are constituted of one hydrocarbon section and one polar group. The hydrocarbon section connects inhibitors and paraffins, but the polar section interferes with the crystallization process and changes the morphology. These polymers absorb on the surface of paraffin crystals or enter in the crystal structures, so they reduce nucleation and growth rates, and finally the amount of deposit.

Some authors studied the morphology of wax crystals and its changes with the addition of copolymers [81-86]. Their results show that wax crystals in the absence of polymer were plate-like crystals that changed to spherulites after a long time. Addition of a small amount of copolymer changed the morphology of the wax crystals from both plate-like and spherulitic to a lot of crystals that are smaller in size. The reason for such an occurrence is because the copolymer can incorporate into the growing crystals and prevent the growth of the crystals, interfering with the crystallization process. The lack of crystal growth and inability to connect and form crystal networks cause the formation of a weaker structure, so the removal of the wax deposit is easier.

1.2.5 Polymer diluent mixtures (equilibrium melting)

For a true reflection of the microstructure and morphology of a blend, the equilibrium melting temperature ($T_m°$) needs to be determined. This parameter is the reference temperature from which the driving force for crystallization is measured [77,87]. $T_m°$ is usually determined by DSC. The Hoffman–Weeks equation predicts a linear relation between T_m and T_c [15], and $T_m°$ is obtained from the intersection of this line with the line given by $T_m = T_c$, implying the

extrapolation to infinite thickness of lamellae. There is consensus that the equilibrium melting temperature of 100% linear HDPE is approximately 140-145 °C. This is the equilibrium melting point of an infinite crystal of 100% linear PE. When branches are introduced this value decreases. Both experimental and theoretical investigations showed that the equilibrium melting temperature decreases as the number of branches (or comonomer content) increases. It was shown [73,80] that the equilibrium melting temperature of the polymer in polymer-diluent blends is lower than that of the pure polymer. Several reasons were given for this: (i) the chemical potential of a polymer decreased by the addition of a miscible diluent, (ii) the thermodynamic stability of polymer crystallization was influenced by the content of side-branches, and (iii) the mean lamellar thickness is decreased during the isothermal crystallization.

1.3 The aims and objectives of this study are:

- To study the influence of the presence of wax on the melting and crystallization behaviour of LLDPE for non-annealed samples.
- To study the influence of the presence of wax on the melting and crystallization behaviour of LLDPE for annealed samples.
- To investigate whether the SSA thermal fractionation technique can fractionate LLDPE and/or wax samples.
- To investigate the interaction of wax with LLDPE in order to ascertain if it can co-crystallize with LLDPE or act as a diluent.
- To investigate how the fraction distribution of LLDPE change with the presence of molten wax.
- To kinetically study the influence of the presence of wax on the overall crystallization rate, mechanism of nucleation and crystal growth for the LLDPE crystals.
- To kinetically study the influence of the presence of LLDPE on the overall crystallization rate, mechanism of nucleation and crystal growth for the wax crystals.
- To evaluate the effectiveness of wax as a phase change material when blended with LLDPE.

1.4 Thesis outline

The outline of this thesis is as follows:

- Chapter 1: General introduction and literature review
- Chapter 2: Materials and methods
- Chapter 3: Results and discussion
- Chapter 4: Conclusions

1.5 References

[1] P. Supaphol, J.E. Spruiell. Isothermal melt- and cold-crystallization kinetics and subsequent melting behaviour in syndiotactic polypropylene: A differential scanning calorimetry study. Polymer 2001; 42:699-712.
DOI: 10.1016/S0032-3861(00)00399-2

[2] C.C. Han, H. Kammer, S.L. Har, T. Winie. Morphologies and kinetics of isothermal crystallization for green polymer blends comprising PHBV and ENR: Influence of rubbery phase. International Journal of Pharmacy and Pharmaceutical Sciences 2011; 3:1-6.
DOI: 10.1002/app.33384

[3] X.F. Lu, J.N. Hay. Isothermal crystallization kinetics and melting behaviour of poly(ethylene terephthalate). Polymer 2001; 42:9423-9431.
DOI: 10.1016/S0032-3861(01)00502-X

[4] R.L. Mazur, E.C. Botelho, M.C. Rezende, M.L. Costa. Evaluation of crystallization kinetics of poly (ether-ketone-ketone) and poly (ether-ether-ketone) by DSC. Journal of Aerospace Technology and Management 2010; 2:155-162.
DOI: 10.5028/jatm.2010.02026310

[5] G. Lamberti, C. Naddeo. Some issues on polymer crystallization kinetics studied by DSC non isothermal tests. Polymer Bulletin 2006; 56:591-598.
DOI: 10.1007/S00289-006-0518-2

[6] K.P. Pramoda, T.S. Chung. Crystallization and melting behavior of zenite thermotropic liquid crystalline polymers. Polymer Engineering & Science 2002; 42:439-451.
DOI: 10.1002/pen.10961

[7] S.L. Everton, A.A. Cabral. Determining the kinetic parameters for isothermal crystallization in a lithium disilicate (Ls_2) glass by OM and DSC. Journal of the American Ceramic Society 2014; 97:157-162.
DOI: 10.1111/jace.12638

[8] S. Song, P. Wu, M. Ye, J. Feng, Y. Yang.Effect of small amount of ultra molecular weight component on the crystallization behaviors of bimodal high density polyethylene. Polymer 2008; 49:2964-2973.
DOI: 10.1016/j.polymer.2008.04.050

[9] A.T. Lorenzo, M.L. Arnal, J. Albuerne, A.J. Müller. DSC isothermal polymer crystallization kinetics measurements and the use of the Avrami equation to fit the data: Guidelines to avoid common problems. Polymer Testing 2007; 26:222-231.
DOI: 10.1016/j.polymertesting.2006.10.005

[10] P.U. Dhanvijay, V.V. Shertukde. Review: Crystallization of biodegradable polymers. Polymer-Plastics Technology and Engineering 2011; 50:1289-1304.
DOI: 10.1080/03602559.2010.543744

[11] M. Avrami. Kinetics of phase change I: General theory. Journal of Chemical Physics 1939; 7:1103-1112.
DOI: 10.1063/1.1750380

[12] M. Avrami. Kinetics of phase change II: Transformation-time relations for random distribution of nuclei. Journal of Chemical Physics 1940; 8:212-224.
DOI: 10.1063/1.1750631

[13] M. Avrami. Granulation, phase change, and microstructure kinetics of phase change III. Journal of Chemical Physics 1941; 9:177-184.
DOI: 10.1063/1.1750872

[14] M. Trujillo, M.L. Arnal, A.J. Müller, M.A. Mujica, C. Urbina de Navarro, R.B. Caribay, P. Dubois. Supernucleation and crystallization regime change provoked by MWNT addition to poly(ε-caprolactone). Polymer 2012; 53:832-841.
DOI: 10.1016/j.polymer.2011.12.028. ISSN: 0032-3861

[15] J.D. Hoffman, J.J. Weeks. Melting process and the equilibrium melting temperature of polychlorotrifluoroethylene.Journal of Research of the National Bureau of Standards-A. Physics and Chemistry 1962; 66A:13-28.
DOI: 10.6028/jres.066A.003

[16] A.M. Díez-Pascual, M. Naffakh, C. Marco, G. Ellis, M.A. Gómez-Fatou. High-performance nanocomposites based on polyetherketones. Progress in Materials Science 2012; 57:1106-1190.
DOI: 10.1016/j.pmatsci.2012.03.003

[17] W.Y. Zhou, B. Duan, M. Wang, W.L. Cheung. Isothermal and non-isothermal crystallization kinetics of poly(L-lactide)/carbonated hydroxyapatite nanocomposite microspheres. Nanotechnology and Nanomaterials 2011; 231-260.
DOI: 10.5772/14715

[18] N.L.A. McFerran, C.G. Armstrong, T. McNally. Nonisothermal and isothermal crystallization kinetics of nylon-12. Journal of Applied Polymer Science 2008; 110:1043-1058.
DOI: 10.1002/app.28696

[19] A. Jeziorny. Parameters characterizing the kinetics of the non-isothermal crystallization of poly(ethylene terephthalate) determined by DSC. Polymer 1978; 19:1142-1144.
DOI: 10.1016/0032-3861(78)90060-5

[20] J. Song, M. Ren, Q. Chen, X. Sun, H. Zhang, C. Song, H. Zhang, Z. Mo. Isothermal and nonisothermal crystallization kinetics of irradiated nylon 1212. Journal of Polymer Science Part B: Polymer Physics 2005; 43:2326-2333.
DOI: 10.1002/polb.20447

[21] T. Liu, Z. Mo, S. Wang. Nonisothermal melt and cold crystallization kinetics of poly(aryl ether ether ketone ketone). Polymer Engineering and Science 1997; 37:568-571.
DOI: 10.1002/pen.11700

[22] J.B. Song, Q.Y. Chen, M.Q. Ren, X.H. Sun, H.L. Zhang, H.F. Zhang, Z. Mo. Effect of partial melting on the crystallization kinetics of nylon-1212. Journal of Polymer Science Part B: Polymer Physics 2005; 43:3222-3230.
DOI: 10.1002/polb.20525

[23] A.J. Müller, M.L. Arnal. Thermal fractionation of polymers. Progress in Polymer Science 2005; 30:559-603.
DOI: 10.1016/j.progpolymsci.2005.03.001

[24] C. Koning, M. van Duin, C. Pagnoulle, R. Jerome. Strategies for compatibilization of polymer blends. Progress in Polymer Science 1998; 23:707-757.
DOI: 10.1016/S0079-6700(97)00054-3

[25] A. Pasupathy, R. Velraj, R.V. Seeniraj. Phase change material-based building architecture for thermal management in residential and commercial establishments. Renewable and Sustainable Energy Reviews 2008; 12:39-64.
DOI: 10.1016/j.rser.2006.05.010

[26] A.M. Khudhair, M.M. Farid. A review on energy conservation in building applications with thermal storage by latent heat using phase change materials. Energy Conservation and Management 2004; 45:263-275.
DOI: 10.1016/S0196-8904(03)00131-6

[27] W. Wang, X. Yang, Y. Fang, J. Ding. Preparation and performance of form-stable polyethylene glycol/silicon dioxide composites as solid-liquid phase change materials. Applied Energy 2009; 86:170-174.
DOI: 10.1016/j.apenergy.2007.12.003

[28] F. Kuznik, D. David, K. Johannes, J. Roux. A review on phase change materials integrated in building walls. Renewable and Sustainable Energy Reviews 2011; 15:379-391.
DOI: 10.1016/j.rser.2010.08.019

[29] C.H. Lee, H.K. Choi. Crystalline morphology in high-density polyethylene/paraffin blend for thermal energy storage. Polymer Composites 1998; 19:704-708.
DOI: 10.1002/pc.10143

[30] Y. Cai, Q. Wei, F. Huang, S. Lin, F. Chen, W. Gao. Thermal stability, latent heat and flame retardant properties of the thermal energy storage phase change materials based on paraffin/high density polyethylene composites. Renewable Energy 2009; 34:2117-2123.
DOI: 10.1016/j.renene.2009.01.017

[31] M.E. Mngomezulu, A.S. Luyt, I. Krupa. Structure and properties of phase change materials based on HDPE, soft Fischer-Tropsh paraffin wax, and wood flour. Journal of Applied Polymer Science 2010; 118:1541-1551.
DOI: 10.1002/app.3252

[32] M.L. Arnal, J.J. Sanchez, A.J. Müller. Miscibility of linear and branched polyethylene blends by thermal fractionation: Use of the successive self-nucleation and annealing (SSA) technique. Polymer 2001; 42:6877-6890.
DOI: 1016/s0032-3861(01)00177-X

[33] C. Piel, P. Starck, J.V. Seppälä, W. Kaminsky. Thermal and mechanical analysis of metallocene-catalyzed ethene–α-olefin copolymers: The influence of the length and number of the crystallizing side chains. Journal of Polymer Science: Part A: Polymer Chemistry 2006; 44:1600-1612.
DOI: 10.1002/pola.21265

[34] A.J. Müller, Z.H. Hernández, M.L. Arnal, J.J. Sánchez. Successive self-nucleation annealing (SSA): A novel technique to study molecular segregation during crystallization. Polymer Bulletin 1997; 39:465-472.
DOI: 10.1007/s002890050174

[35] A.J. Müller, A.T. Lorenzo, M.L. Arnal. Recent advances and applications of "successive self-nucleation and annealing" (SSA) high speed thermal fractionation. Macromolecular Symposia 2009; 277:207-214.
DOI: 10.1002/masy.200950325

[36] I. Krupa, A.S. Luyt. Thermal properties of uncross-linked and cross-linked LLDPE/wax blends. Polymer Degradation and Stability 2000; 70:111-117.
DOI: 10.1016/S0141-3910(00)00097-5

[37] S.P. Hlangothi, I. Krupa, V. Djoković, A.S. Luyt. Thermal and mechanical properties of cross-linked and uncross-linked linear low-density polyethylene-wax blends. Polymer Degradation and Stability 2003; 79:53-59.
DOI: 10.1016/S0141-3910(02)00238-0

[38] I. Krupa, A.S. Luyt. Thermal and mechanical properties of extruded LLDPE/wax blends. Polymer Degradation and Stability 2001; 73:157-161.
DOI: 10.1016/S0141-3910(01)00082-9

[39] M.J. Hato, A.S. Luyt. Thermal fractionation and properties of different polyethylene/wax blends. Journal of Applied Polymer Science 2007; 104:2225-2236.
DOI: 10.1002/app.25494

[40] H.S. Mpanza, A.S. Luyt. Comparison of different waxes as processing agents for low density polyethylene. Polymer Testing 2006; 25:436-442.
DOI: 10.1016/j.polymertesting.2006.01.008

[41] I. Krupa, A.S. Luyt. Physical properties of blends of LLDPE and an oxidized paraffin wax. Polymer 2001; 42:7285-7289.
DOI: 10.1016/S0032-3861(01)00172-0

[42] F. Chen, M.P. Wolcott. Miscibility studies of paraffin/polyethylene blends as form-stable phase change materials. European Polymer Journal 2014; 52:44-52.
DOI: 10.1016/j.eurpolymj.2013.09.027

[43] A. Sari. Form-stable paraffin/high density polyethylene composites as solid–liquid phase change material for thermal energy storage: Preparation and thermal properties. Energy Conversion and Management 2004; 45:2033-2042.
DOI: 10.1016/j.enconman.2003.10.022

[44] M.E. Sotomayor, I. Krupa, A. Várez, B. Levenfeld. Thermal and mechanical characterization of injection moulded high density polyethylene/paraffin wax blends as phase change materials. Renewable Energy 2014; 68:140-145.
DOI: 10.1016/j.renene.2014.01.036

[45] M.A. Al Maadeed, S. Labidi, I. Krupa, M. Ouederni. Effect of waste wax and chain structure on the mechanical and physical properties of polyethylene. Arabian Journal of Chemistry 2014 (published online).
DOI: 10.1016/j.arabjc.2014.01.006

[46] T.N. Mtshali, I. Krupa, A.S. Luyt. The effect of cross-linking on the thermal properties of LDPE/wax blends. Thermochimica Acta 2001; 380:47-54.
DOI: 10.1016/S0040-6031(01)00636-0

[47] L. Wild. Temperature rising elution fractionation.Advances in Polymer Science 1991; 98:1-47.
DOI: 10.1007/3-540-53135-1_4

[48] J. Kong, X. Fan, Y. Xie, W. Qiao. Study on molecular chain heterogeneity of linear low-density polyethylene by cross-fractionation of temperature rising elution fractionation and successive self-nucleation/annealing thermal fractionation. Journal of Applied Polymer Science 2004; 94:1710-1718.
DOI: 10.1002/app.21084

[49] M. Zhang, D.T. Lynch, S.E. Wanke. Effect of molecular structure distribution on melting and crystallization behavior of 1-butene/ethylene copolymers. Polymer 2001; 42:3067-3075.
DOI: 10.1016/S0032-3861(00)00667-4

[50] B. Monrabal. Crystallization analysis fractionation: A new technique for the analysis of branching distribution in polyolefins. Journal of Applied Polymer Science 1994; 52:491-499.
DOI: 10.1002/app.1994.070520403

[51] H. Pasch, R. Brüll, U. Wahner, B. Monrabal. Analysis of polyolefin blends by crystallization analysis fractionation. Macromolecular Materials and Engineering 2000; 279:46-51.
DOI: 10.1002/1439-2054(20000601)279:1<46::AID-MAME46>3.0.CO;2-1

[52] B. Fillon, J.C. Wittmann, B. Lotz, A. Thierry.Self-nucleation and recrystallization of isotactic polypropylene (α phase) investigated by differential scanning calorimetry. Journal of Polymer Science Part B: Polymer Physics 1993; 31:1383-1393.
DOI: 10.1002/polb.1993.090311013

[53] M.L. Arnal, V. Balsamo, G. Ronca, A. Sánchez, A.J. Müller, E. Cañizales, C. Urbina de Navarro. Applications of successive self-nucleation and annealing (SSA) to polymer characterization. Journal of Thermal Analysis and Calorimetry 2000; 59:451-470.
DOI: 10.1023/A:1010137408023

[54] M. Camargo, M.M.C. Forte, C.R. Wolf. Linear low density polyethylene thermal fractionation by DSC technique. International Journal of Polymer Analysis and Characterization 2008; 13:49-65.
DOI: 10.1080/10236660701802593

[55] B. Wolf, S. Kenig, J. Klopstock, J. Militz. Thermal fractionation and identification of low-density polyethylenes. Journal of Applied Polymer Science 1996; 62:1339-1345.

DOI: 10.1002/(SICI)1097-4628(19961128)62:9<1339::AID-APP4>3.0.CO;2-I

[56] P. Starck. Studies of the comonomer distributions in LDPE using temperature rising elution fractionation and stepwise crystallization by DSC. Polymer International 1996; 40:111-122.
DOI: 10.1002/(SICI)1097-0126(199606)40:2<111::AID-PI541>3.0.CO;2-N

[57] J. Varga, J. Menezel, A. Solti. Memory effect of low-density polyethylene crystallized in a stepwise manner. Journal of Thermal Analysis 1976; 10:433-440.
DOI: 10.1007/BF01909895

[58] J. Varga, J. Menezel, A. Solti. The melting of high-pressure polyethylene subjected to stepwise heat treatment. Journal of Thermal Analysis 1979; 17:333-342.
DOI: 10.1007/BF01914024

[59] F. Chen, R.A. Shanks, G. Amarasinghe. Crystallization of single-site polyethylene blends investigated by thermal fractionation techniques. Polymer International 2004; 53:1795-1805.
DOI: 10.1016/S0032-3861(00)00859-4

[60] R.A. Shanks, G. Amarasinghe. Crystallization of blends of LLDPE with branched VLDPE. Polymer 2000; 41:4579-4587.
DOI: 10.1016/S0032-3861(99)00678-3

[61] X. Sun, G. Shen, H. Shen, B. Xie, W. Yang, M. Yang. Co-crystallization of blends of high-density polyethylene with linear low-density polyethylene: An investigation with successive self-nucleation and annealing (SSA) technique. Journal of Macromolecular Science, Part B: Physics 2013; 52:1372-1387.
DOI: 10.1080/00222348.2013.768504

[62] R.L. Morgan, M.J. Hill, P.J. Barham. Morphology, melting behavior and co-crystallization in polyethylene blends: The effect of cooling rate on two homogeneously mixed blends. Polymer 1999; 40:337-348.
DOI: 10.1016/S0032-3861(98)00193-1

[63] M.L. Arnal, E. Cañizales, A.J. Müller. Thermal and morphological evaluation of very low density polyethylene/high density polyethylene blends. Polymer Engineering and Science 2002; 42:2048-2063.
DOI: 10.1002/pen.11096

[64] A.S. Luyt, R. Brüll. Investigation of polyethylene-wax blends by CRYSTAF and SEC-FTIR. Polymer Bulletin 2004; 52:177-183.
DOI: 10.1007/s00289-004-0274-0

[65] J.C. Crause, I. Nieuwoudt. Paraffin wax fractionation: State of the art vs. supercritical fluidfractionation. The Journal of Supercritical Fluids 2003; 27:39-54.
DOI: 10.1016/S0896-8446(02)00185-7

[66] G.N. Sapkale, S.M. Patil, U.S. Surwase, P.K. Bhatbhage. Supercritical fluid extraction. International Journal of Chemical Sciences 2010; 8:729-743 (published online).

[67] A. Keller. A note on single crystals in polymers: Evidence for a folded chain configuration. Philosophical Magazine 1957; 2:1171-1175.
DOI: 10.1080/14786435708242746

[68] U.W. Gedde. Polymer Chemistry. Chapman & Hall, London (1985).

[69] J.D. Menczel, R.B. Prime. Thermal Analysis of Polymers. Fundamentals and Applications. John Wiley & Sons, New Jersey (2009).

[70] G.Z. Papageorgiou, D.S. Achilias, D.N. Bikiaris, G.P. Karayannidis. Crystallization and nucleation activity of filler in polypropylene/surface-treated SiO_2 nanocomposites. ThermochimicaActa 2005; 427:117-128.
DOI: 10.1016/j.tca.2004.09.001

[71] X.L. Jiang, S.J. Luo, K. Sun, X.D. Chen. Effect of nucleating agents on crystallization kinetics of PET. eXPRESS Polymer Letters 2007; 1:245-251.
DOI: 10.3144/expresspolymlett.2007.37

[72] A. Choudhury. Isothermal crystallization and mechanical behavior of ionomer treated sisal/HDPE composites. Materials Science and Engineering A 2008; 491:492-500.
DOI: 10.1016/j.msea.2008.03.011

[73] M. Hayatifar, L. Bernazzani, A.M.R. Galletti. Thermal and structural investigation of random ethylene/1-hexene copolymers with high 1-hexene content. Journal of Thermal Analysis and Calorimetry 2014; 115:1711-1718.
DOI: 10.1007/s10973-013-3445-0

[74] R. Ou, Y. Xie, C. Guo, Q. Wang. Isothermal crystallization kinetics of Kevlar fiber-reinforced wood floor/high-density polyethylene composites. Journal of Applied Polymer Science 2012; 126:E2-E9.

DOI: 10.1002/app.36425

[75] C. Liu, H. Qiu, C. Liu, J. Zhang. Study on crystal process and isothermal crystallization kinetics of UHMWPE/CA-MMT composites. Polymer Composites 2012; 33:1987-1992. DOI: 10.1002/pc.22339

[76] Z. Qiu, T. Ikehara, T. Nishi. Miscibility and crystallization of poly(ethylene oxide) and poly(ε-caprolactone) blends. Polymer 2003; 44:3101-3106. DOI: 10.1016/S0032-3861(03)00167-8

[77] J.W. Huang, Y.L. Wen, C.C. Kang, M.Y. Yeh, S.B. Wen. Crystallization of poly(butylene terephthalate)/poly(ethylene octane) blends: Isothermal crystallization. Journal of Applied Polymer Science 2008; 109:3070-3079. DOI: 10.1002/app.27628

[78] H. Teng, W. Tang, Y. Shi, X. Jin. Crystallization kinetics of homogeneous and heterogeneous LLDPE. Chinese Journal of Polymer Science 2002; 20:339-345.

[79] W. Shao, Y. Zhang, Z. Wang, Y. Niu, R. Yue, W. Hu. Critical content of ultrahigh-molecular-weight polyethylene to induce the highest nucleation rate for isotactic polypropylene in blends. Industry & Engineering Chemistry Research 2012; 51:15953-15961. DOI: 10.1021/ie302542x

[80] C. Li, J. Zhao, D. Zhao, Q. Fan. Linear low-density polyethylene/poly(ethylene-ran-butene) elastomer blends: Miscibility and crystallization behavior. Journal of Polymer Research 2004; 11:323-331. DOI: 10.1007/s10965-005-6569-5

[81] A.L.C. Machado, E.F. Lucas, E. González. Poly(ethylene-co-vinyl acetate) (EVA) as wax inhibitor of a Brazilian crude oil: Oil viscosity, pour point and phase behavior of organic solutions. Journal of Petroleum Science and Engineering 2001; 32:159-165. DOI: 10.1016/S0920-4105(01)00158-9

[82] K.G. Paso, H. Scott Fogler. Bulk stabilization in wax deposition systems.Energy & Fuels 2004; 18:1005-1013. DOI: 10.1021/ef034105+

[83] H.R. Jafari Ansaroudi, M. Vafaie-Sefti, Sh. Masoudi , T. Jafari Behbahani, H. Jafari. Study of the morphology of wax crystals in the presence of ethylene-co-vinyl acetate copolymer. Petroleum Science and Technology 2013; 31:643-651.
DOI: 10.1080/10916466.2011.632800

[84] D.W. Jennings, K. Weispfennig. Effect of shear on the performance of paraffin inhibitors: Coldfinger investigation with Gulf of Mexico crude oils. Energy & Fuels 2006; 20:2457-2464.
DOI: 10.1021/ef0602170

[85] E. Marie, Y. Chevalier, F. Eydoux, L. Germanaud, P. Flores. Control of n-alkanes crystallization by ethylene-vinyl acetate copolymers. Journal of Colloid and Interface Science 2005; 290:406-418.
DOI: 10.1016/j.jcis.2005.04.054

[86] P. Singh, R. Venkatesan, H. Scott Fogler. Morphological evolution of thick wax deposits during aging. American Institude of Chemical Engineers Journal 2001; 47:6-18.
DOI: 10.1002/aic.690470103

[87] L. Mandelkern. Crystallization of Polymers.Volume 1.Equilibrium Concepts. Cambridge, New York (2002).

CHAPTER 2

MATERIALS AND METHODS

2.1 Materials

2.1.1 Linear low-density polyethylene (LLDPE)

LLDPE was supplied in pellet form by Sasol Polymers. It is a 2.13% hexene copolymer with a melt flow index (MFI) of 1.0 g/10 min, an average molecular weight of 191 600 g mol^{-1}, a melting temperature of 124 °C and a density of 0.924 g cm^{-3}. It is generally used for packaging.

2.1.2 Medium-soft paraffin wax (M3 wax)

M3 wax was supplied in powder form by Sasol Wax. It is a paraffin wax consisting of approximately 99% of straight short chain hydrocarbons and few branched chains. It has an average molecular weight of 440 g mol^{-1} and a carbon distribution of C15 – C78. It has a melting temperature range of 40–60 °C, a density of 0.90 g cm^{-3}, and it is primarily used in the manufacturing of candles.

2.2 Methods

2.2.1 Sample preparation

Table 2.1 shows the sample ratios of the blends. All the samples were prepared by melt mixing using a Brabender Plastograph with a 50 mL internal mixer. The samples were prepared at 170 °C, at a speed of 30 rpm for 15 min. A high temperature of about 170 °C was chosen in order to (i) fully melt the crystals, (ii) avoid sample degradation, and (iii) to get the right melt viscosity in order to avoid high torque levels in the Brabender. The blends were physically premixed and fed into the heated mixer. They were then melt pressed at 170 °C for 5 min under 50 kPa using a hydraulic melt press.

Table 2.1 Samplesused in this project

Sample	Ratio (w/w)
LLDPE	
LLDPE/wax	95/5
	90/10
	80/20
	70/30
	60/40
Wax	

2.3 Sample analysis

2.3.1 Differential scanning calorimetry (DSC)

In this study, a power compensated DSC was used. A Perkin Elmer Pyris-1 DSC was used for thermal analysis, thermal fractionation and isothermal crystallization measurements, while a Perkin Elmer DSC7 was used for the non-isothermal crystallization measurements. All the experiments were performed under nitrogen flow (flow rate 20 mL min^{-1}) to minimize oxidative degradation of the samples, and the instruments were calibrated at a heating rate of 10 °C min^{-1} using the onset temperatures of melting of indium and zinc standards, and the melting enthalpy of indium.

2.3.1.1 Thermal analysis

Samples of approximately 5 mg were weighed, encapsulated and sealed in aluminum pans. They were then melted in the DSC for 3 min at 170 °C to erase any previous thermal history. A cooling scan at 20 °C min^{-1} from 170 to 25 °C was recorded; this process imposed a known thermal history on the sample. Finally, a subsequent heating scan at 20 °C min^{-1} from 25 to 170 °C was recorded; this process allowed a sample with a known thermal history to be analysed. The DSC curves were integrated using a sigmoidal baseline. Three samples for each composition

were tested to ensure accuracy and reproducibility. The melting and crystallization temperatures, as well as enthalpies, were determined by keeping the measurement range constant and the data is reported as average values with standard deviations.

2.3.1.2 Thermal treatment

Samples of approximately 5 mg were weighed, encapsulated and sealed in aluminum pans. Two suitable oil baths were used to perform the thermal treatments with a good temperature control. The first oil bath was kept at a constant temperature of 170 °C and the second oil bath was kept at 115 °C. Both oil baths were placed next to each other. The samples were placed all together inside a test tube-like or glass ampoule. The glass ampoule was then purged with nitrogen gas and immediately sealed. The reason for this was to have the samples without oxygen to avoid degradation during the thermal treatments. The glass ampoule was placed in the first oil bath for 10 min to erase all thermal history and fully melt the samples. It was then rapidly removed from the first oil bath and immediately placed inside the second oil bath. It was crucial for this step to be done quickly, so that the samples do not start to crystallize before they are placed inside the second oil bath. The samples remained under isothermal conditions for 48 hours inside the second oil bath at 115 °C. The glass ampoule was then removed from the oil bath and immersed in a water/ice mixture to rapidly quench the samples. The samples were then analysed according to the procedure described in section 2.3.1.1.

2.3.1.3 Self-nucleation (SN)

The SN thermal protocol was performed to determine the ideal self-nucleation temperature ($T_{s(ideal)}$) for thermal fractionation, which is the temperature that causes maximum SN without any annealing. It was performed using pure LLDPE, since this is the blend component that melts at a higher temperature. Samples of approximately 5 mg were weighed, encapsulated and sealed in aluminum pans. A schematic representation of the self-nucleation (SN) experiment is shown in Figure 2.1. The process is described as follows:

(a) The sample was heated from 25 to 170 °C at 20 °C min^{-1} and maintained at that temperature for 3 min to erase thermal history.

(b) The sample was cooled from 170 to 25 °C at 20 °C min^{-1} to create the initial "standard" state and held at that temperature for 3 min.

(c) The sample was heated from 25 °C to a selected thermal treatment temperature or self-seeding temperature (T_s) located in the final melting temperature range of the sample and held at that temperature for 5 min.

(d) The sample was cooled to 25 °C again, where the effects of thermal treatment would be reflected in the crystallization behaviour of the sample.

(e) Finally, the sample was heated to 170 °C, where the effects of thermal treatment would also be reflected by the melting of the sample.

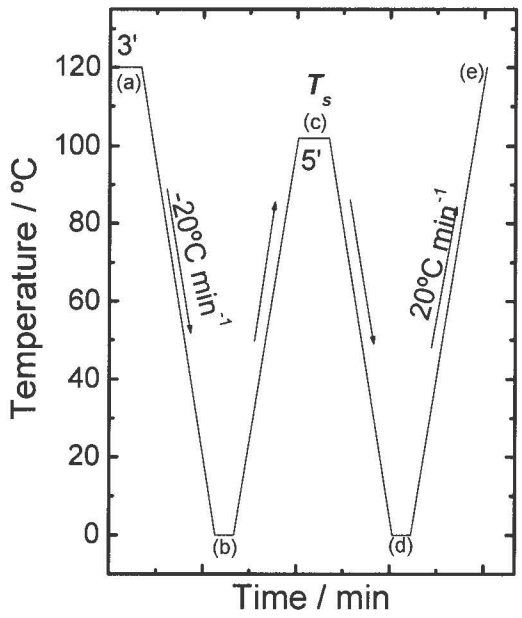

Figure 2.1 Schematic representation of the temperature programme of a self-nucleation (SN) procedure [1]

2.3.1.4 Successive self-nucleation and annealing (SSA)

The SSA thermal protocol was first performed using pure LLDPE, since this is the blend component that melts at a higher temperature. It was again used for the blends, but more steps were added in order to cover the entire melting temperature range of the wax. Samples of approximately 5 mg were weighed, encapsulated, and sealed in aluminum pans. The samples were analyzed according to the SSA treatment comprising eight self-nucleation/annealing cycles with a T_s from 123 to 88 °C, with 5 °C steps and 5 minutes isothermal at each successive temperature. A schematic representation of the SSA thermal fractionation is shown in Figure 2.2. Steps (a)-(d) of the SN experiment were followed as the first cycle of SSA, and then the following steps were performed as the successive cycles:

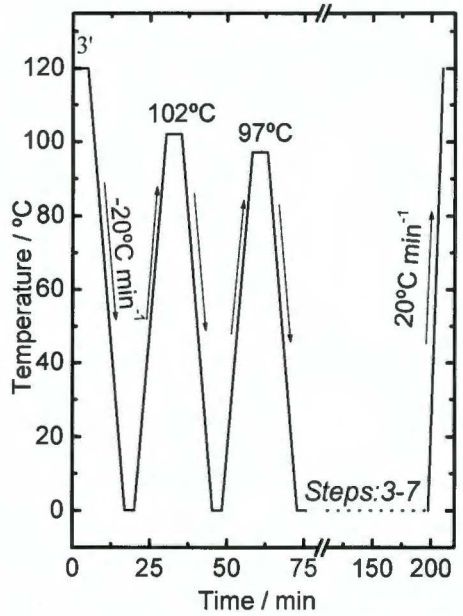

Figure 2.2 Schematic representation of the temperature programme of a successive self-nucleation and annealing procedure (SSA) [2-5]

(e) The sample was heated to a successive predetermined thermal treatment temperature or self-seeding temperature that was 5 °C lower than the previous T_s and held at that

temperature for 5 min. Then the sample was cooled to 25 °C at a rate of 20 °C min^{-1}. This cycle was repeated at increasingly lower T_s values.

(f) The sample was heated to 170 °C at the rate of 20 °C min^{-1}, during which the effects of the SSA cycles would be reflected.

2.3.1.5 Isothermal crystallization

(i) Selection of the crystallization temperatures, T_c

In order to determine suitable crystallization temperatures (T_c) for isothermal measurements, the sample was heated from 25 to 170 °C at 60 °C min^{-1} and held there for 3 min to erase the thermal history. The sample was then cooled from the melt at 60 °C min^{-1} to a pre-established temperature (T_{cl}). It was immediately heated from T_{cl} to 170 °C at 20 °C min^{-1} in order to see if any melting could be detected. If an endotherm was recorded, then the $T_{cl}$was too low, since some crystallization occurredduring the cooling to T_{cl} at 60 °C min^{-1}. Then a test was performed with a higher T_{cl} until no crystallization occurred duringthe previous cooling.

(ii) Isothermal crystallization procedure

A schematic representation of the isothermal crystallization is shown in Figure 2.3. The sample was heated from 25 to 170 °C at 60 °C min^{-1} and held there for 3 min to erase the thermal history. The sample was then cooled from the melt at 60 °C min^{-1} to the established crystallization temperature (T_c) and held there for a time t_c until saturation was reached (at approximately three times the half-crystallization time). The isothermal crystallization of the sample was then recorded. A high cooling rate of about 60 °C min^{-1} was used to minimize crystallization of the sample during cooling. Finally, the sample was heated at 20 °C min^{-1} in order to record the melting behaviour of the isothermally crystallized copolymer.

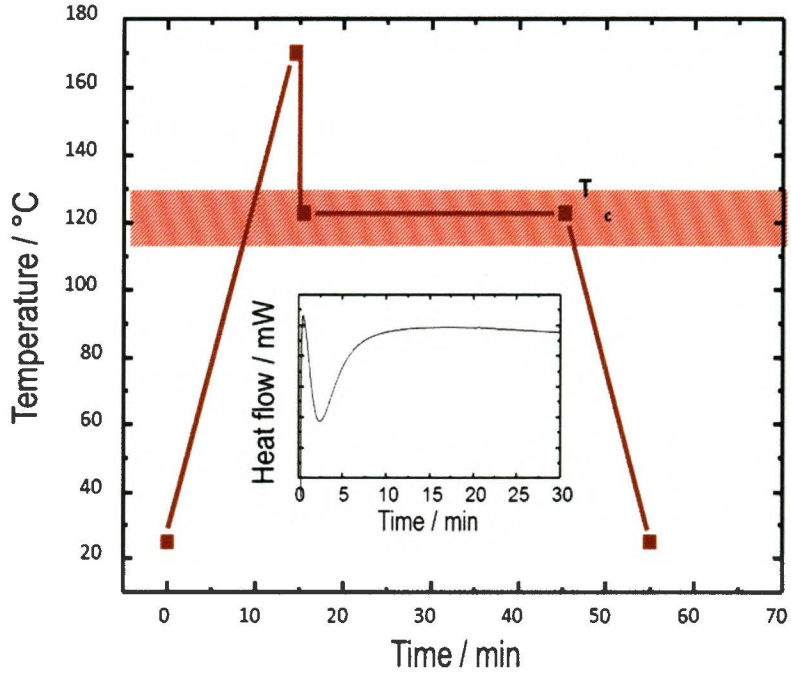

Figure 2.3 Isothermal crystallization experimental procedure [6]

2.3.1.6 Equilibrium melting

To determine the equilibrium melting temperatures, $T_m°$, of the samples, the final step in the isothermal crystallization procedure, whereby the sample was heated at 20 ° C min^{-1} in order to record the melting behaviour of the isothermally crystallized polymer, was used to record the melting of the crystals formed at different crystallization temperatures, T_c. The Hoffman–Weeks extrapolation [7,8] was then applied by plotting the observed melting temperature ($T_{m(obs)}$) against T_c to observe the intersection of this line with another line with a slope equal to 1 ($T_m = T_c$).

2.3.1.7 Non-isothermal crystallization

Attempts were made to investigate the isothermal crystallization of pure wax, but the analyses were not successful due to the fact that wax crystallizes too fast. A non-isothermal approach was therefore used to determine the crystallization kinetics of the wax. The neat wax and the 70/30

w/w LLDPE/wax blend were used to study the crystallization behaviour of wax. A constant sample mass of 10 mg (pure wax) and 5 mg (70/30 w/w LLDPE/wax) at constant scanning rates of 5, 10, 20 and 40 °C min^{-1} were used. In another series of experiments the sample masses were changed inversely proportional to the scanning rates. A sample mass of 10 mg at 5 °C min^{-1}, 5 mg at 10 °C min^{-1}, 2.5 mg at 20 °C $min^{-1}$and 1.25 mg at 40 °C min^{-1} were used for each sample. For non-isothermal crystallization measurements the sample was first heated from 0 to 170 °C to erase the thermal history. Then it was cooled to 0 °C and immediately heated to 170 °C at constant scanning rates of 5, 10, 20 and 40 °C min^{-1}, and the exothermic crystallization peaks were recorded as a function of temperature.

2.3.2 Atomic force microscopy (AFM)

In this study, AFM was used to study the surface topography of the samples and also to distinguish the different phases in the blend. The AFM topography examinations were carried out by an Easyscan AFM from Nanosurf. The analyses were done in a non-contact mode with a Si cantilever having a resonance frequency of 170 MHz.

2.4 References

[1] B. Fillon, J.C. Wittmann, B. Lotz, A. Thierry. Self-nucleation and recrystallization of isotactic polypropylene (α phase) investigated by differential scanning calorimetry. Journal of Polymer Science Part B: Polymer Physics 1993; 31:1383-1393. DOI: 10.1002/polb.1993.090311013

[2] A.J. Müller, Z.H. Hernández, M.L. Arnal, J.J. Sánchez. Successive self-nucleation annealing (SSA): A novel technique to study molecular segregation during crystallization. Polymer Bulletin 1997; 39:465-472. DOI: 10.1007/s002890050174

[3] M.L. Arnal, J.J. Sanchez, A.J. Müller. Miscibility of linear and branched polyethylene blends by thermal fractionation: Use of the successive self-nucleation and annealing (SSA) technique. Polymer 2001; 42:6877-6890. DOI: 1016/s0032-3861(01)00177-X

[4] A.J. Müller, M.L. Arnal. Thermal fractionation of polymers. Progress in Polymer Science 2005; 30:559-603.
DOI: 10.1016/j.progpolymsci.2005.03.001

[5] A.J. Müller, A.T. Lorenzo, M.L. Arnal. Recent advances and applications of 'successive self-nucleation and annealing' (SSA) high speed thermal fractionation. Macromolecular Symposia 2009; 277:207-214.
DOI: 10.1002/masy.200950325

[6] A.T. Lorenzo, M.L. Arnal, J. Albuerne, A.J. Müller. DSC isothermal polymer crystallization kinetics measurements and the use of the Avrami equation to fit the data: Guidelines to avoid common problems. Polymer Testing 2007; 26:222-231.
DOI: 10.1016/j.polymertesting.2006.10.005

[7] J.D. Hoffman, J.J. Weeks. Melting process and the equilibrium melting temperature of polychlorotrifluoroethylene. Journal of Research of the National Bureau of Standards - A. Physics and Chemistry 1962; 66:13-28.
DOI: 10.6028/jres.066A.003

[8] L. Mandelkern. Crystallization of Polymers. Volume 1. Equilibrium Concepts. Cambridge, New York (2002).

CHAPTER 3

RESULTS AND DISCUSSION

3.1 Differential scanning calorimetry (DSC)

The DSC curves for all the investigated samples are shown in Figures 3.1 to 3.3. The DSC first heating curves in Figure 3.1(a) are of the non-annealed samples, whereas those in Figure 3.1(b) for the same samples isothermally crystallized in nitrogen in an oil bath at a crystallization temperature (T_c) of 115 °C and a crystallization time (t_c) of 48 hours, followed by fast quenching in iced water. The purpose was to grow the thickest possible lamellae to observe how the LLDPE crystallization was affected by wax addition.

Figure 3.1(a) does not show a wax melting peak for wax contents up to 10 wt.%, which could be an indication that the wax and LLDPE are miscible at these wax contents or the individual wax chains were trapped in the amorphous part of the LLDPE, leaving too little crystallized wax for the DSC instrument to detect the melting of these wax crystals. However, two separate melting peaks are observed at higher wax contents (20-40 wt.%). The lower temperature melting peak that appears at approximately 30-65 °C is for the wax phase, while the most prominent peak between 110-130 °C is related to the melting of the LLDPE crystals. The DSC heating curves for the annealed samples show a third peak at around 100 °C (Figure 3.1(b) and Table 3.1). This peak corresponds to the melting of the LLDPE crystals that were formed during cooling from 115 °C. A peak shoulder appearing at a slightly higher temperature of about 120 °C is observed at low wax contents, indicating two separate crystal populations that are formed from chains with different crystallizable lengths after being annealed for a certain time, and some degree of heterogeneity in the sequence lengths [1]. Upon annealing, there are two melting peaks that may sometimes merge into a single peak (section 3.2) as a result of the plasticizing/dilution effect of the wax that causes homogeneity in the sequence lengths. This is clearly demonstrated by the disappearance of the peak shoulder as the wax content in the samples increases. It is possible that the wax reduces the nucleation probability, because the equilibrium melting temperature and the accompanying supercooling are changed (section 3.3). During annealing the effect of molecular

weight separation could also significantly contribute to (a) the formation of separate melting peaks in the presence of wax and (b) reversion to the "standard" melting behaviour on the second heating. The melting peak maximum of the LLDPE phase decreased with an increase in wax content because of the dilution effect of the wax. The LLDPE crystals melt in the presence of molten wax, which acts as a diluent or solvent and causes a depression of the melting point. The melting point depression of polymer crystals in the presence of a solvent is a well-known thermodynamic phenomenon which has been described by, for instance, the Flory-Huggins theory [2]. However, the Flory-Huggins theory was developed for very small amounts of solvent present.

The normalised melting and crystallization enthalpy values shown in Table 3.1 were determined according to Equations 3.1 and 3.2.

$$\Delta H_m^n = \Delta H_{m(x \text{ or } y)}/w_{(x \text{ or } y)} \quad (3.1)$$

$$\Delta H_c^n = \Delta H_{c(x \text{ or } y)}/w_{(x \text{ or } y)} \quad (3.2)$$

where ΔH_m^n and ΔH_c^n are the melting and crystallization enthalpies normalised to the amount of the pure components in the sample, ΔH_m and ΔH_c are the melting and crystallization enthalpies of the pure components, and w is the weight fraction of the pure components in the blend; x and y represent LLDPE and wax, respectively.

After the annealed samples were heated, all crystallinity was destroyed, and the effect of the annealing should not be visible in the second heating curves. The DSC cooling curves of the pure components and the blends are shown in Figure 3.2. An increase in wax content results in a slight decrease in the crystallization peak temperatures of LLDPE. This indicates that the polymer was plasticized by the molten wax which increased the LLDPE chain mobility and reduced the temperature at which it started crystallizing.

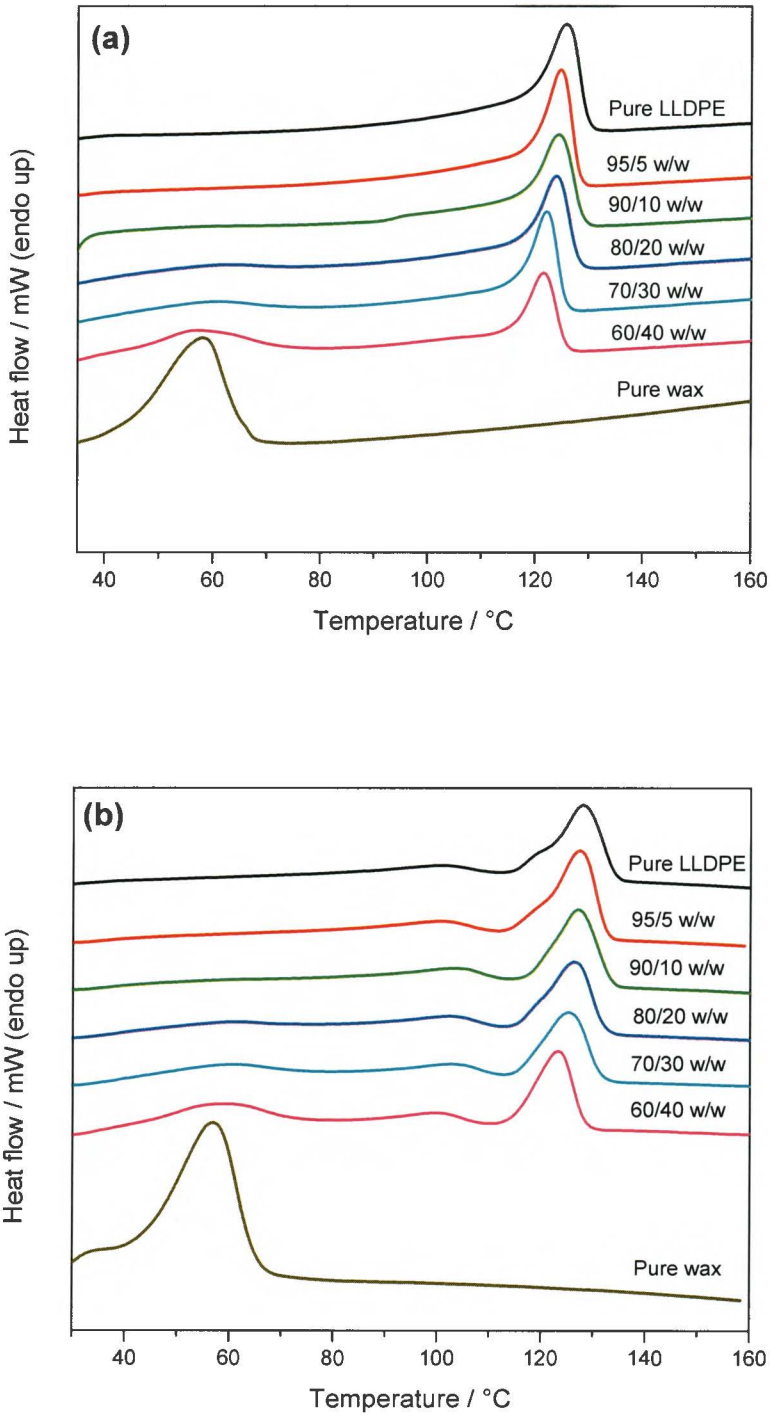

Figure 3.1 DSC first heating curves for (a) non-annealed samples and (b) samples annealed at 115 °C

The DSC second heating curves of the pure components and the blends are shown in Figure 3.3. Since the wax melts before the polyethylene, the LLDPE crystals are surrounded by molten wax, and a melting point depression caused by a solvent is observed, as described in the Flory-Huggins theory [2]. However, the Flory-Huggins theory depends on composition and it was developed for very small amounts of solvent present. In the case of the LLDPE/wax blends having low wax content (up to 10 wt.%), no wax crystallization peak is observed, which is probably due to single wax chains being trapped in the amorphous phase of LLDPE, or co-crystallization of the wax with the LLDPE. However, at higher wax contents a significant fraction of the wax crystallized separately in the amorphous phase of LLDPE, and two separate melting peaks related to wax and LLDPE are observed. This observation was reported in several studies on different polyolefin/wax systems [3-14].

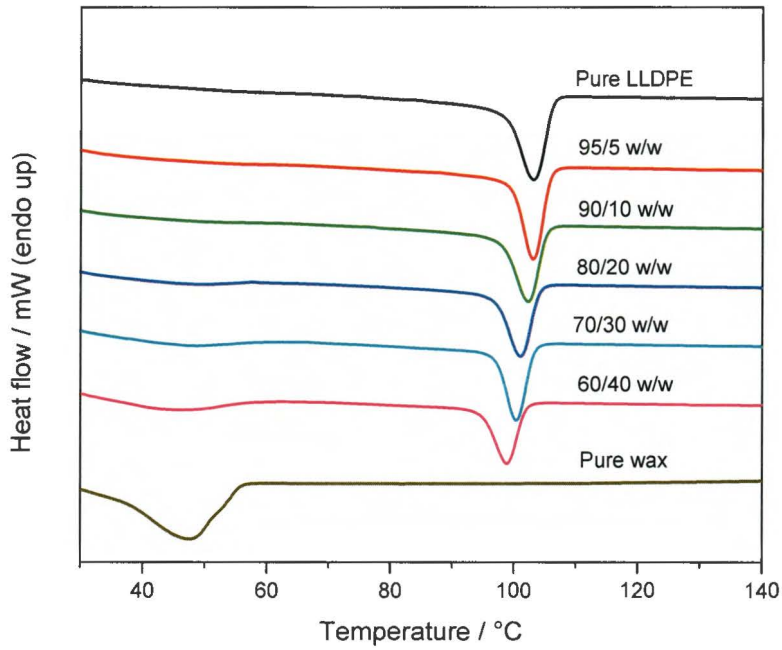

Figure 3.2 DSC cooling curves of the pure components and the blends

Table 3.1 The parameters obtained from DSC measurements for all the samples analysed before and after annealing

Sample	1st Heating						Cooling						2nd Heating					
	Annealed samples			Non-annealed samples			Annealed samples			Non-annealed samples			Annealed samples			Non-annealed samples		
	T_m / °C	ΔH_m/ J g^{-1}	ΔH_m^n/ J g^{-1}	T_m / °C	ΔH_m/ J g^{-1}	ΔH_m^n/ J g^{-1}	T_c/ °C	ΔH_c/ J g^{-1}	ΔH_m^n/ J g^{-1}	T_c/ °C	ΔH_c/ J g^{-1}	ΔH_c^n/ J g^{-1}	T_m / °C	ΔH_m/ J g^{-1}	ΔH_m^n/ J g^{-1}	T_m / °C	ΔH_m/ J g^{-1}	ΔH_m^n/ J g^{-1}
Pure LLDPE	128.7[a] 101.3[b]	37[a] 11[b]	37[a] 11[b]	125.7[a]	88[a]	88[a]	109.3[a]	80[a]	80[a]	103.3[a]	91[a]	91[a]	125.8[a]	69[a]	69[a]	126.1[a]	67[a]	67[a]
95/5w/w LLDPE/wax	128.0[a] 101.3[b]	48[a] 14[b]	50[a] 15[b]	124.7[a]	82[a]	86[a]	109.2[a]	90[a]	95[a]	103.0[a]	81[a]	85[a]	125.1[a]	75[a]	79[a]	124.1[a]	58[a]	61[a]
90/10w/w LLDPE/wax	128.0[a] 103.3[b]	39[a] 17[b]	43[a] 19[b]	124.4[a]	73[a]	81[a]	108.5[a]	78[a]	87[a]	102.6[a]	75[a]	83[a]	124.3[a]	66[a]	73[a]	124.4[a]	56[a]	62[a]
80/20w/w LLDPE/wax	127.3[a] 103.8[b] 60.1[c]	33[a] 13[b] 12[c]	41[a] 16[b] 60[c]	124.1[a] 61.7[c]	68[a] 10[c]	85[a] 50[c]	107.5[a] 54.4[c]	77[a] 13[c]	96[a] 67[c]	101.3[a] 45.3[c]	67[a] 11[c]	84[a] 53[c]	122.2[a] 59.1[c]	66[a] 13[b]	83[a] 65[c]	123.7[a] 58.1[c]	50[a] 11[c]	63[a] 55[c]
70/30w/w LLDPE/wax	126.0[a] 103.5[b] 59.2[c]	22[a] 11[b] 23[c]	31[a] 16[b] 77[c]	122.1[a] 59.7[c]	61[a] 17[c]	87[a] 57[c]	106.4[a] 53.3[c]	75[a] 21[c]	107[a] 70[c]	100.6[a] 48.3[c]	61[a] 20[c]	87[a] 65[c]	122.0[a] 59.1[c]	63[a] 20[c]	90[a] 67[c]	122.1[a] 57.9[c]	44[a] 18[c]	63[a] 60[c]
60/40w/4 5w LLDPE/wax	123.8[a] 101.0[b] 55.8[c]	18[a] 8[b] 44[c]	30[a] 13[b] 109[c]	121.7[a] 56.4[c]	50[a] 31[c]	83[a] 78[c]	105.3[a] 53.9[c]	67[a] 33[c]	115[a] 83[c]	98.9[a] 43.8[c]	50[a] 33[c]	83[a] 82[c]	121.1[a] 58.1[c]	57[a] 34[c]	95[a] 85[c]	121.1[a] 56.1[c]	37[a] 34[c]	62[a] 85[c]
Pure wax	58.7[c]	126[c]	126[c]	58.3[c]	114[c]	114[c]	47.9[c]	123[c]	123[c]	47.6[c]	88[c]	88[c]	58.3[c]	115[c]	115[c]	58.1	90[c]	90[c]

T_m - melting peak temperature, T_c-crystallization peak temperature, ΔH_m - melting enthalpy, ΔH_c - crystallization enthalpy, ΔH_m^n - melting enthalpy normalised with respect to amount of LLDPE or wax; ΔH_c^n - crystallization enthalpy normalised with respect to LLDPE or wax;'a' denotes the melting of the LLDPE phase; 'b' denotes the melting of the LLDPE crystals that were formed during quenching from T_c; 'c' denotes the melting of the wax phase

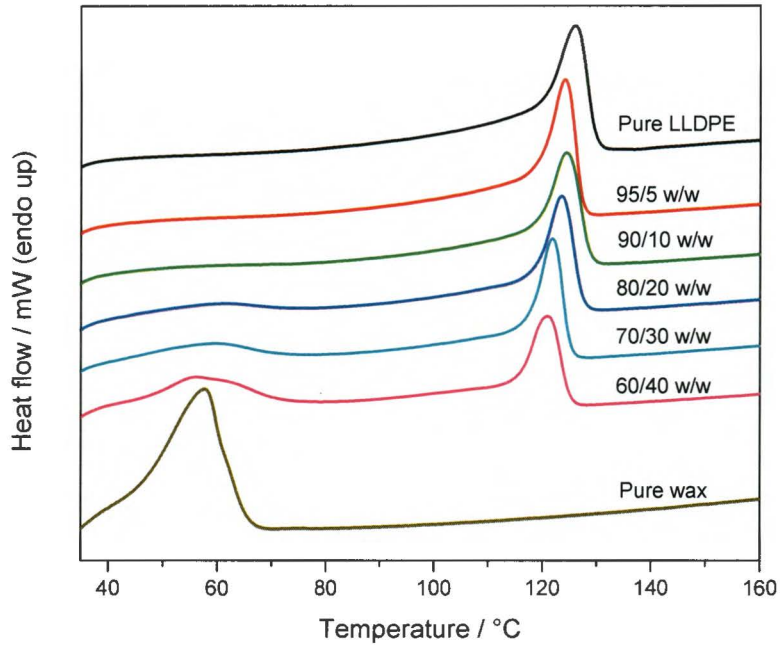

Figure 3.3 DSC second heating curves of the pure components and the blends

The melting temperatures from the DSC first heating curves are shown as a function of wax content in Figure 3.4. It can be clearly seen that an increase in the wax content results in a slight decrease in the melting peak temperatures of the LLDPE (Figure 3.4(a) and (b)). However, the LLDPE had very little influence on the wax melting temperature. The same behaviour was observed for the cooling and second heating of the samples (Figure 3.5). The melting temperature of the LLDPE crystals that were formed during cooling from 115 °C was nearly constant as the wax content increased (Figure 3.4(b)). This is probably because during annealing there is enough time to form more perfect, stable LLDPE crystals, even in the presence of the molten wax.

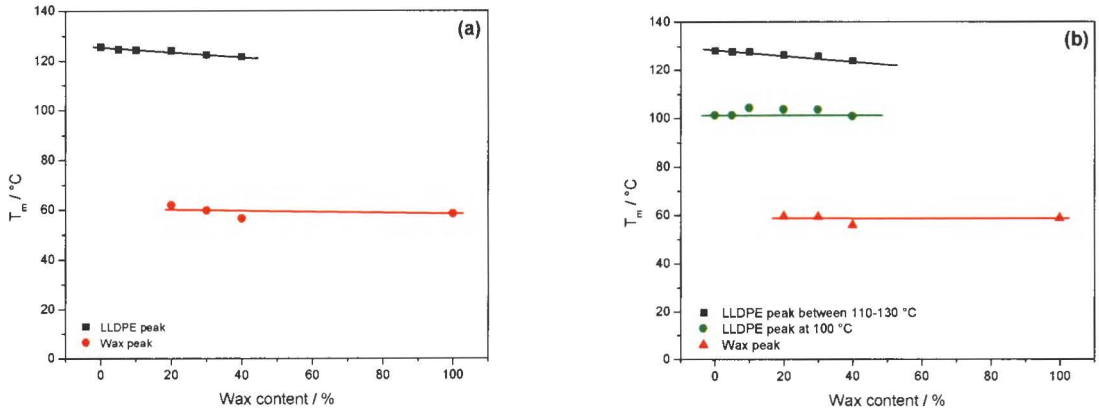

Figure 3.4 DSC first heating melting temperatures as a function of wax content for (a) non-annealed samples and (b) samples annealed at 115 °C

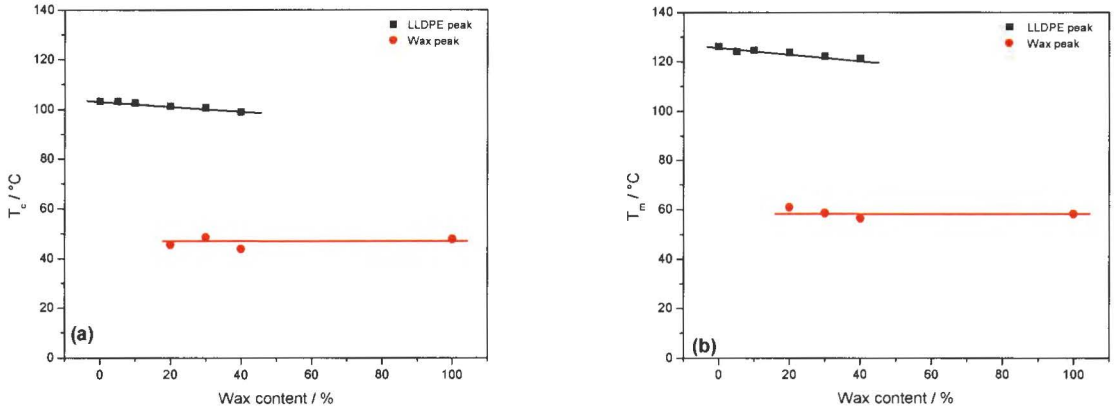

Figure 3.5 DSC (a) crystallization and (b) second heating melting temperatures as a function of wax content for the pure components and the blends

The normalised melting enthalpies (first heating) as a function of wax content are shown in Figure 3.6. If the wax completely crystallized as a separate phase in the blend, one would expect the normalised melting enthalpies of the wax in the blends to be the same as the melting enthalpy of pure wax. In this case the normalised melting enthalpies of the wax in the blends are lower than that of pure wax, but increases with increasing wax content. This is true for both the non-annealed samples and the samples annealed at 115 °C (Figure 3.6 and Table 3.1). A certain fraction of the wax therefore did not crystallize separately when blended with LLDPE. There are

two possible reasons for this observation: (i) the individual wax chains may have been trapped in the amorphous phase of LLDPE, or (ii) part of the wax may have co-crystallized with the LLDPE. It seems as if more wax crystallized separately for the samples annealed at 115 °C (Table 3.2). It is possible that during the annealing process there was enough time for the wax chains to come together and crystallize separately upon further cooling after annealing. The normalised enthalpy values of LLDPE show almost no change within experimental error with an increase in wax content. This indicates that the presence of wax and increasing wax content had little influence on the amount of crystalline LLDPE formed during cooling and annealing. The enthalpy values from the cooling and second heating curves are summarised in the appendix (Figures A.1 and A.2).

Table 3.2 Percentage wax which did not crystallize separately

Sample	Non-annealed sample	Annealed sample
Pure LLDPE	-	-
95/5 LLDPE/wax	-	-
90/10 LLDPE/wax	-	-
80/20 LLDPE/wax	56%	52%
70/30 LLDPE/wax	50%	39%
60/40 LLDPE/wax	32%	13%

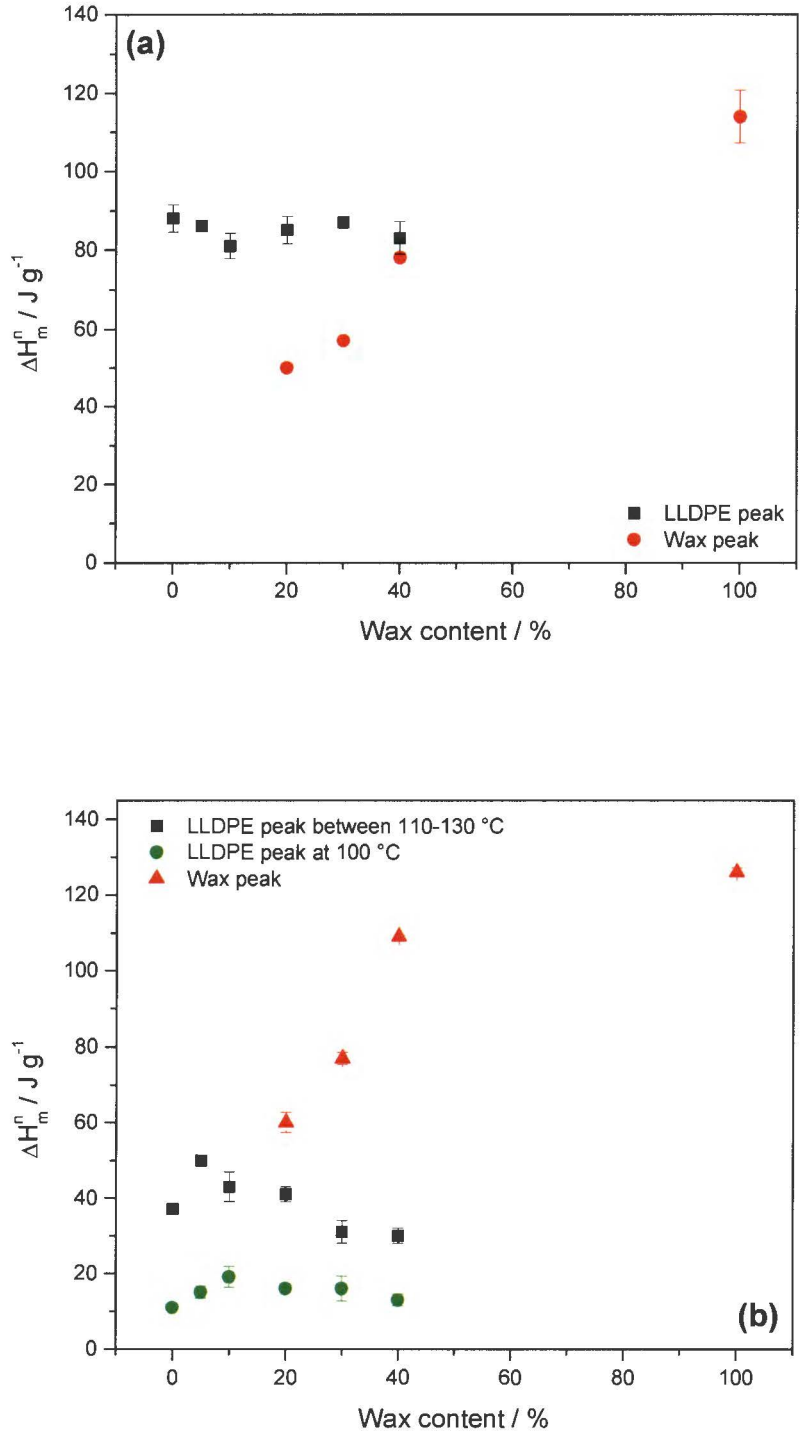

Figure 3.6 DSC normalised melting enthalpies (first heating) as a function of wax content for (a) non-annealed samples and (b) samples annealed at 115 °C

3.2 Thermal fractionation by successive self-nucleation and annealing (SSA)

Self-nucleation was performed to determine the minimum temperature of *Domain II*. Keeping a polymer at this temperature causes maximum self-nucleation without any annealing, and this temperature is therefore the first T_s temperature of the SSA thermal protocol [15]. The DSC cooling and heating curves of pure LLDPE treated at different T_s temperatures are shown in Figure 3.7. The selected self-seeding temperatures (T_s) were chosen to range from 120 to 130 °C. In Figure 3.7(a) the cooling curves were evaluated to determine the different domains, whereas the heating scans shown in Figure 3.7(b) were used to determine whether annealing was present. At low T_s temperatures (120-122 °C) the crystallization exotherm showed a characteristic high temperature tail that indicates immediate recrystallization upon cooling from the T_s temperature. The subsequent melting endotherm shows a high temperature peak that is due to the melting of the annealed crystals at that T_s temperature. Upon annealing there are two melting peaks that may sometime merge into one peak, since the melting temperature of the annealed crystals will decrease with decreasing T_s temperature. It is well known that the melting temperature is not directly related to the nucleation density in the protocol, but it is valuable to determine the transition between *Domain II* and *Domain III* [15,16].

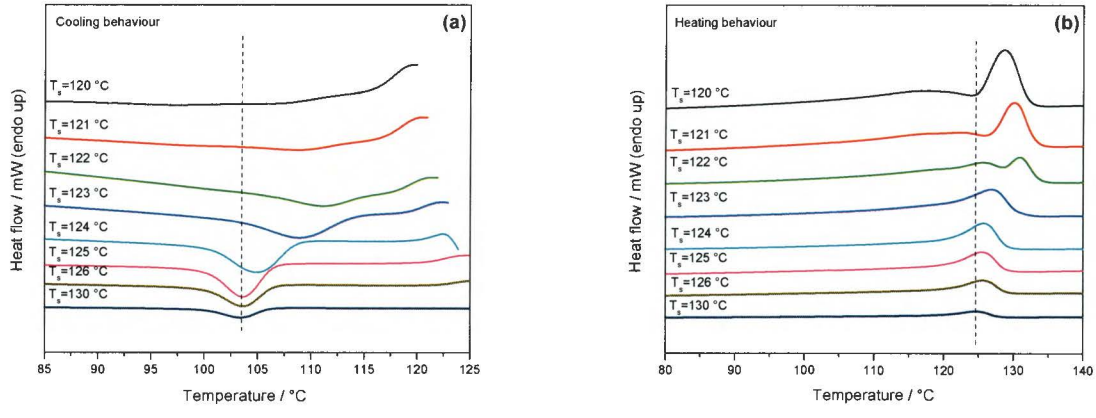

Figure 3.7 Self-nucleation of pure LLDPE: (a) DSC cooling scans from T_s (after the 5 min isothermal step at T_s was complete) and (b) DSC subsequent heating scans after the cooling shown in (a)

The dependence of the crystallization and melting temperatures of pure LLDPE on different T_s temperatures is shown in Figure 3.8. The vertical lines drawn in Figure 3.8(a) indicate the limits between the different domains. The polymer is said to be under *Domain I* when complete melting of the crystallites occurs. In this case complete melting was found to persist when the T_s temperature is equal to or greater than 125 °C, since no significant changes in T_c values are detected after the self-nucleation (SN) protocol. This indicates that a constant nucleation density is achieved. In *Domain II* the temperature is high enough to melt the sample almost completely, but low enough to leave some self-nuclei that provoke nucleation during the subsequent cooling from T_s. Therefore, self-nucleation is only found to persist when the T_s temperature is in the narrow range of 123-124 °C. Therefore, the crystallization temperature increases with decreasing T_s temperatures. When the T_s temperature is lower or equal to 122 °C, there is self-nucleation and annealing, which is *Domain III* behaviour. In this domain the temperature is too low and only part of the crystals will melt. The unmolten crystals will be annealed during the 5 min at T_s, while the rest of the polymer will be self-nucleated during the subsequent cooling from T_s. The melting temperature is not as sensitive to changes in nucleation as the crystallization temperature because of the metastability of polymer crystals (Figure 3.8(b)).

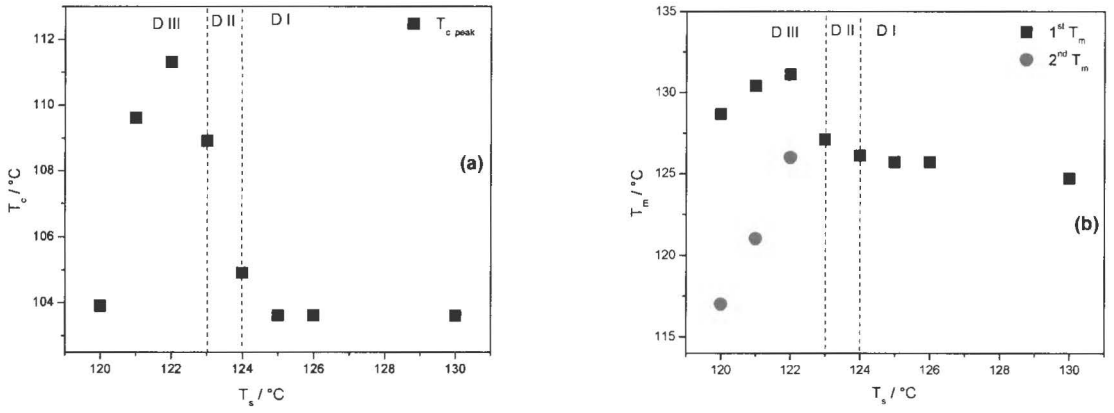

Figure 3.8 Dependence of the (a) crystallization and (b) melting peak temperatures of pure LLDPE on T_s

The classical self-nucleation domains are shown on the original melting trace of LLDPE in Figure 3.9, where the usual three self-nucleation domains can be observed [15]. The vertical lines indicate the temperatures at which the material experiences a self-nucleation domain

transition, whereas the shaded area indicates the temperature range at which *Domain II* is experienced. This is the most important domain, because it is the temperature range in which there is maximum self-nucleation without any annealing. The lowest T_s temperature in this domain should be used as the first T_s temperature for the SSA thermal protocol.

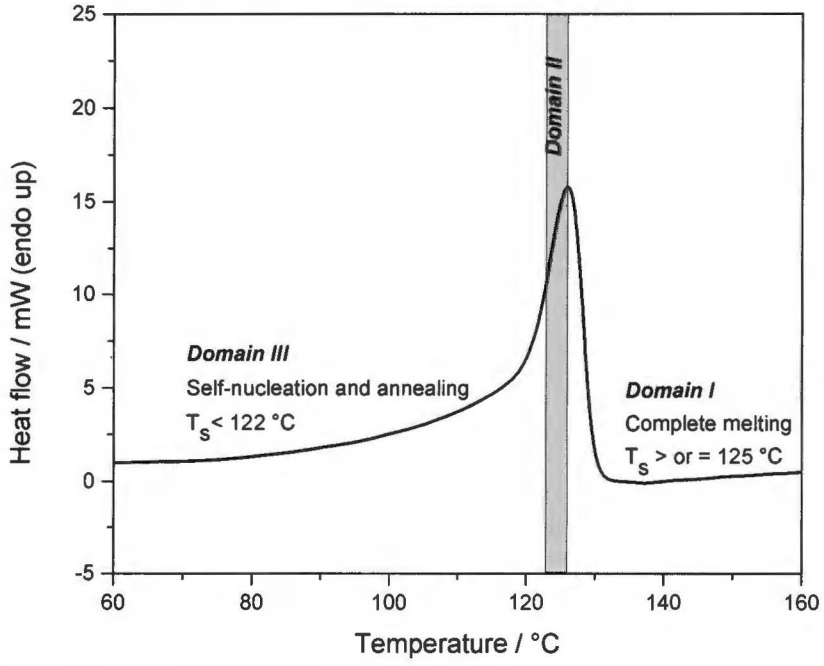

Figure 3.9 Self-nucleation and annealing domains

Table 3.3 shows a summary of the results from the self-nucleation experiment for pure LLDPE. 123 °C was chosen as the ideal self-nucleation temperature for the SSA experiments. This temperature is in agreement with previous reports on specific LLDPE samples [17-18]. However, self-nucleation must be applied to each sample, since the location of self-nucleation domains vary between samples.

Table 3.3 Detailed information from the SN experiment for pure LLDPE

T_s/ °C	T_c/ °C	T_m / °C
120.0	103.9	128.7
		117.0
121.0	109.6	130.4
		121.0
122.0	111.3	131.1
		126.0
123.0	108.9	127.1
124.0	104.9	126.1
125.0	103.6	125.7
126.0	103.6	125.7
130.0	103.6	124.7

Figure 3.10 shows the difference between the DSC heating curves of the non-fractionated and SSA fractionated LLDPE and wax samples. The SSA thermal fractionation technique can easily fractionate LLDPE because it is a copolymer of ethylene and an α-olefin. The α-olefin is a defect since it introduces a branch point, and the SSA fractionation is a function of the branching distribution and content [19]. However, the wax melting behaviour is the same before and after fractionation (Figure 3.10(b)). This is due to the fact that the wax is made of a polydisperse collection of linear chains. It is not sensitive to fractionation, since the technique and especially the fractionation conditions are rather insensitive to molecular weight differences. This is an indication that wax is essentially linear and is not susceptible to thermal fractionation.

It is observed in Figure 3.10(a) that the melting curve of the fractionated LLDPE sample has eight melting peaks after a nine-step SSA protocol was applied. The number of melting peaks produced by SSA depends on how broad the melting temperature range is, and also on the selection of the thermal fractionation conditions. This observation illustrates the capability of the technique to induce thermal fractionation as a result of the broad short chain branching distribution. Each endothermic peak is said to be proportional to the number of crystals with the same stability [16-17]. The highest melting point fraction of the LLDPE corresponds to the

fusion of the thickest lamellae that are formed by the longest uninterrupted linear methylenic sequence. The shorter sequences crystallize in thinner lamellae that melt at lower temperatures.

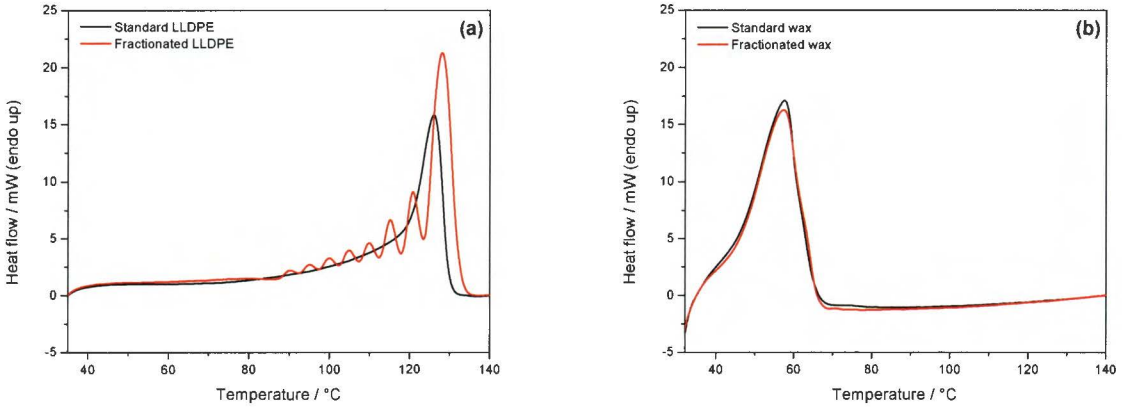

Figure 3.10 Difference between the SSA fractionated and standard (a) LLDPE and (b) wax

The DSC heating curves, after the SSA thermal protocol was applied to the samples are shown in Figure 3.11. The highest melting temperature fraction has slightly lower melting temperature values as the wax content increases. The relative amounts of the different thermal fractions (proportional to the respective areas or enthalpies of fusion) also vary with wax content. The two observations are related to a dilution effect caused by wax addition. The relative importance of the first fraction decreases (its area and height decrease) in comparison with the second and third fraction. It seems as if the low molecular weight wax acts as a 'solvent' for LLDPE, and as a result the diffusion of the chains is higher when the SSA is performed and the SSA fractionation profile will change accordingly. Generally, the fractionation performed by SSA produces different fractions with distinct lamellar thicknesses [16-17,20-22].

There is also no overlap between the wax and LLDPE melting ranges (Figure 3.11). It is well known that in order to observe co-crystallization there must be some degree of melting range overlapping when the pure components and the blends are compared [9,17-18,23-26]. However, different behaviour was observed in previous reports [9,27] where the blends of LDPE and LLDPE with respectively an oxidised and an unoxidised hard wax showed co-crystallization due to the overlap between the melting temperatures of the pure components. This behaviour was explained as follows: the most linear fractions of both materials were able to co-crystallize since

the interaction between LLDPE and wax molecules resulted in a new fraction forming with an intermediate lamellar thickness [24]. Crystal separation and co-crystallization are dependent on the selected PEs, the crystallization conditions, molecular weight, the number of short chain branches (SCBs), and the type of catalyst used [16-18,20].

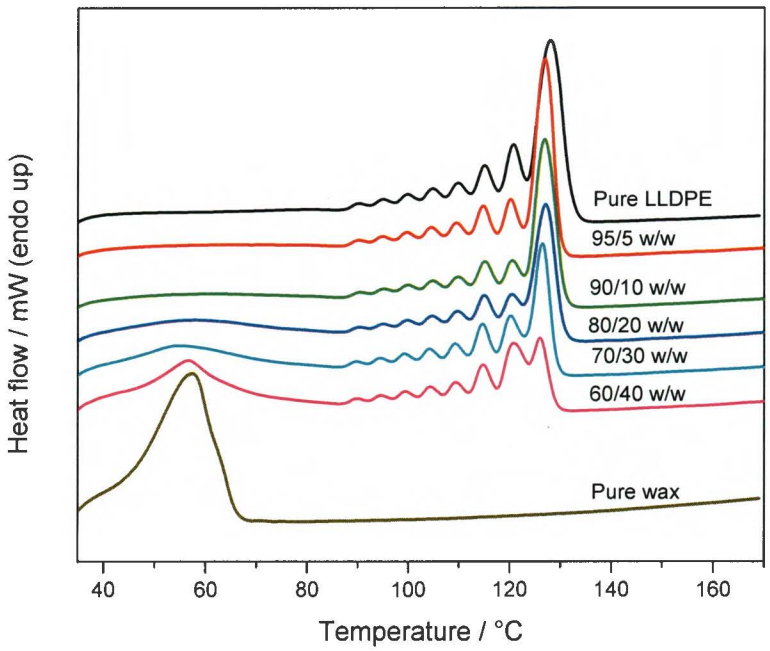

Figure 3.11 Thermal fractionation by SSA of the pure components and the blends (w/w indicates LLDPE/wax weight ratios)

Deconvoluting the SSA traces (or determining the area under each thermal fraction) was done in order to know how the fraction distribution of LLDPE changes because of the presence of molten wax. It also enabled us to observe if the fractionation of the wax has changed as a result of the presence of the LLDPE crystals. The area under each SSA thermal fraction as a function of wax content is tabulated in Table 3.4. The increase in wax content causes the melting enthalpies of the highest melting point fraction in the LLDPE to decrease disproportionately to the LLDPE content in the blend. This is probably due to the dilution effect of the wax that reduces the lamellar thickness and the amount of crystallites formed.

Table 3.4 Area under each SSA thermal fraction as a function of wax content

SSA fraction distribution no.	ΔH_m/ J g^{-1}						
	Pure LLDPE	95/5 w/w LLDPE/ wax	90/10 w/w LLDPE/ wax	80/20 w/w LLDPE/ wax	70/30 w/w LLDPE/ wax	60/40 w/w LLDPE/ wax	Pure wax
1	60.0	51.1	48.2	37.1	26.1	10.2	-
2	9.2	6.3	4.2	4.6	6.3	9.5	-
3	5.8	5.9	5.1	5.1	6.2	5.8	-
4	2.7	2.5	2.1	2.7	2.8	2.7	-
5	2.0	2.1	1.6	2.1	2.2	2.0	-
6	1.3	1.2	1.1	1.1	1.4	1.3	-
7	1.0	0.8	0.8	0.7	0.8	0.8	-
8	0.8	0.7	0.6	0.6	0.7	0.7	-
9	-	-	-	12.2	25.1	35.9	145.0

The experimental and theoretically predicted curves are compared in Figure 3.12. The theoretically predicted curves were constructed by the mathematical weighed sum of the SSA traces of the pure components. At low wax contents up to 10 wt.% the experimental and theoretically predicted fractional peaks of the LLDPE in the blends are almost identical. This indicates that the presence of wax had little influence on the amount of LLDPE crystallites formed. This is probably because the amount of wax is too small to significantly influence the crystallization behaviour of the LLDPE. However, as the wax content increases up to 40 wt.%, the intensity of the experimental peaks is observably lower than the theoretically predicted ones. This is probably related to the chosen ideal self-nucleation temperature in the self-nucleation thermal protocol that is not good, because the DSC results showed no significant change in the LLDPE crystallites with the presence of molten wax (section 3.1). It is further interesting that the experimental wax melting peak for all the blends is smaller than the theoretically predicted one. This is probably because not all of the wax has crystallized because some of the wax chains may have been trapped in the solidified amorphous part of the LLDPE and without enough mobility to grow into sizable wax crystals.

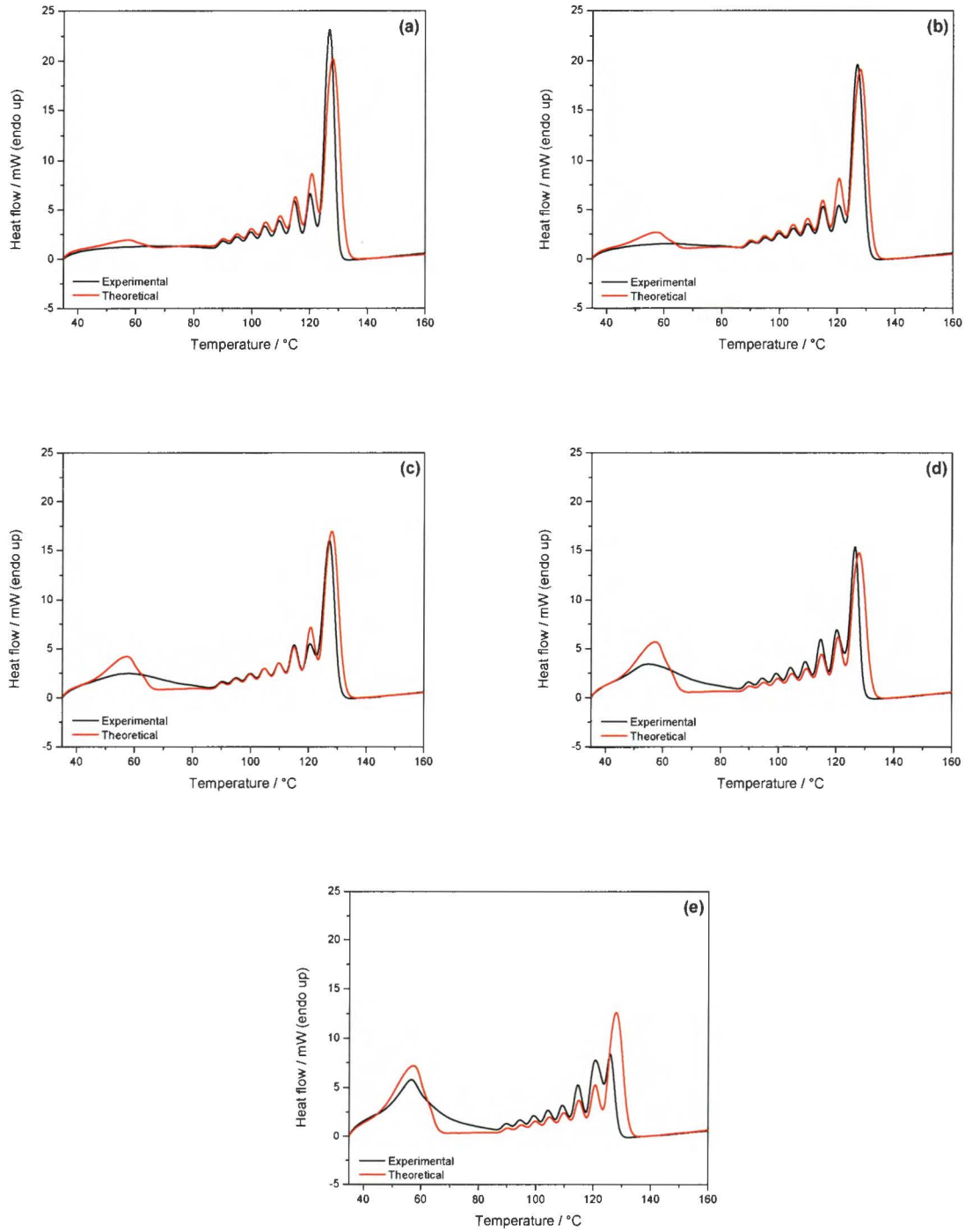

Figure 3.12 Difference between experimental and theoretically predicted curves for (a) 95/5 w/w LLDPE/wax, (b) 90/10 w/w LLDPE/wax, (c) 80/20 w/w LLDPE/wax, (d) 70/30 w/w LLDPE/wax, and (e) 60/40 w/w LLDPE/wax

3.3 Equilibrium melting temperature and melting point depression

In studying the crystallization kinetics of polymer-diluent mixtures, the equilibrium melting temperature ($T_m°$) needs to be determined for a true reflection of the microstructure and morphology of the blend. The equilibrium melting temperature can be determined by crystallizing the samples at different crystallization temperatures (T_c). The melting temperature (T_m) relative to each corresponding crystallization temperature is then recorded from the DSC curves; the values are tabulated in Table 3.5. Figure 3.13 shows the Hoffman-Weeks plots for the determination of the equilibrium melting temperature for pure LLDPE and the blends. The straight line of the observed melting temperature ($T_{m(obs)}$) against T_c intersects with the equilibrium line with a slope equal to 1 ($T_m = T_c$), implying an extrapolation to infinite thickness of lamellae [28].

The values of $T_m°$ obtained from the extrapolations for the different blends are reported in Table 3.6. The equilibrium melting temperatures of the samples decrease with increasing wax content, and is a result of kinetic and thermodynamic factors. The kinetic effects arise because the crystals are formed at temperatures below the equilibrium melting point of the polymer mixture ($T_m°$). The perfect extended chain crystal can only grow at the equilibrium melting temperature $T_m°$, but it would take an infinitely long time to do so. At the crystallization temperatures, that are much lower than the equilibrium melting temperature, thinner lamellae develop (for kinetic reasons, since the crystals formed are the fastest growing crystals, but not the most stable ones, and they are only thin metastable crystals), and therefore they melt at temperatures well below $T_m°$.

Table 3.5 Samples isothermally crystallized at different crystallization temperatures and their corresponding melting temperatures

Sample	T_c / °C	T_m / °C
Pure LLDPE	116.5	127.6
	116.7	127.7
	116.8	127.8
	116.9	127.9
	117.0	128.0
95/5 w/w LLDPE/wax	113.0	125.4
	113.5	125.6
	114.0	126.0
	114.5	126.2
	115.0	126.4
	115.8	126.8
90/10 w/w LLDPE/wax	115.0	126.4
	115.2	126.6
	115.4	126.7
	115.6	126.9
80/20 w/w LLDPE/wax	112.5	123.2
	113.0	123.4
	113.5	123.6
	114.0	123.7
70/30 w/w LLDPE/wax	111.0	123.0
	111.5	123.2
	112.0	123.4
	112.5	123.6
	113.0	124.0
	113.7	123.8
60/40 w/w LLDPE/wax	111.5	121.9
	112.0	122.0
	112.3	122.7
	112.5	122.9
	112.7	123.4

The lower melting temperatures observed after crystallization from solution indicate that a metastable crystalline form is obtained. However, thin plate-like crystals are the usual morphological form observed after crystallization from dilute solution. Therefore, the decrease in $T_m°$ confirms that the chemical potential of a polymer, the thermodynamic stability of the polyethylene crystallites and the mean lamellar thickness decreased during the isothermal crystallization due to the presence of a low molecular weight wax [29-30]. It has been reported that lamellar thickness, crystal type, degree of crystal perfection, and other morphological properties all influence the melting temperatures of polymer blends [31]. Figure 3.14 shows the dependence of the equilibrium melting temperature on the wax content. It is observed that the relationship between $T_m°$ and wax content is not linear but there is a decrease in $T_m°$ with increasing wax content. Similar melting point depression phenomena have been reported for other polymer-diluent mixtures [12,32].

Table 3.6 Equilibrium melting temperatures for pure LLDPE and the blends

Sample	$T_m°$ / °C	R^2
Pure LLDPE	136.0	0.9864
95/5 w/w LLDPE/wax	135.1	0.9950
90/10 w/w LLDPE/wax	134.0	0.9923
80/20 w/w LLDPE/wax	130.0	0.9897
70/30 w/w LLDPE/wax	129.0	0.9225
60/40 w/w LLDPE/wax	128.5	0.9170

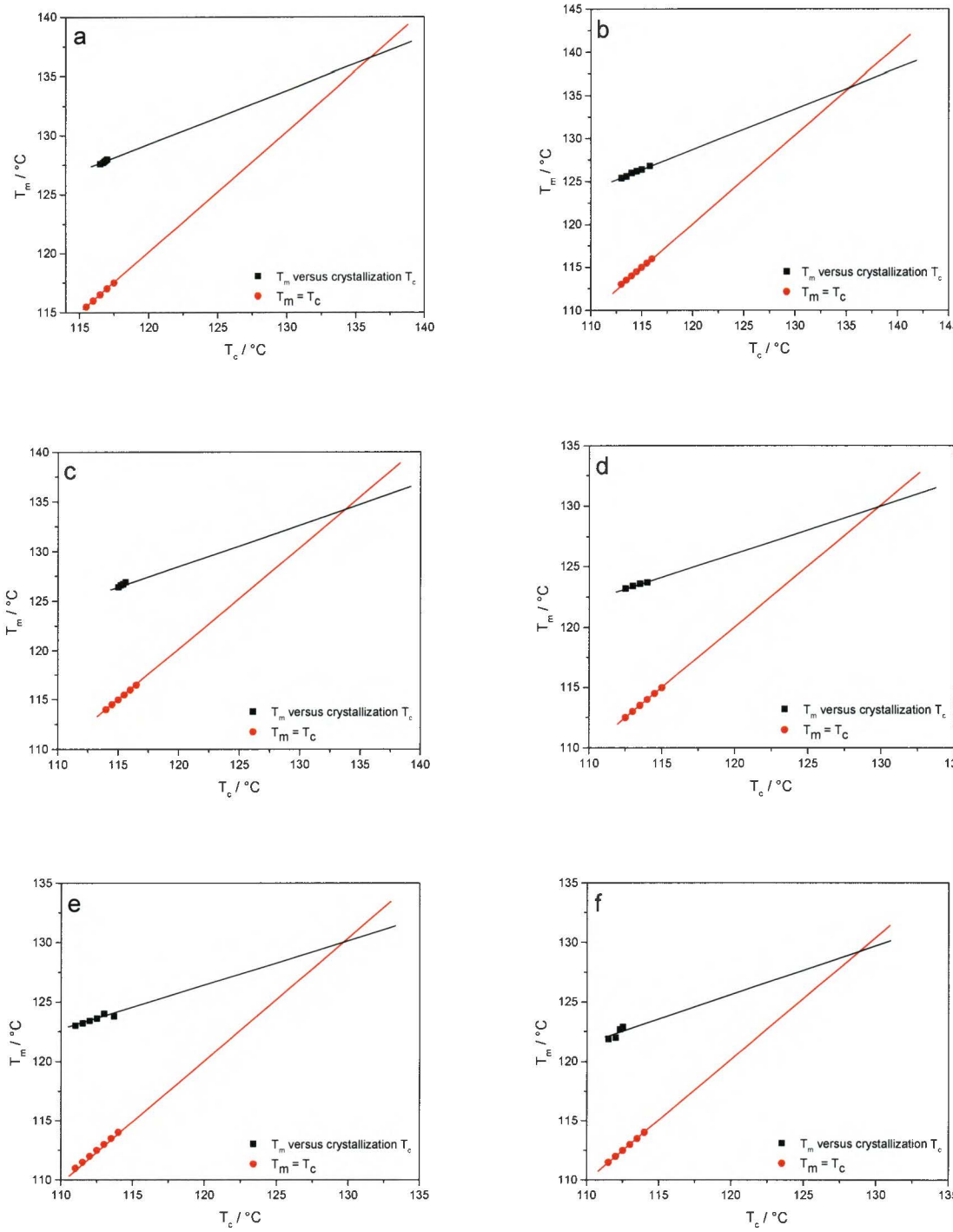

Figure 3.13 Hoffman-Weeks plots of (a) LLDPE, (b) 95/5 w/w LLDPE/wax, (c) 90/10 w/w LLDPE/wax, (d) 80/20 w/w LLDPE/wax, (e) 70/30 w/w LLDPE/wax, and (f) 60/40 w/w LLDPE/wax

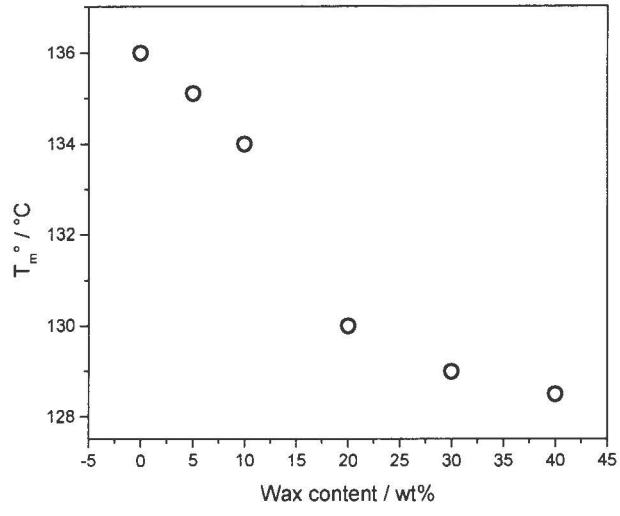

Figure 3.14 The dependence of the equilibrium melting temperature on the wax content

The data were treated according to the Flory-Huggins theory for polymer-diluent mixtures in order to observe if wax behaved like a classic low molecular weight diluent. Equation 3.3 is very similar to the classical expression for the depression of the melting temperature of low molecular weight binary systems. The only difference results from the expression for the activity of the crystallizing polymer component in the molten phase [33]. The values obtained from plotting $[(1/T_m - 1/T_m^\circ)/v_1] \times 10^3$ versus $(v_1/T_m) \times 10^3$ (Equation 3.3) are reported in Table 3.7, and the values plotted in Figure 3.15. A hyperbolic curve is observed, which differs from the simple linear trend expected from the equation. This is due to the non-uniform distribution of short chain branching density along the LLDPE main chain, which can interact with the wax structure [32]. The non-linearity indicates that the interaction between wax and LLDPE is complex and depends on the composition, and therefore the enthalpy of fusion per mole of repeating unit (ΔH_u) cannot be simply obtained. This is because the melting enthalpy per mole of repeat unit is independent of the structure and chemical nature of the diluent [33].

$$\frac{\frac{1}{Tm}-\frac{1}{Tm^\circ}}{v1} = \frac{R}{\Delta Hu}\frac{Vu}{V1}\left(1 - \frac{BV1}{R}\frac{v1}{Tm}\right) \qquad (3.3)$$

Table 3.7 Calculated data for $[(1/T_m - 1/T_m°)/v_1]$ x10^3 versus (v_1/T_m) x 10^3

(v_1/T_m) x 10^3	$[(1/T_m - 1/T_m°)/v_1]$ x10^3
0.402	17.0
0.800	8.22
1.609	4.31
2.441	3.22
3.262	2.37

T_m - apparent melting point; $T_m°$ - equilibrium melting temperature; v_1 - volume fraction of wax; ΔH_u- melting enthalpy per mole of repeating unit; R - gas constant; B - the interaction energy density character of the polymer-diluent pair

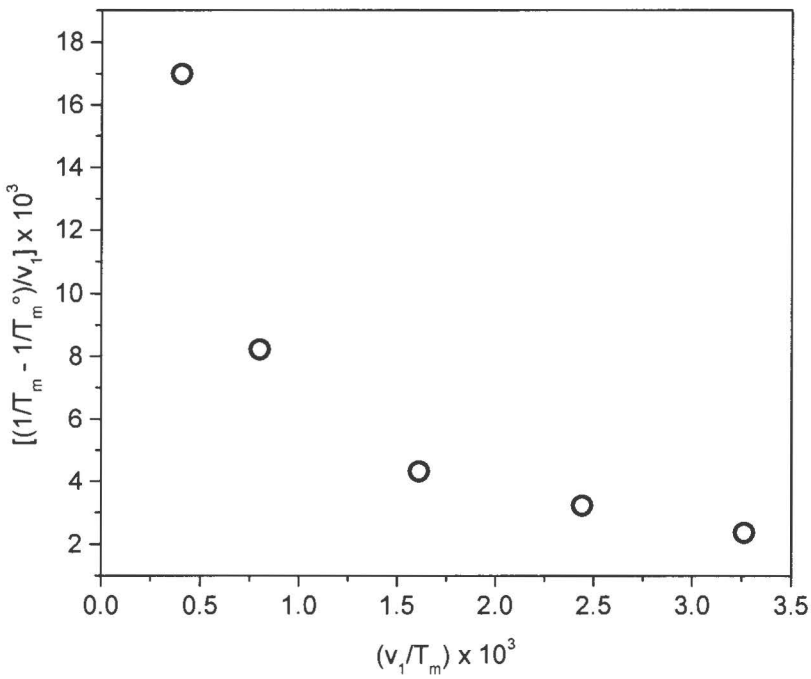

Figure 3.15 Graph of $[(1/T_m - 1/T_m°)/v_1]$ x10^3 versus (v_1/T_m) x 10^3

3.4 Polyethylene crystallization kinetics

The isothermal crystallization curves of all the samples at various T_c temperatures are shown in Figure 3.16. The crystallization temperatures, T_c, differ for the different samples as a result of the

different amounts of wax that has a plasticizing effect on the LLDPE matrix. As the T_c temperatures increase, the peak positions shift along the time axis and become broader and less intense. This is because at higher temperatures the samples require longer times to complete the crystallization process due to an increase in chain mobility. Therefore, the nucleation processes become more difficult, since the chains tend to attach and detach [2,34].

The data presented in Figure 3.17 represents the inverse of the experimentally determined half-crystallization time (the time needed to reach 50% relative crystallinity, or the time that the sample needs to develop half the amount of crystals it will eventually produce) as a function of isothermal crystallization temperature. The inverse of the experimentally determined half-crystallization time is a quantity proportional to the overall crystallization rate (which includes both nucleation and growth). The experimental half-crystallization time is close to the minimum of the isotherms presented in Figure 3.16 and corresponds to the changeover to a slower kinetic process due to impingement of adjacent spherulites. The overall crystallization rate decreased with increasing crystallization temperature. This is attributed to an increase in chain mobility and a decrease in melt viscosity as the crystallization temperatures increase, resulting in the chains attaching to and detaching from the crystal growth front, and causing the nucleation processes to become more difficult because only chain segments that form nuclei with the right stability (large enough surface/volume ratio) survive. The probability of detachment increases as the melting temperature, T_m, is approached. Above T_m no nucleation is possible [2]. This is true for both primary and secondary nucleation, both of which decrease in probability as the T_c increases. In highly flexible polymers that crystallize very fast, like PE, only the curves shown in Figure 3.17 are experimentally possible with standard DSC techniques. The solid lines shown in Figure 3.17 correspond to the Lauritzen-Hoffman (L-H) theory, and Equation 3.4 [35] was used to calculate these lines.

$$\frac{1}{\tau_{50\%}}(T) = G_0^{\tau} exp\left(\frac{-U^*}{R(T_c - T_\alpha)}\right) exp\left(\frac{-K_g^{\tau}}{T\Delta Tf}\right) \qquad (3.4)$$

Where G_o^{τ} is a pre-exponential factor that includes the nucleation and growth rate constant. The first term is controlled by diffusion, and U^* is the activation energy for the transport of the chain

to the growing front (a value of 1500 calmol^{-1} is usually employed). R is the gas constant, T_c the isothermal crystallization temperature, and T_α is the temperature at which chain mobility ceases and which is usually taken as T_g–30 K. The second term is a nucleation term where ΔT is the supercooling defined as ($T_m^\circ - T_c$), with T_m° the equilibrium melting point. The factor f is a temperature correction term equal to $2T_c/(T_c+T_m^\circ)$, and K_g is a constant. In this case, the crystallization rate is approximated to the experimentally determined values of the inverse of half crystallization times ($1/\tau_{50\%}$) obtained by DSC, so that K_g will be proportional to the energy barrier for nucleation and growth. The value of K_g is given by Equation 3.5 according to the L-H theory [35].

$$K_g^\tau = \frac{j b_0 \sigma \sigma_e T_m^0}{k \Delta h_f} \qquad (3.5)$$

where j is taken as 2 for Regime II, b_0 is the diameter of the chain, σ is the lateral surface free energy, σ_e is the fold surface energy, k is the Boltzmann constant and Δh_f is the heat of fusion of a perfect crystal. From the value of K_g, the product $\sigma\sigma_e$ is obtained according to Equation 3.5. Equations 3.6 and 3.7 allow the calculation of σ (and therefore σ_e) and q, the work done by the chain to form a fold.

$$\sigma = 0.1 \Delta h_f \sqrt{a_0 b_0} \qquad (3.6)$$

$$q = 2 a_0 b_0 \sigma_e \qquad (3.7)$$

where $a_0 b_0$ is the cross sectional area of the chain[35].To obtain the parameters of the L-H theory, the following values were used: T_g=231 K, T_g–30K,ΔH=280 J g^{-1}, a_0=4.55 Å, b_0=4.15 Å, ρ_c=1.014 g cm^{-3}, U^*=1500 calmol^{-1}, T_m° corresponds to that reported for each of the samples (Section 3.3, Table 3.6). It is observed that the L-H theory can satisfactorily fit the experimental data for all the wax contents over the full investigated temperature range.

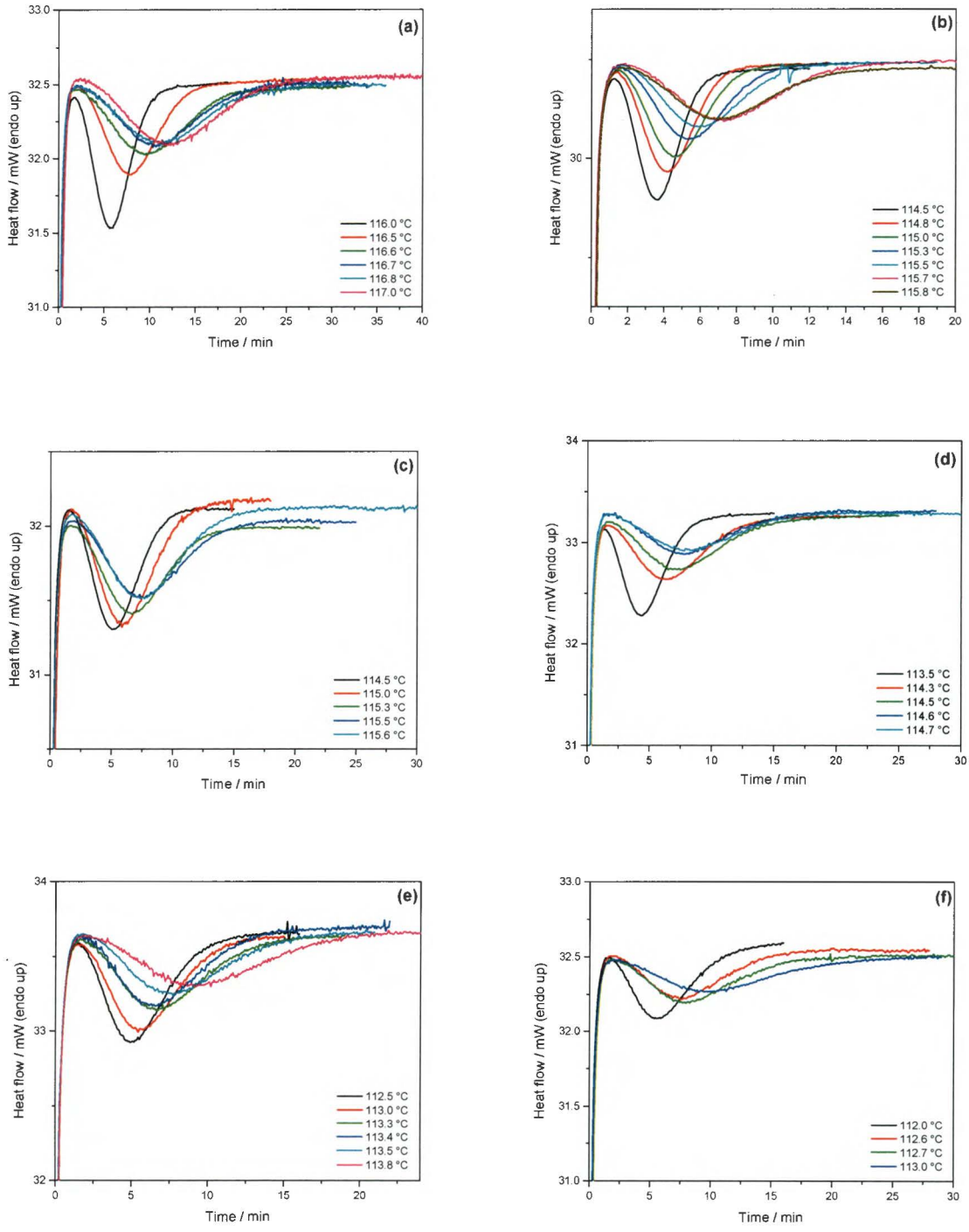

Figure 3.16 Isothermal crystallization curves of (a) LLDPE, (b) 95/5 w/w LLDPE/wax, (c) 90/10 w/w LLDPE/wax, (d) 80/20 LLDPE/wax, (e) 70/30 w/w LLDPE/wax, and (f) 60/40 w/w LLDPE/wax at various T_c temperatures

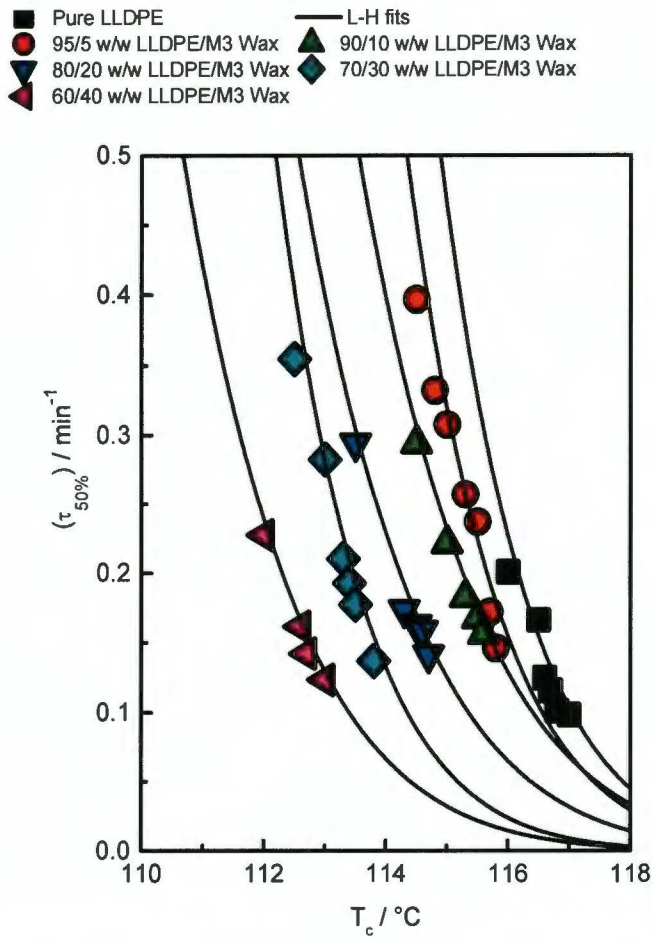

Figure 3.17 Lauritzen-Hoffman (L-H) fits for the overall crystallization rate as a function of the crystallization temperature

Another way to examine the results presented in Figure 3.17 is by taking a constant value of $1/\tau_{50\%}$ (in this case 0.2 min^{-1}) and plotting the crystallization temperature, needed to achieve this constant overall crystallization, as a function of wax content (Figure 3.18(a)). It is clear that the crystallization temperature, T_c, decreases with increasing wax content, which is due to the dilution effect of the wax on LLDPE. Figure 3.18(b) shows a plot of the overall crystallization rate needed to achieve a constant crystallization temperature (115 °C) as a function of wax content. This graph also shows that the overall crystallization rate of LLDPE decreases with increasing wax content. In fact, the dilution effect of the wax is the reason why the equilibrium melting temperature of LLDPE is depressed (Section 3.3, Table 3.6). Therefore, at the same crystallization rate, LLDPE and LLDPE/wax blends have different supercoolings.

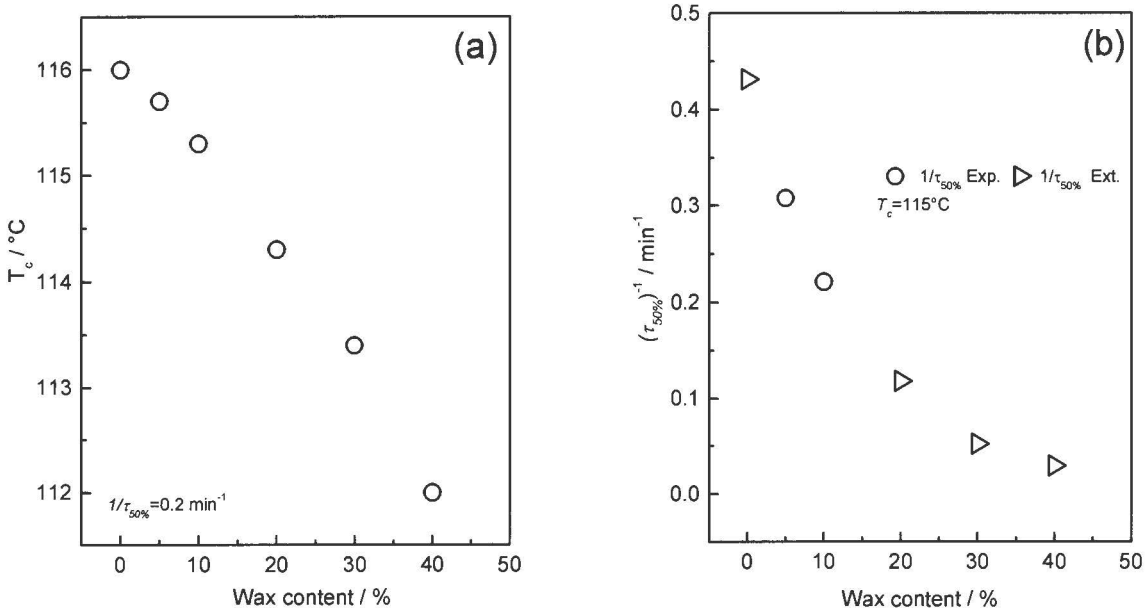

Figure 3.18 (a) Crystallization temperature as a function of wax content at constant $1/\tau_{50\%}$=0.2 min^{-1}; (b) Overall crystallization rate as a function of wax content at constant T_c=115°C

The Avrami theory [36-38] is the most popular theory used to model isothermal crystallization kinetics employing overall crystallization rate data (i.e., data that includes nucleation and growth measurements, like those performed by DSC).Avrami fittings of the data were performed by using a plug-in to the Origin® graphics software, developed by Lorenzo *et al.* [39]. This plug-in allows one to verify the reliability of the procedure by graphically comparing the experimental and calculated Avrami trends. An example of such a comparison is shown in Figure 3.19 for the 80/20 w/w LLDPE/wax blend, isothermally crystallized at 114.7 °C. The comparison between the experimental results and the corresponding Avrami prediction for the isothermally crystallized samples is shown in Figure 3.19. Figure 3.19(a) shows the data obtained from integration of the DSC isotherm and the vertical purple dashed lines indicate the integration range used. The vertical green dashed lines indicate the half crystallization time found experimentally. Figure 3.19(b) shows a plot of 1-V_c or the relative amorphous fraction as a function of crystallization time derived from an integration of the data in Figure 3.19(a). A typical sigmoidal shape describes the kinetics of transformation to the semicrystalline state. In

this case the data is well described by the Avrami equation up to a conversion fraction of 0.8 (or 80%). Figure 3.19(c) shows the experimental data (circles) obtained from the isothermal crystallization and the solid line represents the Avrami fit according to Equation 3.8.

$$1 - V_c = \exp(-K(t-t_0)^n) \qquad (3.8)$$

Analysis of the Avrami plot allows one to determine the Avrami index n from the slope and the overall crystallization rate constant, K, from the intercept of the linear fit [36-38]. In Equation 3.8, the Avrami index can be considered as a first approximation to be composed of two terms:

$$n = n_d + n_n \qquad (3.9)$$

where n_d represents the dimensionality of the growing crystals which can have only integer values of 1, 2 or 3 corresponding to the one-, two- or three-dimensional entities that are formed. The time dependence of the nucleation is represented by n_n. In principle its value should be either 0 or 1, where 0 corresponds to instantaneous nucleation and 1 to sporadic nucleation. t_0 is the induction time (which in this case includes the stabilization time) and was deduced from the time t at which the experiment was started. V_c is the relative volumetric transformed fraction [39]. The normalised crystallization enthalpies as function of the crystallization time from the experimental results correlates well with the Avrami fit (Figure 3.19(d)). This indicates that the Avrami model predicts very well the isothermal crystallization.

The kinetic parameters for all the investigated samples are tabulated in Table 3.8. It can be clearly seen that the values of n did not change significantly with wax addition and with an increase in the T_c temperatures. This indicates that the incorporation of wax does not significantly influence the mechanism of nucleation and growth of the LLDPE crystals under the experimental conditions used [40]. The Avrami index values are between 2.5 and 2.8 for all the samples. These values are close to 3, which is an expected result for LLDPE [41,42], which normally has a high density of active nuclei. This value indicates that the crystal geometry is spherulitic and follows an athermal nucleation which leads to spherulites of roughly the same size during isothermal crystallization [42]. The time dependence of the nucleation indicates an

instantaneous nucleation of spherulites which implies that the nucleation is very fast, and starts almost immediately after the isothermal crystallization temperature has been reached [39]. It is also observed that the half crystallization times for the experimental data ($t_{1/2}$(e)) and the Avrami fittings ($t_{1/2}$(t)) are almost the same, which indicates that the Avrami model very well predicts the crystallinity up to 50% relative crystallinity. This is further supported by the very good correlation coefficients that are close to 1 in all the cases. An R^2 value of at least 0.9990 is usually required for a good fit, because the equation has been linearized by the use of double logarithms [39]. A conversion range of approximately 3–20% is used and this corresponds to the primary crystallization range where the Avrami analysis is most adequate. In such a range the correlation coefficients of the fit are always in excess of 0.999 (Table 3.8).

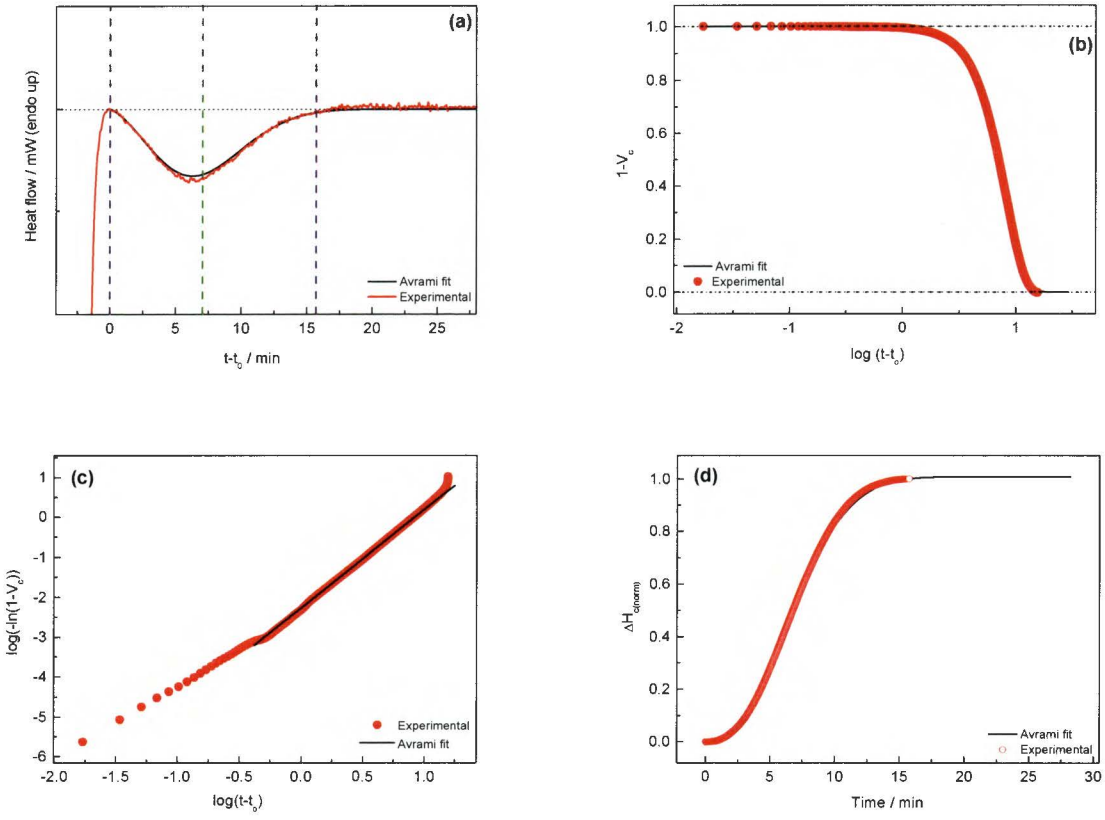

Figure 3.19 Comparison between experimental results and the corresponding Avrami prediction for an 80/20 w/w LLDPE/wax blend isothermally crystallized at 114.7 °C: a) isothermal heat flow; b) unconverted relative fraction; c) Avrami plot; d) normalized ΔH_c as a function of time

Table 3.8 Kinetic parameters for all the investigated samples

	T_c / °C	t_o/ min	ΔH / J g^{-1}	V_c range / %	n	K / min^{-n}	R^2	$t_{1/2}$ (t) / min	$t_{1/2}$ (e) / min	$(\tau_{1/2})^{-1}$/ min^{-1}
LLDPE	116.0	1.84	48	3-20	2.7	0.0092	0.9999	5.02	4.98	0.2008
	116.5	2.21	39	3-20	2.7	0.0054	0.9999	6.11	6.02	0.1661
	116.6	2.30	40	3-20	2.5	0.0039	0.9997	8.30	8.02	0.1247
	116.7	2.43	39	3-20	2.5	0.0028	0.9997	9.06	8.64	0.1157
	116.8	2.21	44	3-20	2.5	0.0020	0.9999	10.1	9.89	0.1011
	117.0	2.86	43	3-20	2.5	0.0021	0.9998	10.5	10.2	0.0983
95/5 w/w LLDPE/ wax	114.5	1.28	35	3-20	2.8	0.0515	0.9999	2.51	2.52	0.3968
	114.8	1.38	34	3-20	2.8	0.0318	0.9999	3.02	3.01	0.3322
	115.0	1.60	32	3-20	2.6	0.0308	0.9999	3.31	3.25	0.3077
	115.3	1.68	30	3-20	2.6	0.0187	0.9998	4.00	3.89	0.2571
	115.5	1.73	40	3-20	2.7	0.0150	0.9999	4.27	4.22	0.2370
	115.7	1.99	39	3-20	2.7	0.0061	0.9999	5.82	5.81	0.1721
	115.8	1.92	41	3-20	2.8	0.0038	0.9999	6.52	6.85	0.1460
90/10 w/w LLDPE/ wax	114.5	1.50	39	3-20	2.7	0.0250	0.9999	3.39	3.40	0.2941
	115.0	1.85	36	3-20	2.6	0.0140	0.9999	4.55	4.52	0.2212
	115.3	1.77	20	3-20	2.8	0.0064	0.9999	5.43	5.47	0.1828
	115.5	2.21	20	3-20	2.5	0.0077	0.9999	6.03	5.98	0.1672
	115.6	1.84	44	3-20	2.6	0.0057	0.9998	6.49	6.41	0.1560
80/20 w/w LLDPE/ wax	113.5	1.43	37	3-20	2.8	0.0237	0.9998	3.39	3.40	0.2941
	114.3	1.82	37	3-20	2.5	0.0093	0.9999	5.84	5.76	0.1736
	114.5	1.80	19	3-20	2.5	0.0071	0.9999	6.21	6.14	0.1629
	114.6	2.24	35	3-20	2.5	0.0131	0.9993	6.83	6.31	0.1585
	114.7	1.79	32	3-20	2.5	0.0054	0.9998	7.22	7.09	0.1410
70/30 w/w LLDPE/ wax	112.5	1.43	33	3-20	2.7	0.0457	0.9999	2.78	2.82	0.3546
	113.0	1.63	29	3-20	2.7	0.0240	0.9999	3.53	3.54	0.2825
	113.3	1.82	30	3-20	2.5	0.0145	0.9998	4.84	4.76	0.2101
	113.4	1.77	29	3-20	2.7	0.0090	0.9999	5.16	5.19	0.1927
	113.5	1.72	31	3-20	2.6	0.0073	0.9999	5.61	5.64	0.1773
	113.8	2.16	24	3-20	2.7	0.0033	0.9999	7.41	7.31	0.1368
60/40 w/w LLDPE/ wax	112.0	1.99	22	3-20	2.5	0.0157	0.9999	4.49	4.40	0.2273
	112.6	2.07	21	3-20	2.5	0.0058	0.9998	6.27	6.19	0.1616
	112.7	1.84	23	3-20	2.6	0.0041	0.9999	7.11	7.04	0.1421
	113.0	2.38	20	3-20	2.5	0.0035	0.9999	8.23	8.11	0.1233

Table 3.9 The Lauritzen-Hoffman theory parameters for LLDPE and the blends

System	$K_g x10^{-4} / K^2$	σ / erg cm^{-2}	σ_e / erg cm^{-2}	q $x10^{13}$ / erg	R^2
LLDPE	20.2	12.3	187.1	7.07	0.90197
95/5 w/w LLDPE/wax	18.0	12.3	166.6	6.29	0.94429
90/10 w/w LLDPE/wax	14.1	12.3	130.7	4.94	0.99832
80/20 w/w LLDPE/wax	15.0	12.3	139.7	5.28	0.98686
70/30 w/w LLDPE/wax	20.2	12.3	188.3	7.11	0.98260
60/40 w/w LLDPE/wax	16.0	12.3	149.1	5.63	0.98928

Even though the model of nucleation and growth proposed by Lauritzen and Hoffman has been under much criticism lately, it is still one of only a few models that provide easy to use analytical expressions capable of fitting the experimental data (even though the physical meaning of some of the fitting parameters could be questionable) and it is therefore widely used. Although the LH theory was originally derived for growth only (i.e., secondary nucleation), it can describe the experimental data shown in Figure 3.17. The first term in Equation 3.4 is controlled by diffusion and the second term is a secondary nucleation term, which has contributions from both nucleation and growth [42]. One of the most important parameters that can be obtained through L–H treatment is the nucleation parameter (K_g), which is related to the product of lateral and fold surface free energies (Equation 3.5) [43]. The L-H parameters for the LLDPE in the LLDPE/wax blends are tabulated in Table 3.9.It can be seen that that the nucleation parameter (K_g), fold surface energy (σ_e), and the work done by the chain to form a fold (q) (obtained using Equations 3.5, 3.6 and 3.7) do not show a specific trend, and the correlation coefficient values are much lower than the preferred value of 0.99.No definite conclusions can therefore be drawn, and a much larger number of data points are needed to obtain values that can be trusted and discussed.

3.5 Wax crystallization kinetics

Since the isothermal crystallization analyses for pure wax was not successful due to its very fast crystallization, a non-isothermal approach was used to determine the crystallization kinetics of the wax. Pure wax and the 70/30 w/w LLDPE/wax blend were used to study the crystallization behaviour of the wax. The DSC curves of (a) pure wax and (b) wax in the 70/30 LLDPE/wax blend at different scanning rates of 5, 10, 20 and 40 °C $min^{-1}$are shown in Figure 3.20. In this case the same sample mass was used for all the analyses. As the cooling rate increased, the exothermic crystallization peaks became more intense and shifted to lower temperatures, which is a normal observation in thermal analysis because of differences in heat transfer and supercooling effects.

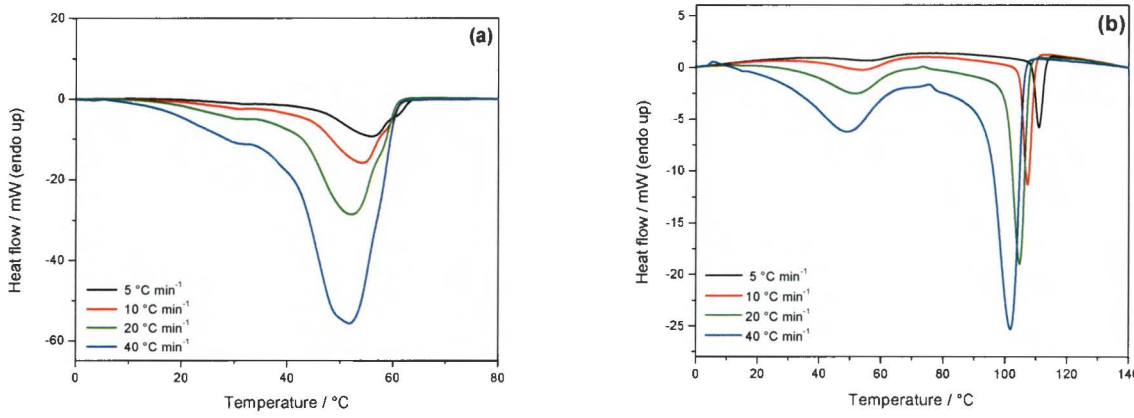

Figure 3.20 DSC curves of (a) pure wax at a constant sample mass of 10 mg and (b) 70/30 LLDPE/wax blend at a constant sample mass of 5 mg for different scanning rates of 5, 10, 20 and 40 °C min^{-1}

Figure 3.21 shows the DSC curves of (a) pure wax and (b) wax in the 70/30 LLDPE/wax blend for sample masses inversely proportional to the scanning rates. The crystallization peak sizes and shapes of the wax in the blend, for the samples analysed at different cooling rates and sample masses, are almost the same. This shows that the supercooling effects could be eliminated by reducing the sample mass in proportion to the increasing cooling rate [16]. The faster the cooling rate, the smaller the sample mass should be, in order to reduce the thermal gradients in the sample caused by the heat transfer from the sample pan to the sample. The crystallization

temperatures and enthalpies determined from the DSC curves in Figures 3.20 and 3.21 are summarized in Table 3.10. It can be seen that all these values strongly depend on the cooling rate, except where the sample mass was reduced in proportion to the increasing cooling rate. The cooling rate still has an effect, but it is much less pronounced.

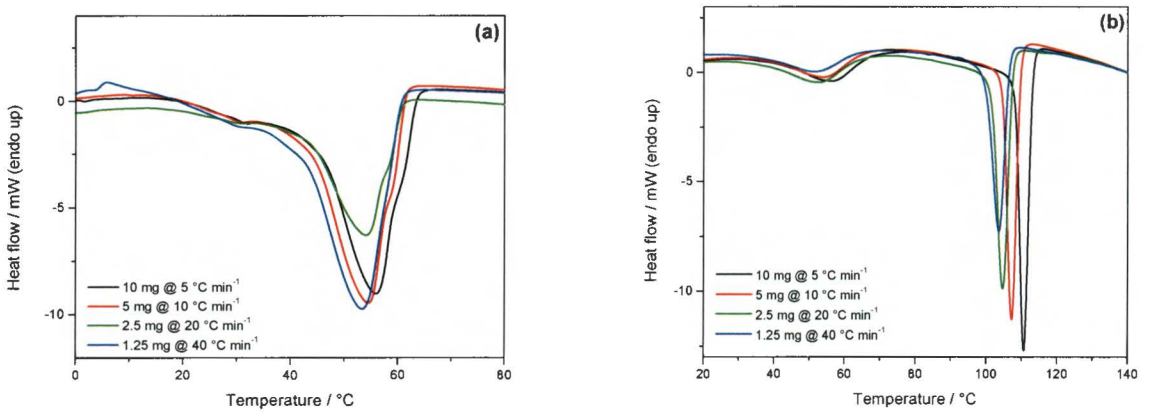

Figure 3.21 DSC curves of (a) pure wax and (b) 70/30 LLDPE/wax blend using sample masses inversely proportional to the scanning rate

In order to obtain the kinetic information, the experimental data presented in Figures 3.20 and 3.21 needed to be converted to relative crystallinity (X_t),which was obtained by partial integration of the crystallization exotherm at specific temperature intervals divided by the total area of the crystallization exotherm [42]. The relative crystallinity curves are shown in Figure 3.22. These curves show an approximately reversed sigmoidal shape, with a fast primary crystallization in the early stages and a slow secondary crystallization at later stages. As the cooling rate increased, the relative crystallinity of the sample at a specific crystallization temperature decreased (Figures 3.22). This is attributed to the smaller time scale which did not allow the polymer to crystallize completely [44].

Table 3.10 Parameters of samples crystallized non-isothermally

Sample	Cooling rate /°C min^{-1}	Sample mass / mg	ΔH_c / J g^{-1}	T_c / °C
Pure wax	5	10	115	56.2
	10	10	98	54.4
	20	10	88	52.7
	40	10	82	52.1
Pure wax	5	10	115	56.2
	10	5	119	54.9
	20	2.5	110	54.3
	40	1.25	117	53.9
70/30 w/w LLDPE/wax	5	5	15	56.8
	10	5	23	53.7
	20	5	30	51.6
	40	5	30	48.6
70/30 w/w LLDPE/wax	5	10	24	56.2
	10	5	23	53.7
	20	2.5	23	53.0
	40	1.25	20	51.3

The data can further be analysed by converting the temperature scale of the X_t function into a time scale, using Equation 3.10,

$$t = \frac{|To - T|}{\phi} \qquad (3.10)$$

where T is the temperature at time t, T_o is the onset temperature of crystallization at $t = 0$, and φ is the cooling rate. The relative crystallinity as function of time can then be obtained and the converted curves are shown in Figure 3.23. It can be clearly seen that all the curves showed similar sigmoidal shapes and the time for complete crystallization increased as the cooling rate decreased. The crystallization time was significantly increased when the cooling rate was 5 °C min^{-1}. This is probably because the slow cooling rate provided better diffusivity for the

molecules, because of their low viscosity, and allowed more time for the chains to crystallize [44-45].

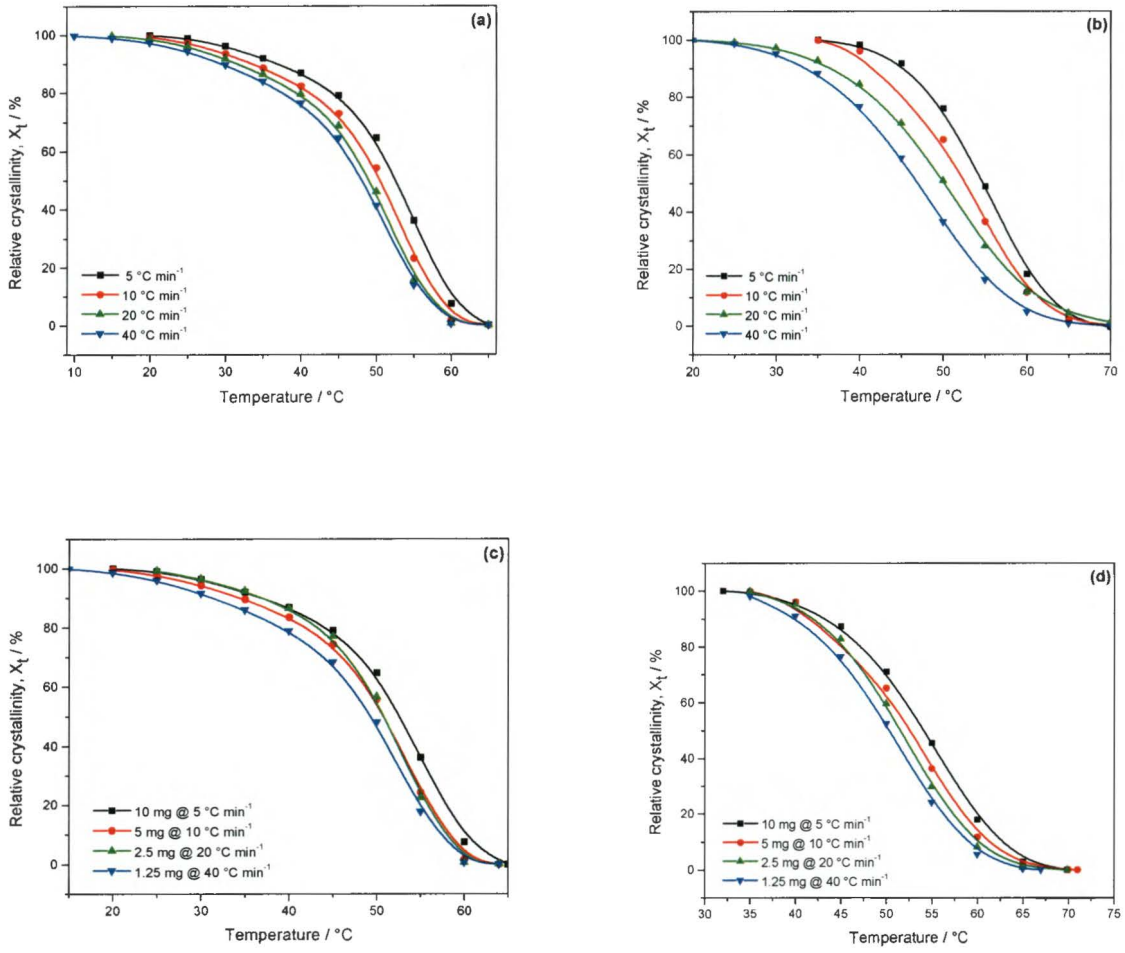

Figure 3.22 Plot of X_t versus crystallization temperature for(a) pure wax at a constant sample mass of 10 mg, (b) 70/30 LLDPE/wax blend at a constant sample mass of 5 mg, (c) pure wax and (d) 70/30 LLDPE/wax blend using sample masses inversely proportional to the scanning rates

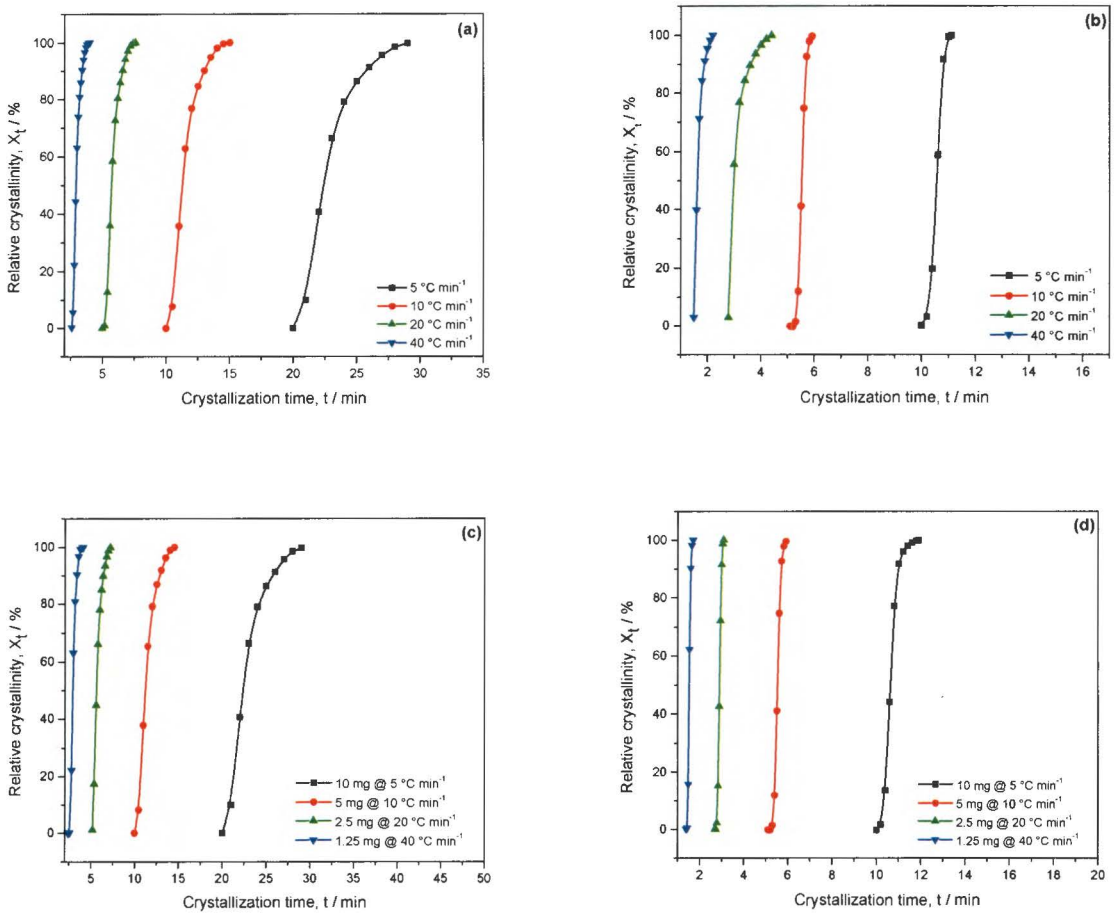

Figure 3.23 Plot of X_t versus crystallization time for (a) pure wax at a constant sample mass of 10 mg, (b) 70/30 LLDPE/wax blend at a constant sample mass of 5 mg, (c) pure wax and (d) 70/30 LLDPE/wax blend using sample masses inversely proportional to the scanning rates

Jeziorny-modified Avrami equation

To study the kinetic parameters for the non-isothermal crystallization processes, several methods were developed by Jeziorny [46] and Mo [47-49], and their models are based on the Avrami equation [35-37]. Equation 3.12 is the logarithmic form of Equation 3.11.

$$1 - X_t = \exp(-Zt^n) \qquad (3.11)$$

$$\ln[-\ln(1 - X_t)] = \ln Z + n\ln t \quad (3.12)$$

where X_t, Z and n respectively denote the relative crystallinity, crystallization rate constant and Avrami exponent. Both Z and n do not have the same physical meaning as in isothermal crystallization, because under non-isothermal crystallization the temperature changes constantly. This affects the rate of crystal formation since it is temperature dependent. In this case both Z and n can be considered as adjustable parameters for data fitting [45]. Considering the non-isothermal character of the investigated process, Jeziorny [46] suggested that the value of Z should be revised using the cooling rate, φ (Equation 3.13).

$$\ln z_c = (\ln Z)/\varphi \quad (3.13)$$

The plots of $\ln[-\ln(1-X_t)]$ versus $\ln t$ should give straight lines and the values of n and Z can be determined from the slope and intercept, respectively. These plots for the non-isothermal crystallization of pure wax and wax in the 70/30 w/w LLDPE/wax blend are shown in Figure 3.24. It can be seen that the linearity of the plots is very poor, suggesting that the Avrami analysis does not effectively describe the non-isothermal crystallization kinetics in this case. Each curve shows a slight deviation and exhibits an almost parallel linear portion at the beginning of crystallization, indicating a similar nucleation mechanism and crystal growth geometries for the primary crystallization process at different cooling rates. However, the linear lines tend to level off during the later stage of crystallization, which is usually attributed to the presence of secondary crystallization caused by the slower crystallization and further perfection of crystals in the later stage.

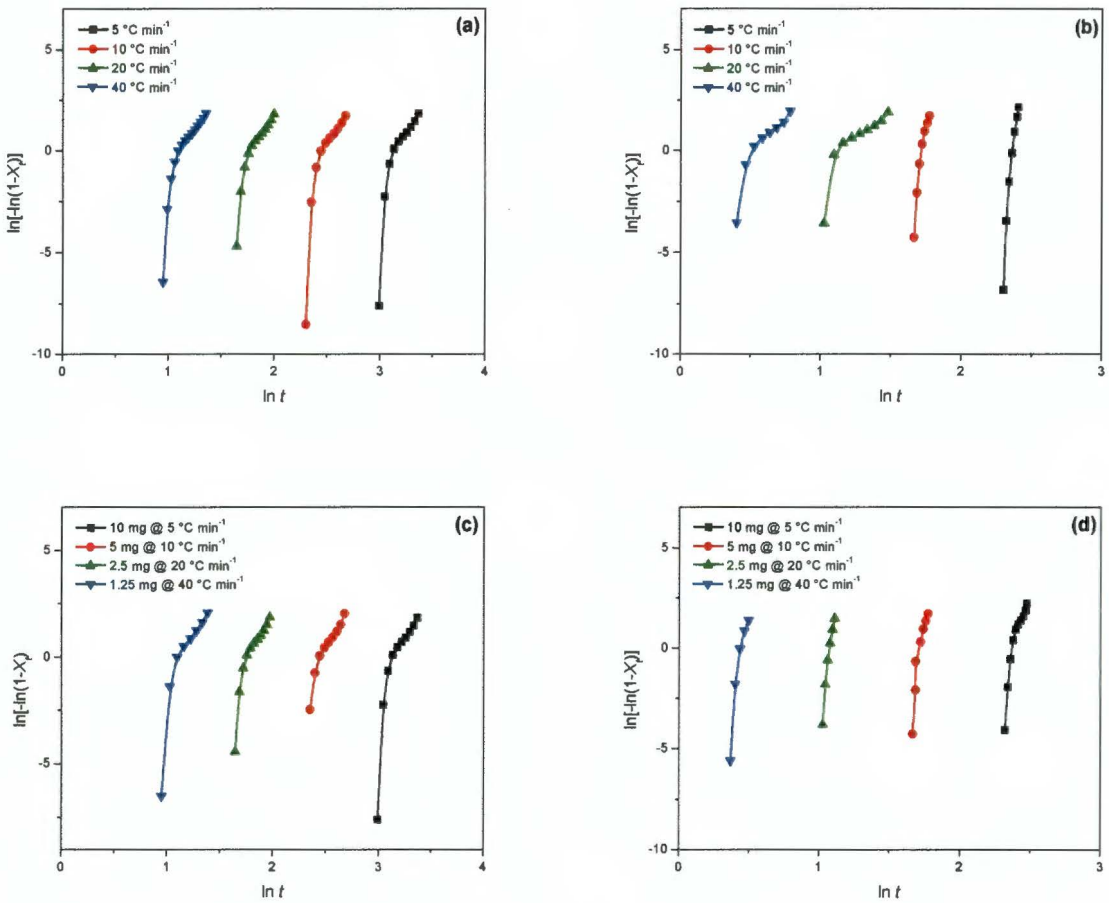

Figure 3.24 Plots of ln[-ln(1-X_t)] as a function of ln t for (a) pure wax at a constant sample mass of 10 mg, (b) 70/30 LLDPE/wax blend at a constant sample mass of 5 mg, (c) pure wax and (d) 70/30 LLDPE/wax blend using sample masses inversely proportional to the scanning rates

Ozawa equation

The Ozawa theory is an extension of the Avrami theory based on the assumption that non-isothermal crystallization may be equivalent to a series of infinitesimal small isothermal crystallization steps. According to the Ozawa theory [50], the evolution of X_t as a function of cooling rate for a given temperature T can be calculated using Equations 3.14 and 3.15.

$$1 - X_t = \exp\,[-K(t) / \varphi^m] \qquad (3.14)$$

$$\ln[-\ln(1 - X_t)] = \ln K(t) - m \ln \varphi \qquad (3.15)$$

where X_t is the relative crystallinity at temperature t, and m is the Ozawa exponent which depends on the nucleation and crystalline growth mechanisms and which is similar to the Avrami exponent n. $K(t)$ is a temperature cooling function, and is related to the overall crystallization rate. Equation 3.15 is the logarithmic form of Equation 3.14.

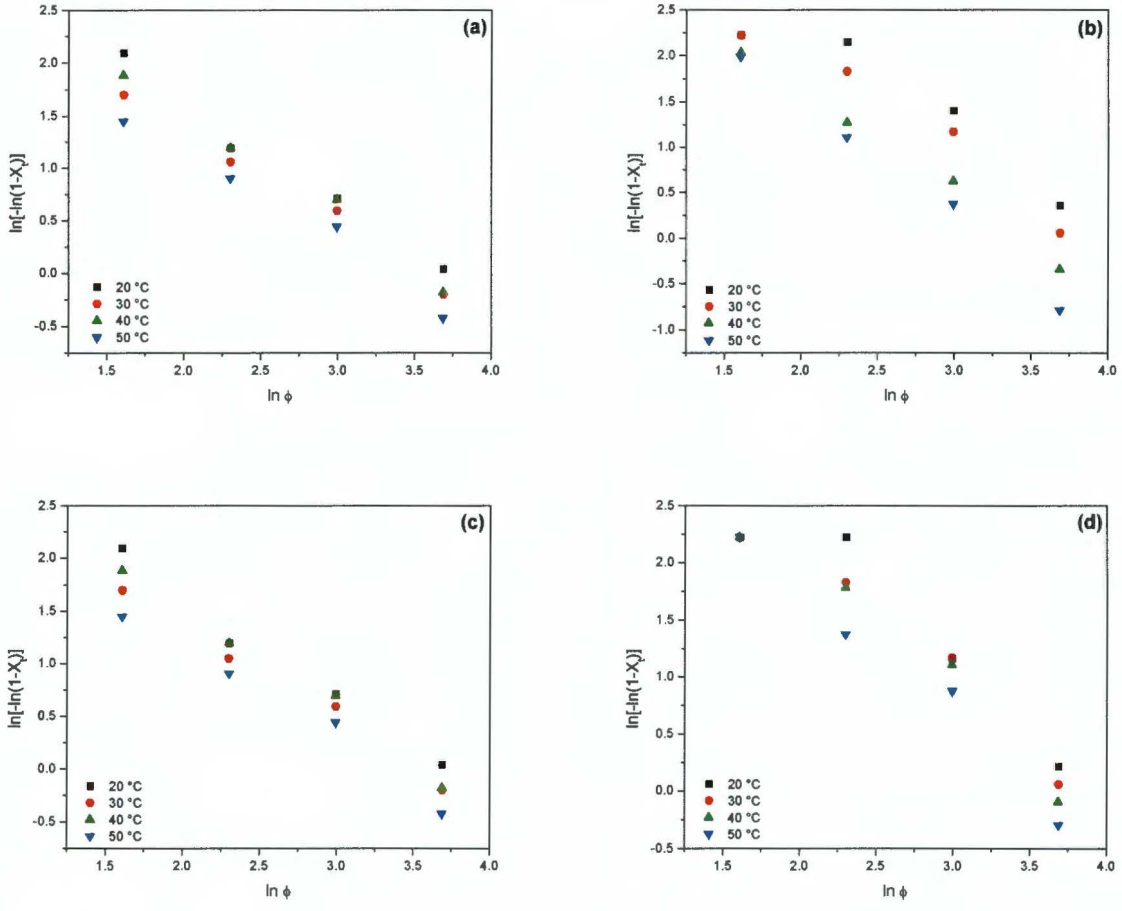

Figure 3.25 Ozawa plots of ln[-ln(1-X_t)]versus ln φ for (a) pure wax and (b) 70/30 w/w LLDPE/wax at different temperatures

The Ozawa plots of ln[-ln(1 - X_t)] versus ln φ in the temperature range of 20-50 °C for pure wax and the 70/30 w/w LLDPE/wax blend are shown in Figure 3.25. These plots were generated by taking a temperature, T, and plotting the crystallinity at that temperature against the corresponding cooling rate. All the plots are almost linear, and the X_t values calculated at

different temperatures decreased with increasing cooling rate. Linear regression analysis of the data in Figure 3.25 gave the values in Table 3.11. The ln *K(t)* values for the wax in the blend are higher than those of the unblended wax, which implies that the wax in the blend crystallized faster than the unblended wax. There are two possible reasons for this observation: (i) The LLDPE crystals could have acted as nucleation sites for wax crystallization, or (ii) less wax could have crystallized in the blend causing an increase in the rate of crystallization. Although there is some variation in the values of *m*, the values for all the samples are approximately 1, indicating that the crystal growth is one-dimensional (fibrillar/rod-like) with athermal nucleation, and that all the crystals started to grow at the same time [42]. The Ozawa approach very well describes the non-isothermal crystallization kinetics of wax.

Table 3.11 Non-isothermal crystallization kinetic parameters based on the Ozawa equation

Sample	Temperature / °C	*m*	Ln *K(t)*
[a]Pure wax	20	0.96	3.55
	30	0.89	3.14
	40	0.97	3.46
	50	0.88	2.92
[a]70/30 w/w LLDPE/wax	20	0.91	3.95
	30	1.03	4.05
	40	1.12	3.86
	50	1.31	4.13
[b]Pure wax	20	0.96	3.55
	30	0.89	3.14
	40	0.97	3.46
	50	0.88	2.92
[b]70/30 w/w LLDPE/wax	20	1.02	4.16
	30	1.03	4.05
	40	1.10	4.17
	50	1.16	4.12

'a' is for the same sample mass and 'b' is for sample masses inversely proportional to the scanning rates

Mo method (combination of Avrami and Ozawa equations)

The Mo method was developed by Liu *et al.* [48], and the simplified formula is:

$$\log Z_t + n \log t = \log K_t - m \log \varphi \tag{3.16}$$

$$\log \varphi = \log F(T) - a \log t \tag{3.17}$$

where a is the ratio of the Avrami exponent, n, to the Ozawa exponent, m. $F(T) = [K_t/Z_t]^{1/m}$ refers to the cooling rate chosen at the unit crystallization time when the measured system reached a given degree of crystallinity. At a given degree of crystallinity, the plots of log φ versus log t are shown in Figure 3.26. The values of $F(T)$ and a are tabulated in Table 3.12. According to Equation 3.17, $F(T)$ is the rate of crystallization at various degrees of crystallinity and is attributed to the amount of cooling required at a specific degree of crystallinity in unit time. The $F(T)$ values do not change with increasing degree of conversion in the case where the sample masses were changed, while it increased significantly with increasing degree of conversion where the sample mass was kept constant. This is probably due to the heat transfer and supercooling effects that were eliminated when the sample mass was changed, hence the same crystallization behaviour. The $F(T)$ values are significantly higher where the sample mass was changed, but the reason for this is unclear but must be related to the fact that $F(T)$ has no real physical significance and cannot be directly related to the rate of crystallization. The 'a' parameter for all the samples is approximately 1, which is in good agreement with the Ozawa exponent, indicating that the crystal growth of wax is one-dimensional (fibrillar/rod-like) with athermal nucleation signifying that the crystals started to grow at the same time [42]. This further implies that the ratio of n to m remained constant at different crystallinities and sample masses, indicating that the wax has short chains that pack parallel to each other [33]. We tried to confirm this through atomic force microscopy analysis, and although we did not get very convincing results, the micrograph in Figure 3.27 may confirm our conclusion from the crystallization kinetics results.

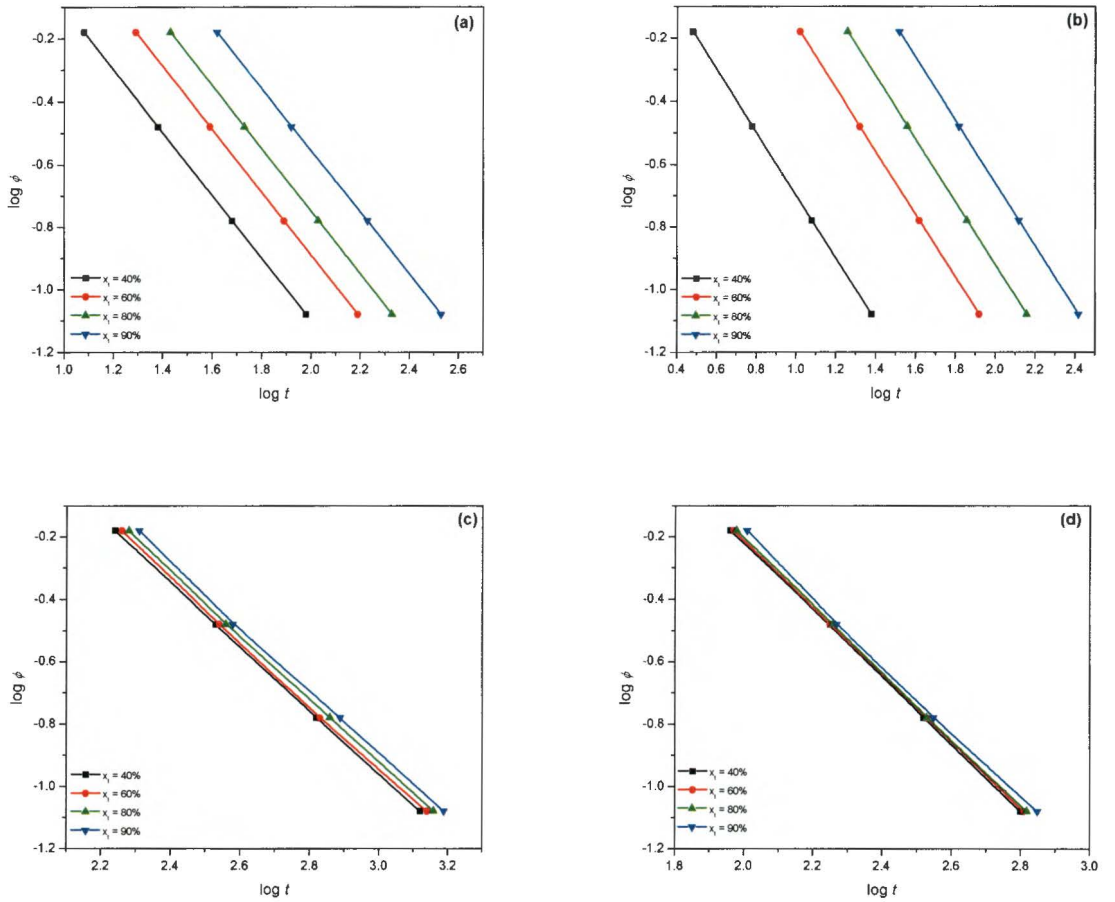

Figure 3.26 Plots of log φ as a function of log t at different relative crystallinities for (a) pure wax at a constant sample mass of 10 mg, (b) 70/30 LLDPE/wax blend at a constant sample mass of 5 mg, (c) pure wax and (d) 70/30 LLDPE/wax blend using sample masses inversely proportional to the scanning rates

Table 3.12 Non-isothermal crystallization kinetic parameters from a combination of the Avrami and Ozawa equations

X_t / %	40	60	80	90
10 mg wax samples cooled at 5, 10, 20 and 40 °C min^{-1}				
F(T) / °C s^{-1}	7.9	12.6	20.0	25.1
a	1.0	1.0	1.0	1.0
Wax: 10 mg at 5 °C min^{-1}, 5 mg at 10 °C min^{-1}, 2.5 mg at 20 °C min^{-1}, 1.25 mg at 40 °C min^{-1}				
F(T) / °C s^{-1}	125.9	125.9	125.9	158.5
a	1.0	1.0	1.0	1.0
5 mg 70/30 LLDPE/wax samples cooled at 5, 10, 20 and 40 °C min^{-1}				
F(T) / °C s^{-1}	2.0	6.3	12.6	20.0
a	1.0	1.0	1.0	1.0
70/30 LLDPE/wax: 10 mg at 5 °C min^{-1}, 5 mg at 10 °C min^{-1}, 2.5 mg at 20 °C min^{-1}, 1.25 mg at 40 °C min^{-1}				
F(T) / °C s^{-1}	85.1	85.1	85.1	87.1
a	1.1	1.1	1.1	1.1

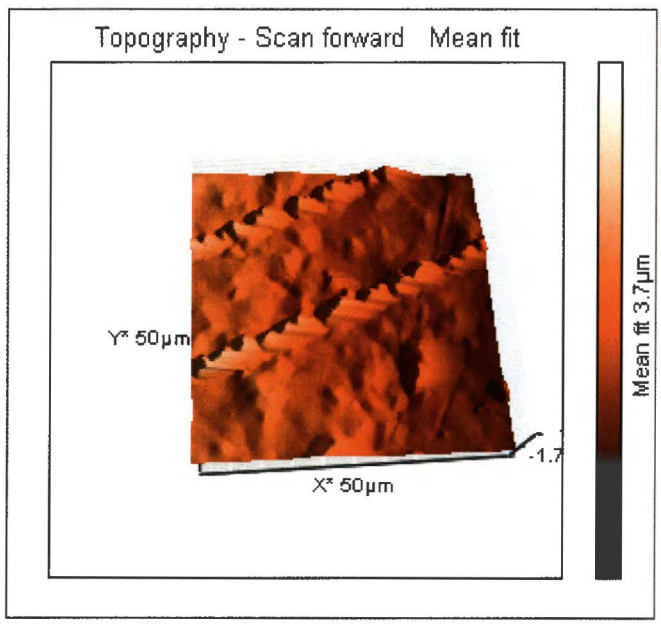

Figure 3.27 AFM micrographs for the 70/30 w/w LLDPE/wax blend

References

[1] T. Poltimäe, E. Tarasova, A. Krumme, J. Roots, A. Viikna. Thermal analyses of blends of hyperbranched linear low-density polyethylene (LLDPE) with high-density polyethylene and LLDPE prepared by dissolving method. Materials Science 2011; 17:254-259. DOI: 10.5755/J01.ms.17.3.589

[2] R.J. Young, P.A. Lovell. Introduction to Polymers, 3rd Edition.CRC Press, New York (2011).

[3] J.A. Molefi, A.S Luyt, I. Krupa. Comparison of LDPE, LLDPE and HDPE as matrices for phase change materials based on a soft Fischer-Tropsch paraffin wax. Thermochimica Acta 2010; 500:88-92. DOI: 10.1016/j.tca.2010.01.002

[4] M.E. Mngomezulu, A.S. Luyt, I. Krupa. Structure and properties of phase change materials based on HDPE, soft Fischer-Tropsch paraffin wax and wood flour. Journal of Applied Polymer Science 2010; 118:1541-1551. DOI: 10.002/app.32521

[5] I. Krupa, A.S. Luyt. Thermal properties of polypropylene/wax blends. Thermochimica Acta 2001; 372:137-141. DOI: 10.1016/S0040-6031(01)00450-6

[6] I. Krupa, A.S. Luyt. Thermal properties of uncross-linked and cross-linked LLDPE/wax blends. Polymer Degradation and Stability 2000; 70:111-117. DOI: 10.1016/S0141-3910(00)00097-5

[7] S.P. Hlangothi, I. Krupa, V. Djoković, A.S. Luyt. Thermal and mechanical properties of cross-linked and uncross-linked linear low-density polyethylene-wax blends.Polymer Degradation and Stability 2003; 79:53-59. DOI: 10.1016/S0141-3910(02)00238-0

[8] I. Krupa, A.S. Luyt. Thermal and mechanical properties of extruded LLDPE/wax blends. Polymer Degradation and Stability 2001; 73:157-161. DOI: 10.1016/S0141-3910(01)00082-9

[9] M.J. Hato, A.S. Luyt. Thermal fractionation and properties of different polyethylene/wax blends. Journal of Applied Polymer Science 2007; 104:2225-2236.

DOI: 10.1002/app.25494

[10] H.S. Mpanza, A.S. Luyt. Comparison of different waxes as processing agents for low density polyethylene. Polymer Testing 2006; 25:436-442.
DOI: 10.1016/j.polymertesting.2006.01.008

[11] I. Krupa, A.S. Luyt. Physical properties of blends of LLDPE and an oxidized paraffin wax. Polymer 2001; 42:7285-7289.
DOI: 10.1016/S0032-3861(01)00172-0

[12] F. Chen, M.P. Wolcott. Miscibility studies of paraffin/polyethylene blends as form-stable phase change materials. European Polymer Journal 2014; 52:44-52.
DOI: 10.1016/j.eurpolymj.2013.09.027

[13] A. Sari. Form-stable paraffin/high density polyethylene composites as solid–liquid phase change material for thermal energy storage: Preparation and thermal properties. Energy Conversion and Management 2004; 45:2033-2042.
DOI: 10.1016/j.enconman.2003.10.022

[14] M.E. Sotomayor, I. Krupa, A. Várez, B. Levenfeld. Thermal and mechanical characterization of injection moulded high density polyethylene/paraffin wax blends as phase change materials. Renewable Energy 2014; 68:140-145.
DOI: 10.1016/j.renene.2014.01.036

[15] B. Fillon, J.C. Wittmann, B. Lotz, A. Thierry.Self-nucleation and recrystallization of isotactic polypropylene (α phase) investigated by differential scanning calorimetry. Journal of Polymer Science Part B: Polymer Physics 1993; 31:1383-1393.
DOI: 10.1002/polb.1993.090311013

[16] A.J. Müller, M.L. Arnal. Thermal fractionation of polymers. Progress in Polymer Science 2005; 30:559-603.
DOI: 10.1016/j.progpolymsci.2005.03.001

[17] M.L. Arnal, J.J. Sanchez, A.J. Müller. Miscibility of linear and branched polyethylene blends by thermal fractionation: Use of the successive self-nucleation and annealing (SSA) technique. Polymer 2001; 42:6877-6890.
DOI: 1016/s0032-3861(01)00177-X

[18] J. Kong, X. Fan, Y. Xie, W Qiao. Study on molecular chain heterogeneity of linear low-density polyethylene by cross-fractionation of temperature rising elution fractionation and

successive self-nucleation/annealing thermal fractionation. Journal of Applied Polymer Science 2004; 94:1710-1718.
DOI: 10.1002/app.21084

[19] C. Piel, P. Starck, J.V. Seppälä, W. Kaminsky. Thermal and mechanical analysis of metallocene-catalyzed ethene–α-olefin copolymers: The influence of the length and number of the crystallizing side chains. Journal of Polymer Science: Part A: Polymer Chemistry 2006; 44:1600-1612.
DOI: 10.1002/pola.21265

[20] M.L. Arnal, V. Balsamo, G. Ronca, A. Sánchez, A.J. Müller, E. Cañizales, C. Urbina de Navarro. Applications of successive self-nucleation and annealing (SSA) to polymer characterization. Journal of Thermal Analysis and Calorimetry 2000; 59:451-470.
DOI: 10.1023/A:1010137408023

[21] A.J. Müller, Z.H. Hernández, M.L. Arnal, J.J. Sánchez. Successive self-nucleation and annealing (SSA): A novel technique to study molecular segregation during crystallization. Polymer Bulletin 1997; 39:465-472.
DOI: 10.1007/s002890050174

[22] A.J. Müller, A.T. Lorenzo, M.L. Arnal. Recent advances and applications of "successive self-nucleation and annealing" (SSA) high speed thermal fractionation. Macromolecular Symposia 2009; 277:207-214.
DOI: 10.1002/masy.200950325

[23] M. Camargo, M.M.C. Forte, C.R. Wolf. Linear low density polyethylene thermal fractionation by DSC technique. International Journal of Polymer Analysis and Characterization 2008; 13:49-65.
DOI: 10.1080/10236660701802593

[24] X. Sun, G. Shen, H. Shen, B. Xie, W. Yang, M. Yang. Co-crystallization of blends of high-density polyethylene with linear low-density polyethylene: An investigation with successive self-nucleation and annealing (SSA) technique. Journal of Macromolecular Science, Part B: Physics 2013; 52:1372-1387.
DOI: 10.1080/00222348.2013.768504

[25] R.L. Morgan, M.J. Hill, P.J. Barham. Morphology, melting behavior and co-crystallization in polyethylene blends: The effect of cooling rate on two homogeneously mixed blends. Polymer 1999; 40:337-348.
DOI: 10.1016/S0032-3861(98)00193-1

[26] M.L. Arnal, E. Cañizales, A.J. Müller. Thermal and morphological evaluation of very low density polyethylene/high density polyethylene blends. Polymer Engineering and Science 2002; 42:2048-2063.
DOI: 10.1002/pen.11096

[27] A.S. Luyt, R. Brüll. Investigation of polyethylene-wax blends by CRYSTAF and SEC-FTIR. Polymer Bulletin 2004; 52:177-183.
DOI: 10.1007/s00289-004-0274-0

[28] J.D. Hoffman, J.J. Weeks. Melting process and the equilibrium melting temperature of polychlorotrifluoroethylene. Journal of Research of the National Bureau of Standards-A. Physics and Chemistry 1962; 66:13-28.
DOI: 10.6028/jres.066A.003

[29] L. Mandelkern. Crystallization of Polymers.Volume 1. Equilibrium Concepts. Cambridge, New York (2002).

[30] M. Hayatifar, L. Bernazzani, A.M. Raspolli Galletti. Thermal and structural investigation of random ethylene/1-hexene copolymers with high 1-hexene content. Journal of Thermal Analysis and Calorimetry 2014; 115:1711-1718.
DOI: 10.1007/s10973-013-3445-0

[31] C. Li, J. Zhao, D. Zhao, Q. Fan. Linear low-density polyethylene/poly(ethylene-ran-butene) elastomer blends: Miscibility and crystallization behavior. Journal of Polymer Research 2004; 11:323-331.
DOI: 10.1007/s10965-005-6569-5

[32] H. Liang, F. Xie, B. Chen, F. Guo, Z. Jin, F. Luo. Miscibility and melting behavior of poly(ethylene terephthalate)/poly(trimethylene terephthalate) blends. Journal of Applied Polymer Science 2007; 107:431-437.
DOI: 10.1002/app.27081

[33] M.A. Al Maadeed, S. Labidi, I. Krupa, M. Ouederni. Effect of waste wax and chain structure on the mechanical and physical properties of polyethylene. Arabian Journal of Chemistry 2014 (published online).
DOI: 10.1016/j.arabjc.2014.01.006

[34] J.W. Huang, Y.L. Wen, C.C. Kang, M.Y. Yeh, S.B. Wen. Crystallization of poly(butylene terephthalate)/poly(ethylene octane) blends: Isothermal crystallization. Journal of Applied Polymer Science 2008; 109:3070-3079.
DOI: 10.1002/app.27628

[35] M. Trujillo, M.L. Arnal, A.J. Müller, M.A. Mujica, C. Urbina de Navarro, B. Ruelle, P.Dubois. Supernucleation and crystallization regime change provoked by MWNT addition to poly(ε-caprolactone). Polymer 2012; 53: 832-841.
DOI: 10.1016/j.polymer.2011.12.028

[36] M. Avrami. Kinetics of phase change I: General theory. Journal of Chemical Physics 1939; 7:1103-1112.
DOI: 10.1063/1.1750380

[37] M. Avrami. Kinetics of phase change II: Transformation-time relations for random distribution of nuclei. Journal of Chemical Physics 1940; 8:212-224.
DOI: 10.1063/1.1750631

[38] M. Avrami. Granulation, phase change, and microstructure kinetics of phase change III. Journal of Chemical Physics 1941; 9:177-184.
DOI: 10.1063/1.1750872

[39] A.T. Lorenzo, M.L. Arnal, J. Albuerne, A.J. Müller. DSC isothermal polymer crystallization kinetics measurements and the use of the Avrami equation to fit the data: Guidelines to avoid common problems. Polymer Testing 2007; 26:222-231.
DOI: 10.1016/j.polymertesting.2006.10.005

[40] Q. Guo, C. Harrats, G. Groeninckx, M.H.J. Koch. Miscibility, crystallization kinetics and real-time small-angle X-ray scattering investigation of the semicrystalline morphology in thermosetting polymer blends of epoxy resin and poly(ethylene oxide). Polymer 2001; 42:4127-4140.
DOI: 10.1016/S0032-3861(00)00813-2

[41] M.R. Nouri, J.N. Hay. Isothermal crystallization kinetics and melting behaviour of metallocene-catalyzed polyethylenes. Iranian Polymer Journal 2007; 16:105-112.

[42] J.D. Menczel, R.B. Prime. Thermal Analysis of Polymers.Fundamentals and Applications.John Wiley & Sons, New Jersey (2009).

[43] J.W. Huang, Y.L. Wen, C.C. Kang, M.Y. Yeh, S.B. Wen. Crystallization of poly(butylene terephthalate)/poly(ethylene octene) blends: Isothermal crystallization. Journal of Applied Polymer Science 2008; 109:3070-3079.
DOI: 10.1002/app.27628

[44] H.A.M Saeed, Y.A. Eltahir, Y. Xia, W. Yimin. Non-isothermal crystallization kinetics and nucleationactivity of hyperbranched polyester (HBPET) in recycled PET. Polymer Bulletin 2014; 71:595-612.
DOI: 10.1007/s00289-013-1080-3

[45] R. Ou, C. Guo, Y, Xie, Q. Wang. Non-isothermal crystallization kinetics of Kevlar fiber-reinforced wood flour HDPE composites. BioResources 2011; 6:4547-4565.
DOI: 10.1002/app.36425

[46] A. Jeziorny. Parameters characterizing the kinetics of the non-isothermal crystallization of poly(ethylene terephthalate) determined by DSC. Polymer 1978; 19:1142-1144.
DOI: 10.1016/0032-3861(78)90060-5

[47] J. Song, M. Ren, Q. Chen, X. Sun, H. Zhang, C. Song, H. Zhang, Z. Mo. Isothermal and nonisothermal crystallization kinetics of irradiated nylon 1212. Journal of Polymer Science Part B: Polymer Physics 2005; 43:2326-2333.
DOI: 10.1002/polb.20447

[48] T. Liu, Z. Mo, S. Wang. Nonisothermal melt and cold crystallization kinetics of poly(aryl ether ether ketone ketone). Polymer Engineering and Science 1997; 37:568-571.
DOI: 10.1002/pen.11700

[49] J.B. Song, Q.Y. Chen, M.Q. Ren, X.H. Sun, H.L. Zhang, H.F. Zhang, Z. Mo. Effect of partial melting on the crystallization kinetics of nylon-1212. Journal of Polymer Science Part B: Polymer Physics 2005; 43:3222-3230.
DOI: 10.1002/polb.20525

[50] T. Ozawa. Kinetics of non-isothermal crystallization. Polymer 1971; 12:150-158.
DOI: 10.1016/0032-3861(71)90041-3

CHAPTER 4

CONCLUSIONS

Crystallinity and crystalline morphology have an influence on the properties of a polymer (blend). It is therefore important to understand the influence of other components in a blend on the crystallization behaviour of a particular component.

LLDPE/wax blends were successfully prepared by melt-mixing and annealing in an oil bath. The results showed that the wax acted as a solvent or plasticizer in the LLDPE matrix for the non-annealed samples. This was evidenced by (i) the reduction of the melting and crystallization temperatures of the LLDPE phase, and (ii) the reduction of the temperature at which crystallization started. For the annealed samples, the LLDPE melting peak showed the development of a peak shoulder, and a separate peak due to the melting of the LLDPE crystals formed during cooling from 115 °C. The molten wax reduced the nucleation probability of the LLDPE, because the peak shoulder disappeared with increasing wax content. However, the melting peak of the LLDPE crystals that formed during cooling from 115 °C persisted as the wax content increased. The LLDPE had very little influence on the wax melting and crystallization temperatures. However, a certain fraction of the wax did not crystallize separately when blended with LLDPE, which was attributed to trapping of individual wax chains in the amorphous phase of LLDPE. The normalised melting enthalpies of the LLDPE in the blend showed almost no change with an increase in the wax content. The equilibrium melting temperatures of LLDPE in the LLDPE/wax blends were lower than that of pure LLDPE, and decreased with an increase in wax content, which indicates that the chemical potential of the LLDPE and its thermodynamic stability was reduced upon wax addition.

Through thermal fractionation by SSA, it was shown thatLLDPE can be thermally fractionated whereas the medium-soft paraffin wax was not susceptible to thermal fractionation owing to its linear short chain hydrocarbons. There was no overlap between the wax and LLDPE melting temperature ranges, indicating that they formed lamellae with widely different thicknesses.

The overall crystallization rate of LLDPE decreased with an increase in wax content due to the dilution effect of wax. The mechanism of nucleation and growth was not affected for either LLDPE or wax by the presence or content of the other component in the blend. For LLDPE an Avrami exponent of approximately 3 for all the samples confirmed the three-dimensional athermal and instantaneous nucleation of spherulites, while for wax the exponents were determined to be approximately 1, indicating that the crystal growth of the wax was one-dimensional fibrillar/rod-like with athermal nucleation. The isothermal crystallization kinetics for LLDPE could be well predicted by the Avrami and Lauritzen-Hoffman models.

In applying non-isothermal kinetics to the crystallization of wax, which was the only option because of its rapid crystallization, we used the mass compensation principle by decreasing the sample mass in relation to the increased cooling rates. This took into account the supercooling effects and thermal gradients in the samples, and the kinetics results showed that the wax in the blend crystallized faster than the unblended wax.

In conclusion, a phase-change material should be able to absorb the maximum amount of thermal energy during a phase change, even when mixed with a polymer. The results described in this thesis showed that, although wax crystallized faster when blended with LLDPE; it had a lower crystallinity, which directly impacts on its effectiveness as a phase-change material for thermal energy storage.

Recommendations for futurework:

- Determine the lamellar thickness of the crystals in the samples and the contribution of each phase to the crystalline superstructure using small-angle X-ray scattering (SAXS) and wide-angle X-ray scattering (WAXS).
- Do the same study presented in this thesis on nano filler containing LLDPE/wax blends.
- Study the possible nucleating effect of LLDPE on wax, in the absence and presence of a nanofiller.

ACKNOWLEDGEMENTS

First and foremost, I would like to thank God for His will to plan and complete this thesis despite all difficulties, and for the support and endless efforts of a large number of individuals and institutions.

I would like to express my sincere gratitude to my supervisors, **Prof. Adriaan Stephanus Luyt and Prof. Alejandro Jesus Müller** for their compassionate, excellent supervision. Their broad knowledge, dedication, andenthusiasm are what brought success in this work. You really made me believe that I had so much strength and courage to persevere even when it was tough. Despite the difficulties I encountered, you made me realize that in each and every end of the tunnel, there is a little light in the end. I aspire to emulate you.

My heartfelt gratitude goes to all the colleagues in the Polymer Research Group of UFS (Qwaqwa campus), Ms. Mamohanoe Molaba, Ms. Thollwana Makhetha, Ms. Cheryll-Ann Clarke, Ms. Motshabi Sibeko, Ms. Puseletso Mofokeng, Mr. Tsietsi Tsotetsi, Mr. Tyson Mosoabisane, Mr. Shale Sefadi, Mr. Khotso Mpitso, Mr. Benison Motloung and Dr. Duško Dudić. Special thanks to Mr. Jonas Mochane for the fruitful discussions we had and for always being determined to see me through. Thank you once again.

I would like to thank my former Polymer Science colleagues who are currently in CSIRand SASOL Companies; Mr. Tladi Mofokeng, Mr. Mfiso Mngomezulu, Dr. Thabang Mokhothu, Dr. Tshwafo Motaung and Dr. Jonathan Molefi for their time, effort and positive comments they always made to this study.

Special thanks to Mr. Alfred Maduba for the constant support, encouragement and patience throughout my studies.

Lastly, I am very grateful for the financial support I received from the National Research Foundation (NRF) and Sasol Inzalo Foundation (SaIF), South Africa.

Appendix A

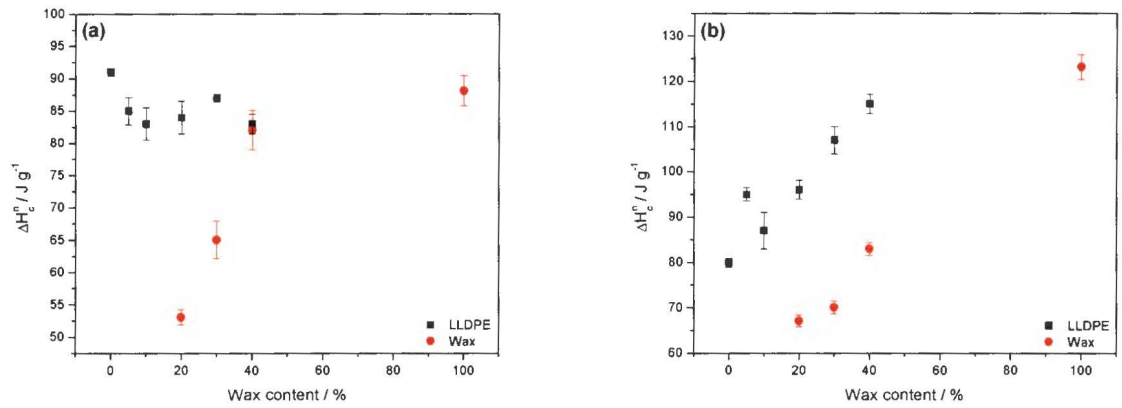

Figure A.1 DSC normalised crystallization enthalpies as a function of wax content for (a) non-annealed samples and (b) samples annealed at 115 °C

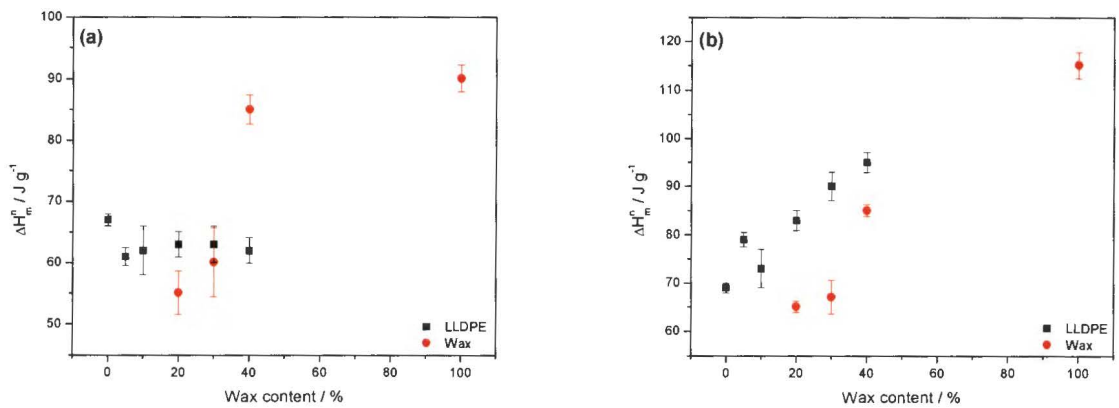

Figure A.2 DSC normalised melting enthalpies (second heating) as a function of wax content for (a) non-annealed samples and (b) samples annealed at 115 °C